SUPRACHOROIDAL DRUG DELIVERY TO THE EYE USING HOLLOW MICRONEEDLES

A Dissertation
Presented to
The Academic Faculty

by

Samirkumar R Patel

In Partial Fulfillment
of the Requirements for the Degree
Chemical Engineering in the
School of Chemical and Biomolecular Engineering

Georgia Institute of Technology
May 2011

SUPRACHOROIDAL DRUG DELIVERY TO THE EYE USING HOLLOW MICRONEEDLES

Approved by:

Dr. Mark R Prausnitz, Advisor
School of Chemical and Biomolecular Engineering
Georgia Institute of Technology

Dr. Henry F Edelhauser, Co-advisor
Department of Ophthalmology
Emory University

Dr. Andreas Bommarius
School of Chemical and Biomolecular Engineering
Georgia Institute of Technology

Dr. John Nickerson
Department of Ophthalmology
Emory University

Dr. Athanasios Nenes
School of Chemical and Biomolecular Engineering
Georgia Institute of Technology

Date Approved: Jan 24, 2011

Dedicated to my parents, Rajnikant and Indiraben Patel,
who taught me to value education.

I've lost many battles but never lost sight of the war
- Hank Moody

ACKNOWLEDGEMENTS

I'd like to start off by thanking my two advisors, Dr. Mark Prausnitz and Dr. Henry Edelhauser, who have been a large reason for not just the completion of my thesis but also in the overall success of the work. They have, despite my nebulous approach to graduate work, directed me down a path that has yielded some great results. In particular I would like to thank Dr. Prausnitz for putting up with my circuitous writing style and helping me to become a better communicator. Dr. Edelhauser has been with me every step of the way in the experiments we have done. He has helped me to understand the value in some of the most basic experiments and methods. I am indebted to you both. I'd also like to thank the rest of my committee members: Dr. Andreas Bommarius, Dr. Anthanasios Nenes and Dr. John Nickerson, who have put in the time and effort to help review this work and make it better.

This work involved a number of direct collaborators who I am very appreciative of. I'm grateful to Angela Lin for help in imaging the eye using microcomputed tomography. Dr. Damian Berzovsky MD has been instrumental in conducting all of the in vivo experiments with me and for making the work fun. Together we usually managed to find a way to make things bounce in the right direction. Dr. Bernard McCarey provided great advice for many of the rabbit experiments and also made the 'radio hour' lunches at Emory more enjoyable. Drs. Louise Bergman MD and Lennart Berglin MD from Sweden were also very helpful in the studies and their jovial attitude made the time pass quickly. I'd also

like to thank a number of undergraduate students who have contributed to my graduate work: Nicole Devlin, Sahaja Bandhari, Iva Franjkic, Adam Tallarita, Eric Powers, and Xi Wong (Emory). I would also like to thank Dr. Uday Kompella (University of Colorado) for his advice on many experiments. Specifically I'd like to thank him and his lab, especially Rinku Baid, for supplying some custom formulations for the experiments in this work.

There are also a number of people that I have had the pleasure of working with throughout this time that have complemented my research experience. I've enjoyed working with Susan Lee from University of Southern California on magnetic resonance imaging of the eye. I'm also grateful for the opportunity to work with Dr. Tim Olsen MD and Kathy Wabner on pig studies over at Emory. Both were extremely helpful and patient. I've also had the pleasure of visiting University of Wisconsin at Madison and collaborating with Dr. Bahoe Tian and Dr. Paul Kaufman MD who I have learned a lot about glaucoma from. I'd also like to thank Dr. Young bin Choy who I worked with on various eye experiments at Georgia Tech. I'd also like to thank Dr. Mark Allen for use of the laser facility, the Emory histology, and Brad Parker and Jeff Andrews for helping build some of the devices used in this research.

I'd like to say a special thanks to Drs. Harvinder Gill and Vladimir Zarnitsyn who have both been great role models for me in the lab and also great friends. Dr. Zarnitsyn, in addition to contributing technically to my research, has always been a good sounding board for just about anything.

There's one special lady I have to thank. Out of all the ladies that have come and gone since I've started graduate school she has always been there. She's ready to listen to whatever I have to say and treated me like I am someone special. Whenever I needed something she seemed to manage to get it done even if it was on short notice. Donna Bondy, I say to you in the best possible goat voice, "thank you." I'd also like to express my gratitude towards Pat Nichols and Jill Edelhauser who made me feel comfortable to work at Emory.

I've been fortunate to have many friends from the department who have also been great to hang out with outside the lab. I'd like to thank Avishek Aiyer, Dr. Kaushik Chowdhury, Dr. Mita Das, Dr. Kevin Gallagher, Dr. Jyoti Gupta, Josh Hutchenson, Anwesha Paladi, Dr. Ed Park and Dr. Sean Sullivan. Many thanks to past and present Drug Delivery Lab members: Dr. Samantha Andrews, Brian Bondy, Dr. Seong-O Choi, Dr. Leonard Chu, Chris Edens, Dr. Daniel Hallow, Dr. Jason Jiang, Dr. Yeuchun Kim, Yoo Chun Kim, Dr. Jeong-Woo Lee, Ying Liu, Dr. Saffar Mansoor, James Norman, Dr. JungHwan Park, and Aritra Sengupta,

I'd also like to acknowledge the support of all the teachers and mentors throughout my education that brought me to graduate school. In particular, I'd like to thank Dr. Shelley Rabel who helped me to start off my graduate work in confidence.

In conclusion, I'd like to thank my family. Both my mother, Indiraben Patel, and my father, Rajnikant Patel, have provided immeasurable support throughout my life. I'd also like to thank my brother Ashishkumar Patel, whose jokes and lightheartedness always helped to put things in perspective.

TABLE OF CONTENTS

	Page
ACKNOWLEDGEMENTS	iv
LIST OF TABLES	xii
LIST OF FIGURES	xiii
LIST OF SYMBOLS AND ABBREVIATIONS	xxiv
SUMMARY	xxv
CHAPTER	
1 Introduction	1
2 Background	4
2.1 Anatomy of the Eye	4
2.2 Eye Diseases	7
2.2.1 Introduction	7
2.2.2 Glaucoma	7
2.2.3 Age Related Macular Degeneration	8
2.2.4 Diabetic Retinopathy	9
2.3 Ocular Drug Delivery Methods	10
2.3.1 Introduction	10
2.3.2 Systemic	12
2.3.3 Extraocular	13
2.3.3.1 Topical	13
2.3.3.2 Iontophoresis	
2.3.3.3 Periocular	16
2.3.4 Intraocular	17

2.3.4.1 Intravitreal Injections 17

2.3.4.2 Intravitreal Implants 19

2.3.4.3 Suprachoroidal Delivery 19

2.4 Microneedles and Their Applications in Drug Delivery 20

2.4.1 Introduction 20

2.4.2 Poke and Apply 22

2.4.3 Coat and Poke 23

2.4.4 Poke and Release 27

2.4.5 Poke and Flow 28

3 Materials and Methods 32

3.1 Feasibility of Suprachoroidal Delivery Using a Hollow Microneedle 32

3.1.1 Materials 32

3.1.2 Experimental Procedure 34

3.2 Spread of Injections in the Suprachoroidal Space 36

3.2.1 Hollow Glass Microneedle Device 36

3.2.2 Injections of India Ink 38

3.2.3 Snap Freezing of the Eye 39

3.2.4 Histological Analysis 39

3.2.5 Quantification of the Spread of India Ink 40

3.2.6 Hollow Metal Microneedle Device 41

3.2.7 Injections of Latex in Human Eyes 42

3.3 In Vivo Ocular Clearance of Molecules and Particles 45

3.3.1 Materials 45

3.3.2 Injection Procedure 46

3.3.3 Fluorescence Measurements 47

3.3.4 Imaging Delivery Within Suprachoroidal Space 49

4 Results 50

4.1 Feasibility of Suprachoroidal Delivery Using a Hollow Microneedle 50

4.1.1 Introduction 50

4.1.2 Imaging Delivery in to the Suprachoroidal Space 51

4.1.3 Effect of Operating Parameters on Particle Delivery in to the Suprachoroidal Space of Pig Eyes 58

4.1.4 Effect of Intraocular Pressure 63

4.1.5 Discussion 65

4.1.6 Conclusion 69

4.2 Spread of Injections in the Suprachoroidal Space 70

4.2.1 Introduction 70

4.2.2 India Ink Spread in the Suprachoroidal Space of Rabbit Eyes In Vivo 71

4.2.2.1 Imaging Spread and Hollow Glass Microneedle Device Reliability 71

4.2.2.2 Quantifying Spread of India Ink in the Suprachoroidal Space 77

4.2.3 Spread of Latex in Human Eyes 88

4.2.4 Discussion 95

4.2.5 Conclusion 100

4.3 In Vivo Ocular Clearance of Molecules and Particles 101

4.3.1 Introduction 101

4.3.2 Comparison of Suprachoroidal and Intravitreal Injections 102

4.3.3 Injection of Macromolecules in to the Suprachoroidal Space 110

4.3.4 Injection of Particles in to the Suprachoroidal Space 117

4.3.5 Discussion 126

4.3.6 Conclusion 130

5 Conclusion 131

6 Discussion and Future Work 136

REFERENCES 140

VITA 147

LIST OF TABLES

Page

Table 4.1.1 Statistical comparison of injection success rates of particles of different sizes at different microneedle lengths. Values in the table are p values determined using ANOVA. Statistical significance between particle sizes at a given microneedle length was considered to be $p<0.05$ and indicated by an asterisk (*). 61

Table 4.2.1 Table of statistics from injections of India ink within the suprachoroidal space of live rabbits. 73

Table 4.2.2 Table showing the characteristics of the human eyes used and the experimental parameters tested. The eyes were obtained as quickly as possible from the time of death. The longest time between death and injection was less than 8 hours 89

LIST OF FIGURES

Page

Figure 2.1.1 Image of the anatomy of the eye highlighting the major tissues. Image of the eye was adapted from National Eye Institute, National Institutes of Health, with permission. 6

Figure 2.1.2 The suprachoroidal space is located between two posterior tissues, the sclera and choroid. This region expands when there is a buildup of fluid between these two layers to form the suprachoroidal space. Image of the eye was adapted from National Eye Institute, National Institutes of Health, with permission. 7

Figure 2.3.1 Local drug delivery methods to the back of the eye. There are a variety of ways to locally deliver drugs to the back of the eye. Some of these approaches are highlighted above: (a, b) topical, (c, j) injections, (d, g, h, i) implants, and (e, f) microneedles. 11

Figure 2.4.1 Microneedle strategies for drug delivery into tissues. (a) Poke and apply: Insert microneedles into the tissue to form pores, remove microneedles and then apply the drug formulation to the surface of the tissue. (b) Coat and poke: Coat microneedles with a drug formulation, insert microneedles into a tissue to dissolve off the coating formulation within the tissue and remove microneedles to leave the deposited drug in the tissue. (c) Poke and release: Encapsulate drug in a biodegradable microneedle, insert microneedles into the tissue and leave them there, and as the microneedle degrades the drug is released into the surrounding tissue. (d) Poke and flow: Insert a hollow microneedle into a tissue, apply pressure to the fluid in the microneedle to flow the fluid into the tissue, and remove hollow microneedle after the desired volume has been injection, leaving behind fluid in the tissue. Adapted from Arora et al 2008. 21

Figure 2.4.2 (a) A brightfield image of a single solid stainless steel microneedle. The surface of the microneedle can be coated with a liquid formulation. (b) As an example, it can be coated with an aqueous formulation of sulforhodamine B (red liquid). Scale bar: 500 μm 24

Figure 2.4.3 Brightfield and fluorescent images showing the variety of materials that can be coated onto solid stainless steel microneedles: (a) calcein, (b) vitamin B, (c) bovine serum albumin conjugated with Texas Red, (d) plasmid DNA conjugated with YOYO-1, (e) modified vaccinia virus - Ankara conjugated with YOYO-1, (f) 1-μm diameter barium sulfate particles and (g) 10-μm diameter latex particles. Scale bar: 200 μm. Adapted from Gill and Prausnitz 2007b. 26

Figure 2.4.4 An array of carboxymethylcellulose (CMC) microneedles of 600 μm in length and a base of 300 μm. Scale bar: 500 μm. Adapted from Lee et al 2008. 28

Figure 2.4.5 (a) Front and (b) side view of a single hollow glass microneedle. The microneedle has a beveled tip and an approximately elliptical orifice. Scale bar: 250 μm. Adapted from Jiang et al 2009. 30

Figure 3.1.1 Experimental approach to microneedle infusion into the suprachoroidal space. (a) Comparison of a hollow microneedle mounted in an insertion device (above) and the tip of a 30 gauge hypodermic needle (below). Scale bar: 1mm. (b) Schematic diagram of the experimental set up used to study suprachoroidal injection. The eye was placed on a custom-made mold with a channel through which suction was applied to hold the eye in place. A cannula inserted through the optic nerve of the eye allowed application of intraocular pressure. The microneedle was inserted into the sclera using the custom-made insertion device. Image of the eye was adapted from National Eye Institute, National Institutes of Health with permission. 33

Figure 3.2.1 A custom hollow microneedle device for injection of fluids in vivo in to the rabbit suprachoroidal space. The main housing of the custom device (1-3) contains a shaft through which a hollow glass microneedle can be inserted through. The tip of the microneedle extends from the tip of the cap on the housing (2). The cap can be rotated so as to allow the desired amount of the glass microneedle to protrude from the device. The microneedle length is adjusted using this rotatable cap. The back end of the device is connected to a metal luer adapter containing an olive shaped gasket (4). One end of the adapter is screwed onto to the device which tightens onto the glass microneedle and holds it in place. The other end of the luer adapter is attached to extension tubing which is attached to a glass syringe. Scale bar: 1 cm. 37

Figure 3.2.2 India ink surface area coverage quantification process. (a) Eyes were enucleated after injection of India ink. (b) Enucleated eyes were placed in glycerol for 6-8 minutes causing the sclera to become transparent. (c) The eye was removed when the India ink could clearly be seen. Images of the eye were taken using digital camera. The India ink could clearly be seen and measurements were taken of the spread. (d) Using the images and measurements a digital map of the spread was made for each injection. On this digital map the location of the limbus, the injection site (asterisk), and the optic nerve were designated. 41

Figure 3.2.3 Comparison of hollow metal microneedle to a 30 gauge hypodermic needle. The hollow metal microneedle is on the left attached to a standard luer adapter (in white) which could be easily attached to any syringe. The total length of the microneedle is less than a millimeter which is similar to just the orifice opening of the 30 gauge hypodermic needle. 42

Figure 3.2.4 Latex surface area quantification procedure. (a) First the whole eye was frozen. The globe was dissected using a blade into “petals” starting from the optic nerve. (b) The cuts were made up to the cornea leaving the cornea intact. The petals were opened up from the optic nerve. The petals contained the tissues of the globe (sclera, choroid and retina) and exposed the vitreous (1) inside as a frozen white ball. (c) The vitreous was removed carefully leaving the globe tissues and anterior segments of the eye. The petals were laid flat with the cornea in the center and the choroid and retina (2) were slowly pulled away. Image (c) shows petals with choroid and retina still attached (2) and choroid and retina removed (3). (d) Once all the petals were removed the latex (4) on the sclera that could be easily distinguished from the white sclera with the transparent cornea (5) in the center of the petals. 44

Figure 3.3.1 Representative baseline fluorescence scan of the rabbit eye in vivo. (a) The baseline scan is performed through the visual axis, dotted box area. (b) The scan of that region gives fluorescence measurements along this axis and assigns a relative position (x-axis). The fluorescence reading is plotted on the y-axis. The peaks provide an indication as to the position of key regions of the eye such as the retina, lens and cornea. The image of the eye is roughly scaled to match the position axis of the scan for reference. Image of the eye was adapted from National Eye Institute, National Institutes of Health with permission. 48

Figure 4.1.1 Imaging of fluid infusion into the suprachoroidal space. Brightfield microscopic images of a cross section of a frozen eye (a) showing normal ocular tissue (b) showing the delivery of sulforhodamine B (pink) between the sclera and choroid (i.e., in the suprachoroidal space) Scale bar: 500 μm. 53

Figure 4.1.2 Imaging of sulforhodamine B (pink) infusion into the suprachoroidal space. Brightfield view of a frozen eye from the vitreous side (a) showing the sample with choroid and retina still attached in some locations and (b) with choroid and retina completely removed. 54

Figure 4.1.3 Imaging of particle infusion into the suprachoroidal space. Image of a cryosection of a pig eye with no infusin into the suprachoroidal space. (a) The layers of the eye are (1) sclera, (2) choroid, and (3) retina. Collaged fluorescence microscopy images of tissue cryosections show the delivery of (b) 500 nm particles into a rabbit eye, (c) 500 nm particles into a pig eye, and (d) 1000 nm particles into a human eye, all ex vivo. Each image also displays an inset with a magnified view of the microneedle insertion site. These images show targeted delivery of particles into the suprachoroidal space and indicate that the microneedle did not penetrate into the choroid or retina. Scale bar: 500 μm. 56

Figure 4.1.4 Microcomputed tomography images of suprachoroidal delivery of barium sulfate particles. (a) Two-dimensional axial cross section of a pig eye imaged after injection of 1 μm barium sulfate particles. The arrow points to the thin white strip of particles in the suprachoroidal space. (b) Two-dimensional cross sections were reconstructed to form a three-dimensional map showing the distribution of particles, which have spread circumferentially in all directions around the microneedle insertion site (arrow) in the suprachoroidal space. Scale bar: 5 mm. 58

Figure 4.1.5 The effect of infusion pressure and microneedle length on the success rate of suprachoroidal delivery for (a) 20 nm, (b) 100 nm, (c) 500 nm and (d) 1000 nm particles into pig eyes. A total of five infusions were attempted at each condition studied. Increasing microneedle length and increasing infusion pressure increased the delivery success rate for all particle sizes (ANOVA $p<0.05$). 60

Figure 4.1.6 Effect of particle size on particle distribution in the eye. Collaged fluorescence microscopy images of tissue cryosections show the delivery of (a) 20 nm particles and (b) 1000 nm particles into the suprachoroidal space of pig eyes ex vivo. The images show that 20 nm particles spread in the suprachoroidal space and within the sclera. However, the 1000 nm particles are primarily in the suprachoroidal space. The insertion sites are magnified in the insets. Scale bar: 500 μm. 62

Figure 4.1.7 The effect of infusion pressure and microneedle length on the success rate of suprachoroidal delivery of 1000 nm particles at simulated IOP levels of (a) 18 mmHg and (b) 36 mmHg. A total of five infusions were attempted at each condition studied. The delivery success rate generally increased with an increase in IOP. IOP significantly affected delivery success rate as a function of infusion pressure when using 800, 900, and 1000 μm long microneedles ($p<0.05$). 64

Figure 4.2.1 Images showing a view of an India ink injection into the suprachoroidal space through the pupil. (a) India ink (black) is not visible in the back of the eye when looking away from the injection site (arrow) and as you look towards the injection site (b) more India ink can be seen until the back of the eye looks completely black (c) In this eye, a hollow glass microneedle, 700 μm in length, was used to inject 50 μL into the suprachoroidal space. 72

Figure 4.2.2 Images of a frozen rabbit eye after India ink injections into the suprachoroidal space. (a) A view from the back of the whole eye shows the India ink has reached all the way to the optic nerve, (b) A view of the sclera, choroid and retina tissues after they are removed as a cup from the equator. The equator (E) is marked with double arrows. This view shows the back of the eye from the inside and the India ink within those layers. (c) The vitreous is free from the India ink and the injection site (IS) is marked. The India ink (II) can also be seen as a ring near the equator (E) in the portion of the eye that is left after removing the posterior cup (b). 74

Figure 4.2.3 A whole rabbit eye after fixation in glutaraldehyde. A section of the globe removed near the injection site is flipped over to reveal the Inida ink (black) within the tissues of the globe. A view of the inside of the eye shows that no India ink appears in the vitreous but some can be seen in the remaining tissues of the globe. 76

Figure 4.2.4 Histological cross section of the rabbit eye showing India ink within the suprachoroidal space. (a) The India ink can be seen in black located between the sclera and choroid layers of the eye tissue. Scale bar: 200 μm. (b) A magnified view of the India ink in the suprachoroidal space. Scale bar: 25 μm. 77

Figure 4.2.5 Injections of India ink were done on live rabbits in the superior temporal quadrant of the eye. The eyelids were pushed back to access the insertion site (*) more clearly. The image shows the approximate location of the injection site (*). It also shows the direction towards the nose (N) indicated by the arrow for reference and orientation of future images. 79

Figure 4.2.6 Digitized distribution of India ink within the suprachoroidal space of rabbit eyes. An asterisk indicates the injection site, the arrow points to the location of the optic nerve, and the letter N indicates the direction towards the nose. Scale bar: 5 mm. 80

Figure 4.2.7 A graph showing the surface area covered from 30, 50 or 100 μL (x-axis) of India ink injected in the suprachoroidal space in vivo in rabbits using a glass microneedle. The chorioretinal surface area (left y-axis) covered increases with increasing volume. The surface area per volume of India ink (right y-axis) injected decreases as the volume injected increases. A minimum of n=3 injections were performed for each volume and standard deviations are shown. 82

Figure 4.2.8 A graph showing the percentage surface area covered from a microneedle injection of India ink in the suprachoroidal space in vivo in rabbits. The percent area is on the y-axis and the volumes injected on the left. Error bars represent standard deviations. Each value is statistically different (ANOVA $p<0.05$) from each other indicating that the percent covered is increasing with increasing volumes. 85

Figure 4.2.9 Graph showing the distance covered from a microneedle injection of different volumes of India ink in the suprachoroidal space of rabbit eyes in vivo. The y-axis represents the maximum distance traveled in the two directions and the x-axis shows the two directions measured. The max distance towards the optic nerve is the maximum distance the India ink covers from the limbus to the back of the eye. The max lateral distance is the maximum total distance the India ink covers parallel to the limbus (i.e. around the eye) The asterisks indicate the distances that are statistically significant between the different injection volumes (ANOVA $p<0.05$). 87

Figure 4.2.10 Representative images of the spread of latex in the suprachoroidal space after injection of (a) 50 µL, (b) 100 µL, and (c) 150 µL using a hollow metal microneedle. The white petals are the sclera with pink latex on top of them. Some of the sclera is pigmented (b) and is darker than others. The choroid and retina have been removed and the cornea is in the center. The injection site is marked with an asterisk. Scale bar: 10 mm. 90

Figure 4.2.11 Graph showing the surface area covered from a single microneedle injection of latex in the suprachoroidal space of fresh human cadaver eyes The x-axis displays the volume delivered. The surface area covered (diamond markers) show the surface area covered using the left y-axis. The surface area per volume of fluid (square markers) is plotted against the right y-axis. Error bars are standard deviations. 91

Figure 4.2.12 Graph showing the percent area covered from a microneedle injection of latex in the suprachoroidal space of fresh human cadaver eyes. Error bars are standard deviations. 92

Figure 4.2.13 Graph showing the distance covered from a microneedle injection of latex in the suprachoroidal space of human cadaver eyes. The y-axis represents the maximum distance traveled in the two directions and the x-axis shows the two directions measured. The max distance towards the optic nerve is the maximum distance the latex covers from the limbus to the back of the eye. The max lateral distance is the maximum total distance the latex covers parallel to the limbus (i.e. around the eye). The asterisks indicate the distances that are statistically significant between the different injection volumes (ANOVA $p<0.1$). 95

Figure 4.3.1 Representative baseline scan of the rabbit eye in vivo with no injection. The baseline profile was obtained from a single scan of the eye along the visual axis. The x-axis, position, represents the visual axis of the eye while the y-axis shows the measurement of the fluorescent intensity at that position. The position of eye tissues are estimated from peaks observed in the baseline scan. The peak to the furthest left is the retina while the two peaks at the furthest right are the cornea. Just to the left of the cornea are two additional peaks which demarcate the lens. 103

Figure 4.3.2 Representative concentration profiles of sodium fluorescein in the rabbit eye in vivo over time after an intravitreal injection of 50 µL using a 30 g needle. Each profile was created from a single scan of the eye along the visual axis. The x-axisx-axis, position, represents the visual axis of the eye with the cornea located to the right of the x-axis in the anterior segment. The approximate position of eye tissues is estimated from baseline scans of the eye. 105

Figure 4.3.3 Average concentration of sodium fluorescein in the vitreous over time after an intravitreal injection of 50 µL (6 µg/mL) using a 30g needle. The concentration drops over time and the fluorescein is cleared from the vitreous within 24 hours after injection. (n=3 and error bars are standard deviations). 106

Figure 4.3.4 Representative concentration profiles of sodium fluorescein in the rabbit eye in vivo over time after a suprachoroidal injection of 50 µL using a microneedle. Each profile was created from a single scan of the eye along the visual axis. The x-axis, position, represents the visual axis of the eye with the cornea located to the right of the x-axis in the anterior segment. The approximate position of eye tissues is estimated from baseline scans of the eye. The arrow points to the peak of the concentration profile occurring in the suprachoroidal space. 107

Figure 4.3.5 Average concentration of sodium fluorescein in the suprachoroidal space over time after a suprachoroidal injection of 50 µL (600 µg/mL) using a microneedle. The concentration drops over time and the fluorescein is cleared from the vitreous within 24 hours after injection. (n=3 and error bars are standard deviations). 108

Figure 4.3.6 Graph showing the ratio of concentrations of sodium fluorescein within two locations in the eye after intravitreal (squares) and suprachoroidal injections (triangles). The ratio represents the ability of the injection to target the chorioretinal tissues. For an intravitreal injection the ratio is the concentration in the vitreous near the retina to that near the lens. For a suprachoroidal injection the ratio is the concentration in the suprachoroidal space to the concentration in the vitreous near the lens. The graph shows that the ratio is higher for a suprachoroidal injection and is statistically different at all time points after administration than an intravitreal injection. Error bars are standard deviations. n=3 per injection. 110

Figure 4.3.7 Representative fluorescence intensity profiles of 40kDa dextran tagged with FITC in the rabbit eye in vivo over time after a suprachoroidal injection of 50 µL using a microneedle. Each profile was created from a single scan of the eye along the visual axis. The x-axis, position, represents the visual axis of the eye with the cornea located to the right of the x-axis in the anterior segment. The approximate position of eye tissues is estimated from baseline scans of the eye. The scans show that the peak intensity remains in the suprachoroidal space. 112

Figure 4.3.8 Representative fluorescence intensity profiles of 250kDa dextran tagged with FITC in the rabbit eye in vivo over time after a suprachoroidal injection of 50 µL using a microneedle. Each profile was created from a single scan of the eye along the visual axis. The x-axis, position, represents the visual axis of the eye with the cornea located to the right of the x-axis in the anterior segment. The approximate position of eye tissues is estimated from baseline scans of the eye. The scans show that the peak intensity remains in the suprachoroidal space. 113

Figure 4.3.9 Representative fluorescence intensity profiles of bevaciszumab tagged with Alexa Fluor 488 in the rabbit eye in vivo over time after a suprachoroidal injection of 50 µL using a microneedle. Each profile was created from a single scan of the eye along the visual axis. The x-axis, position, represents the visual axis of the eye with the cornea located to the right of the x-axis in the anterior segment. The approximate position of eye tissues is estimated from baseline scans of the eye. The scans show that the peak intensity remains in the suprachoroidal space. 114

Figure 4.3.10 Average fluorescence intensity of 40 kDa dextran tagged with FITC in the suprachoroidal space over time after a suprachoroidal injection of 50 µL using a microneedle. The fluorescence intensity drops over time and the dextran is cleared from the vitreous within 24 hours after injection. (n=2 and error bars are standard deviations). 115

Figure 4.3.11 Average fluorescence intensity of 250 kDa dextran tagged with FITC in the suprachoroidal space over time after a suprachoroidal injection of 50 µL using a microneedle. The fluorescence intensity drops over time and the dextran is cleared from the vitreous in approximately 24 hours after injection. (n=2 and error bars are standard deviations). 116

Figure 4.3.12 Average fluorescence intensity of bevacizumab tagged with Alexa Fluro 488 in the suprachoroidal space over time after a suprachoroidal injection of 50 µL using a microneedle. The fluorescence intensity drops over time and bevacizumab is cleared from the vitreous in approximately 24 hours after injection. (n=2 and error bars are standard deviations). 117

Figure 4.3.13 Representative fluorescence intensity profiles of 20 nm particles in the rabbit eye in vivo over time after a suprachoroidal injection of 50 µL using a microneedle. Each profile was created from a single scan of the eye along the visual axis. The x-axis, position, represents the visual axis of the eye with the cornea located to the right of the x-axis in the anterior segment. The approximate position of eye tissues is estimated from baseline scans of the eye. The scans show that the peak intensity remains in the suprachoroidal space and does not return to baseline in the time tested. 119

Figure 4.3.14 Representative fluorescence intensity profiles of 500 nm particles in the rabbit eye in vivo over time after a suprachoroidal injection of 50 µL using a microneedle. Each profile was created from a single scan of the eye along the visual axis. The x-axis, position, represents the visual axis of the eye with the cornea located to the right of the x-axis in the anterior segment. The approximate position of eye tissues is estimated from baseline scans of the eye. The scans show that the peak intensity remains in the suprachoroidal space and does not return to baseline in the time tested. 120

Figure 4.3.15 Average fluorescence intensity of 20 and 500 nm particles in the suprachoroidal space over time after a suprachoroidal injection of 50 µL using a microneedle. The fluorescence intensity does not drop over the time tested (ANOVA $p<0.05$) indicating the particles are still present in the suprachoroidal space in a similar concentration to the initial amount. (n=2 and error bars are standard deviations). 121

Figure 4.3.16 Average fluorescence intensity of 1 and 10 µm particles in the suprachoroidal space over time after a suprachoroidal injection of 100 µL using a microneedle. The fluorescence intensity does not drop over the time tested (ANOVA $p<0.05$) indicating the particles are still present in the suprachoroidal space in a similar concentration to the initial amount. (n=2 and error bars are standard deviations). 122

Figure 4.3.17 Fundus photography of rabbit eyes injected with (a,b) 1 μm and (c,d) 10 μm particles in the suprachoroidal space and with (e,f) no injection. Images a, c, and e are color fundus images that show the ocular anatomy while b, d, and f are fluorescence images of the fundus that show the location of fluorescent particles. Arrows indicate the location of the optic cup. The bright particles can be seen in the fluorescent images after suprachoroidal injection (b,d). 124

Figure 4.3.18 Cross-section of rabbit eye tissue 28 days after a suprachoroidal injection of 500 nm particles in a rabbit eye in vivo. The arrow points to fluorescent particles in the suprachoroidal space. This confirms that the particles are still present in the suprachoroidal space even after 28 days. Scale bar: 500 μm. 125

Figure 4.3.19 Cross-section of rabbit eye tissue approximately 60 days after a suprachoroidal injection of (a) 1 μm and (b) 10 μm particles in a rabbit eye in vivo. The arrows points to fluorescent particles in the suprachoroidal/choroidal space. The sclera (S) and the choroid (C) can be seen with portions of the retina (R). This confirms that the particles are still present in the suprachoroidal space even after 60 days. Scale bar: 500 μm. 126

LIST OF SYMBOLS AND ABBREVIATIONS

AMD	Age-related Macular Degeneration
ANOVA	Analysis of Variance
BSS	Balanced Salt Solution
BSA	Bovine Serum Albumin
CMC	Carboxymethyl Cellulose
Gd-DTPA	Gadolinium DiethyleneTriamine Pentaacetic Acid
HBSS	Hanks Balanced Salt Solution
IACUC	Institutional Animal Care and Use Committee
IS	Injection Site
IOP	Intraocular Pressure
IVT	Intravitreal
kDa	kilo Daltons
MRI	Magnetic Resonance Imaging
µCT	Microcomputed Tomography
PLGA	Poly(lactic-co-glycolic acid)
SCS	Suprachoroidal Space

SUMMARY

Delivering drugs to effectively treat diseases of the back of the eye can be a challenging task. Although pharmacological therapies exist, drug delivery devices and techniques are not very effective at targeting delivery of drugs to the diseased tissues. This work introduces a novel approach to effectively deliver drugs to target tissues such as the choroid and retina. The approach involves a device, a hollow microneedle, to administer the drug formulation into a unique location in the eye, the suprachoroidal space. This new route of administration and a device to accomplish the delivery may provide an effective way to treat diseases of the choroid and retina.

The first part of the work determines the ex-vivo feasibility of delivering materials within the suprachoroidal space. The results show that fluids and particles can be delivered into the suprachoroidal space of rabbit, pig and human eyes using a hollow microneedle. It further examines the important parameters for injection of the particles within the suprachoroidal space. The data shows that injection pressure and microneedle length are important parameters for effective delivery of particles. The results lead to a theory on the mechanism by which the particles are delivered into the suprachoroidal space.

The second part of the research aims to develop a reliable in vivo delivery device and study the surface area coverage of materials injected into the suprachoroidal space. A hollow glass microneedle device is developed and for the first time shown to be effective in delivering a fluid into the suprachoroidal space in vivo. Up to 100 µL of India ink could be delivered into rabbit eyes in

vivo and the spread within the suprachoroidal space is characterized. The results show that a single microneedle injection can cover a significant percentage of the available suprachoroidal space. This is the first study to examine the spread of a material injected into the suprachoroidal space of a live animal. A hollow metal microneedle device is also developed and shown to be effective. The device was able to inject up to 150 μL of latex into suprachoroidal space of fresh human cadaver eyes. The spread of latex is characterized and the results also show that a significant portion of the suprachoroidal space can be covered.

The final part of the study examines the clearance of materials injected into the suprachoroidal space of rabbit eyes in vivo. First a comparison of a suprachoroidal injection to a conventional intravitreal injection shows that a suprachoroidal injection is more targeted to the chorioretinal tissues. In addition hollow microneedles are shown to effectively target macromolecules and a therapeutic antibody to the chorioretinal tissues. A study of the clearance kinetics show half lives within the suprachoroidal space on the order of several hours. Nano- and microparticles were also injected into the suprachoroidal space and showed very effective targeting. These non-degradable particles are shown to be present in the suprachoroidal space for months. Basic visual safety assessments identified no adverse effects from the injection of these materials. This represents the first study to compare intraocular clearance kinetics between a suprachoroidal injection and an intravitreal injection. It is also the first study to examine the clearance of a variety of materials from within the suprachoroidal space.

Overall this work shows that microneedles have the capability to deliver a variety of materials into the suprachoroidal space of rabbit, pig, and human eyes. The injection can be done in a minimally invasive way with the proper design of an injection device and can target the chorioretinal tissues more effectively than the currently used method. In addition particles have long residence times in the suprachoroidal space, so a particle based drug formulation could provide sustained delivery to the eye. This work represents the first comprehensive study on using the suprachoroidal space as a drug delivery route and also the first study to use hollow microneedles to deliver formulations into the eye in vivo.

CHAPTER 1

INTRODUCTION

The leading causes of blindness in the industrialized world are diseases that affect the back of the eye (del Amo and Urtti 2008). These diseases include age-related macular degeneration (AMD), diabetic retinopathy and uveitis, among others. An increasing number of pharmacological therapies exist to combat these diseases, but there are limited options for delivering these drugs effectively to their targets in the posterior segment of the eye. Delivering drugs to the posterior segment is hard primarily because of difficult access to the target tissues and the eye's natural barriers that prevent foreign material from moving into them. The target tissues vary depending on the disease and sometimes even the stage of the disease, but are often the choroid and retina, as in the case of AMD, diabetic retinopathy and uveities (Kimura et al 2001, Zarbin and Szirth 2007). Therefore, an effective drug delivery system targeting the back of the eye would provide a significant improvement in the management of these vision-threatening diseases.

An effective drug delivery system for the back of the eye should embody four general characteristics. First, it should be minimally invasive and safe, so as to avoid complications caused by the procedure. Second, the drug should be administered in such a way that it is well targeted to the desired tissues and limit exposure to other regions of the eye. This would allow for high bioavailability while reducing adverse events and toxicity in surrounding tissues. Third, it should be capable of sustained delivery of the drug to reduce the frequency of

administration and allow for better therapeutic control. Finally, administration of the drug should be as simple as possible, requiring only a routine office visit or, ideally, permitting self administration. A simple, reliable procedure can help reduce errors and compliance problems. Current methods of drug delivery to the posterior segment cannot meet all of these requirements.

Current local posterior segment drug delivery methods can be characterized by two overarching strategies: periocular or intravitreal (Ghate et al 2007, Kim et al 2007). The periocular strategy deposits a drug on the outer surface of the globe and either relies on diffusion, natural transport mechanisms of the eye or an applied biophysical driving force (e.g. iontophoresis) to deliver the drug inward towards its intraocular target. Periocular methods are usually minimally invasive, but often suffer from poor targeting, low bioavailability and limited sustained release capabilities. The intravitreal method involves placing the drug formulation directly into the vitreous of the eye; the drug can then diffuse outward towards the retina and choroid. This is often accomplished by an intravitreal injection or an implant, which introduces the drug directly into the back of the eye and can be designed for sustained release. However, intravitreal delivery is invasive, carries a risk of endophthalmitis, and often exposes unintended tissues to the drug.

The research presented here aims to improve upon these two strategies by introducing a new approach, directly delivering drugs between and within tissues of the posterior segment. More specifically we believe that it would be advantageous to deliver drugs into the suprachoroidal space; a virtual space

located between the sclera and choroid layers of the globe. This would place the drug in direct contact with the chorioretinal surface and target the delivery to the diseased tissues. We further propose to accomplish the delivery using a hollow microneedle. Hollow microneedles, because of their size, can target the suprachoroidal space in a minimally invasive way. This work aims to show that this route of administration coupled with a microneedle device can have the potential to meet many of the requirements for an effective delivery device.

The overall objectives of this research are to (1) determine the feasibility of a hollow microneedle to deliver into the suprachoroidal space, (2) characterize the spread of injected fluids within the suprachoroidal space, and (3) determine the clearance of materials injected into the suprachoroidal space in vivo. Accordingly the main body of the thesis is divided into three parts:

1. Demonstrate the feasibility of a hollow microneedle to deliver fluids and particles into the suprachoroidal space using hollow microneedles in vitro and characterize the important parameters for delivery
2. Develop an effective in vivo device to inject into the suprachoroidal space and characterize the spread of the injected material in the suprachoroidal space.
3. Determine the in vivo clearance of small molecules, macromolecules and particles from within the suprachoroidal space and demonstrate effective targeting as compared to conventional delivery.

CHAPTER 2

BACKGROUND

2.1 Anatomy of the Eye

The eye is carefully organized to allow light transmission in order to provide sight. (Figure 2.1.1) The tissues and fluids that make up the eye are centered on this function as well as the need to keep the eye free from disease. The front surface of the eye is bathed with a multilayered tear film designed to keep the surface of the eye wet and foreign particles from remaining on the eye. It is slowly flowing and is drained through the nasal lachrymal duct, upon blinking. (Zignani et al 1995) These natural functions of the eye are key barriers preventing many topically applied drugs from reaching their targets in the eye. The cornea is essentially the transparent window in which most of the refractive power of the eye lies. The size and arrangement of the collagen fibers that make up the bulk of the cornea are the key to its transparency. It contains an epithelium and is divided into five layers, the bulk of which is the stroma. (Meek and Fullwood 2001)

The sclera, which is considered to be the white of the eye, makes up the remaining periphery portion of the eye and is continuous with the corneal stroma. The sclera is also made up primarily of collagen fibers, but their arrangement is quite different than the cornea. The corneal stroma is characterized with more uniform collagen fibril diameters and an ultrastrustructure that is more regularly packed than the sclera. (Meek and Fullwood 2001) On the surface of the sclera is the conjunctiva which contains tiny blood vessels which are normally invisible but become obvious when the eye is irritated. The front portion of the eye (anterior segment) can be loosely defined as the portion of the eye anterior to the lens. This is made up of primarily the cornea, iris, pupil, aqueous humor, and lens. The anterior segment that holds the aqueous humor is further divided in anterior and posterior chambers. (Kaufman and Alm 2002) Aqueous humor is generated from the ciliary body and excreted into the posterior chamber and

eventually flows into the anterior chamber. It is drained through the trabecular meshwork and Schlemm's canal. This maintenance of the flow is critical in controlling the intraocular pressure. (Brubaker 1982)

The structures behind the lens make up the posterior segment of the eye. The bulk of the posterior portion is made of a clear gel called the vitreous humor which resides in the vitreous chamber, and makes up nearly 80% of the volume of the eye. The vitreous bathes one of the most important layers for vision, the retina. The retina lines 2/3 of the circumference of the posterior eye and provides the photochemicals and neurological connections for processing light to the visual cortex and converting it into vision. The central region of the retina, located in the back of the eye near the optic disc, is the macula. The macula is approximately 1.5 mm in diameter and the center of the macula which provides the clearest vision is the fovea. (Kaufman and Alm 2002)

The layer directly above the retina is the choroid. The choroid is a large network of blood vessels whose purpose is to provide nourishment to the photoreceptors present in the retina. The choroid along with the iris and ciliary body make up what is called the uvea. The layer above the choroid is the sclera, whose primary purpose is structural. It provides the housing for the contents of the eye and a protective function. The densely packed collagen fibers that make up the sclera play an important role in this function. The sclera is hydrated and its elastic nature allows for deformation of the tissue without being punctured. (Lens et al 1999)

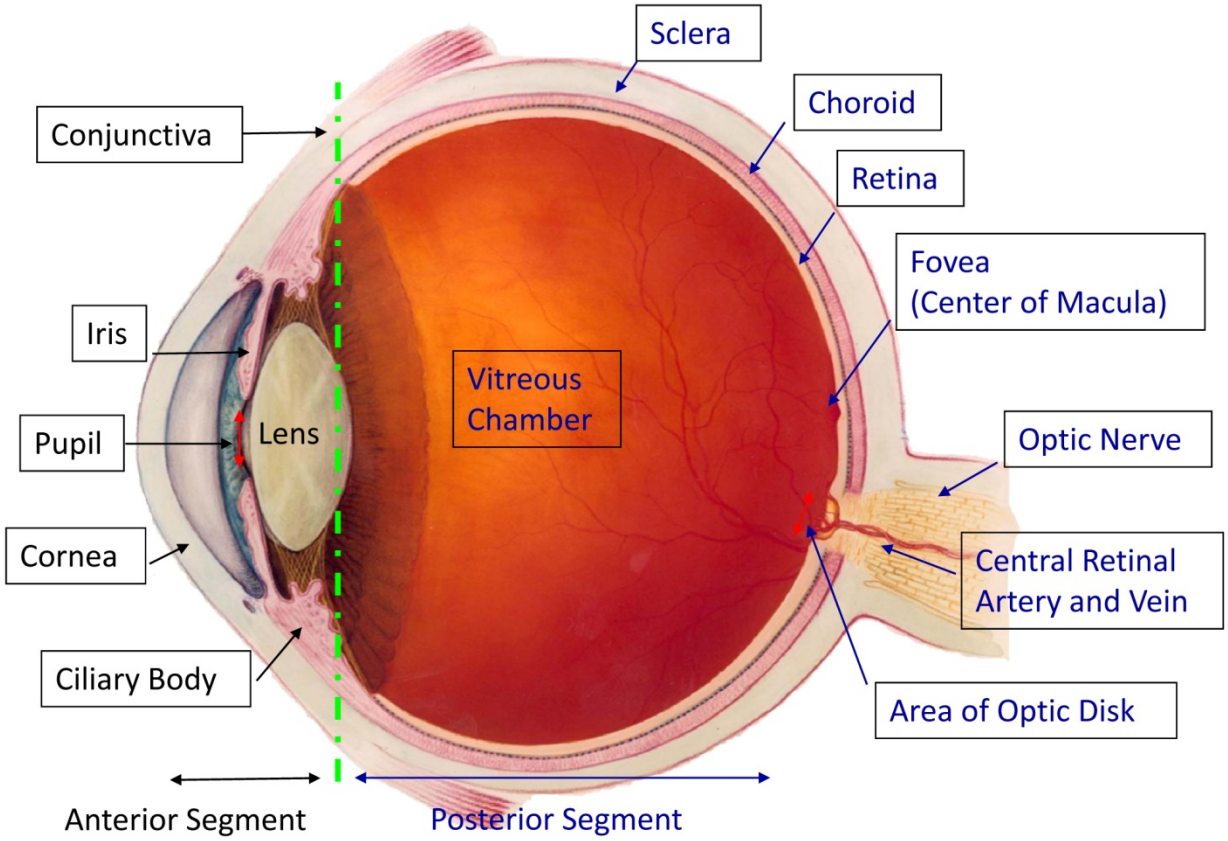

Figure 2.1.1 Image of the anatomy of the eye highlighting the major tissues. Image of the eye was adapted from National Eye Institute, National Institutes of Health, with permission.

One important region of the eye to highlight is the suprachoroidal space. The suprachoroidal space is a virtual space in the eye that becomes evident when there is fluid buildup between the sclera and choroid layers of the eye (Emi et al 1989, Krohn and Bertelsen 1997). Figure 2.1.2 shows the location of this region within the eye. This region is particularly attractive because it can accommodate a fluid and it is adjacent to the choroid and retina. These two tissues are the targets for many diseases such as age related macular degeneration, uveitis, and diabetic retinopathy which lead to blindness. The suprachoroidal space is often associated with the drainage of aqueous humor from the anterior portion as it is part of the uveoscleral outflow system (Krohn 2004). It is most often relevant in cases where there is fluid buildup in the suprachoroidal space as a result of complications from vitreoretinal surgery. In

standard cases the fluid is drained from the eye naturally and the choroid and retinal layers return back to their original position. In severe cases a choroidal hemorrhage may develop and surgical intervention may be necessary. (Healey et al 2007)

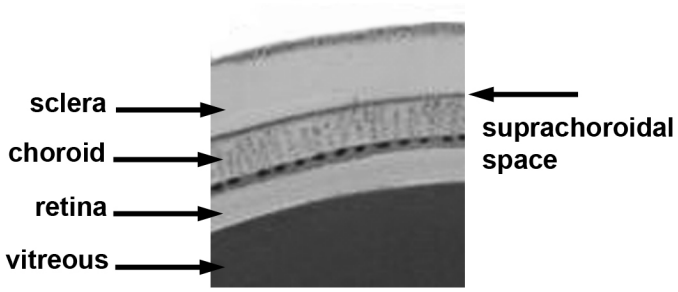

Figure 2.1.2 The suprachoroidal space is located between two posterior tissues, the sclera and choroid. This region expands when there is a buildup of fluid between these two layers to form the suprachoroidal space. Image of the eye was adapted from National Eye Institute, National Institutes of Health, with permission.

2.2 Eye Diseases

2.2.1 Introduction

Blindness and low vision are significant impairments affecting the adult population. One in 28 Americans over the age of 40 suffers from some sort of visual impairment. The prevalence rates of visual impairment increase with age and because of an increasing elderly population, effective treatment of these diseases is a growing need. The most common diseases that cause visual loss are age related macular degeneration (AMD), glaucoma, diabetic retinopathy, and cataract formation (Congdon et al 2004). Below is a summary of these diseases and their treatment modalities.

2.2.2 Glaucoma

Glaucoma is a disease that occurs when there is a disruption in the production and/or drainage of aqueous humor in the eye. The aqueous humor is

in the anterior portion of the eye and is produced by the ciliary body. (Lee and Higginbotham 2005) The fluid flows around the iris and through the pupil into the anterior chamber and out through drainage canals located in the trabecular meshwork. When either too much fluid is produced or not enough is drained, the buildup causes the internal pressure in the eye to become elevated. As a result, glaucoma is marked by an increase in eye pressure. If this imbalance goes untreated, vision will be negatively impacted. (Brubaker 1982)

There are various medications for glaucoma aimed at controlling the fluid flow and most come in the form of topically applied drops. The target for many of the drugs lies in the area of drainage of the aqueous humor (trabecular meshwork) or the production of the aqueous humor (ciliary body). (Alward 1998) The flow and pressure must be maintained at a normal level at all times in the eye and so ideally drug concentrations should be maintained at a therapeutic level in these areas for an extended period of time. Unfortunately topical eye drops are currently the standard method of delivery of medication and usually require a dosing regimen of multiple times a day. (Lee and Higginbotham 2005) This can often lead to non-compliance and poor management of intraocular pressure. When medications are not able to control this, surgery may be necessary. (Clement and Goldberg 2011) Inadequate control of glaucoma over a long period of time can have serious consequences to vision. The pressure has an impact on all the tissues in the eye and is a major cause of optic nerve damage. The need for proper management of glaucoma is immediate as it is one of the leading causes of blindness in United States. (Wax et al 2002)

2.2.3 Age Related Macular Degeneration (AMD)

Age related macular degeneration is a disease that affects the central part of the retina, the macula. Light is focused onto this region of the retina and provides central vision. Any alteration to the macula is detrimental to central field of vision. ARMD is separated into two types: wet and dry. The wet form occurs when blood vessels leak near the macula and scarring develops altering the macula and preventing clear vision. Dry AMD occurs when cells of the retina

begin to die and the retina begins to thin. Unfortunately no therapy is available for the dry form of ARMD, however the wet form usually involves the use of laser therapy to prevent blood leakage into the retina. Intravitreal injections can also be made to target the drug towards the retina. Current research involves looking at a variety of drugs to combat the growth and leakage of blood vessels. (Ozkiris and Erkilic 2005)

Pegaptanib sodium, which is marketed as Macugen® was the first drug to be approved for intravitreal injection for the treatment of ARMD. Clinical trials have showed effectiveness of the aptamer at preventing further degradation of vision as compared to a sham. (Fattal and Bochot 2006) Since then other anti-VEGF drugs have gained attention. Most notably is ranibizumab, or Lucentis®, which was approved in 2006 for AMD. This is a humanized antibody fragment specifically designed for ocular therapy. Though not approved for ocular therapy, the complete human antibody has also gained interest. Bevacizumab , or Avastin®, is cheaper and doctors have been looking to it as an alternative to the more expensive therapy of Lucentis. (Steinbrook 2006)

Other drugs include corticosteroids such as triamcinolone acetonide. (Myles et al 2005) Choroidal neovascularization also develops in many patients with wet ARMD. Here blood vessel growth in the choroid becomes abnormal and penetration of blood vessels into the retinal space causes vision impairment. The targets for many of the drugs that are prescribed for these conditions are the choroid and retina which are in the posterior portion of the eye. (Kimura et al 2001)

2.2.4 Diabetic Retinopathy

Diabetic retinopathy causes damage to the retina as a result of diabetes. High sugar levels in the blood cause changes in the blood vessels in the retina which either leak (non-proliferative diabetic retinopathy) or cause abnormal growth (proliferative diabetic retinopathy). Both forms of the disease have the potential to cause total blindness and because the number of people with diabetes is on the rise, there is a need for effective treatment of this disease.

(Ockrim and Yorston 2010) Almost half of the world's diabetic population has some degree of diabetic retinopathy. Among those, diabetic macular edemea is the leading cause of blindness. Current treatment involves the use of laser therapy or a surgical procedure called vitrectomy. These are usually performed well after the establishment of diabetic retinopathy and, as a result, earlier treatment with medication is desired. (Mohamed et al 2007)

Research involving the use of antiangiogenics, steroids and neuroprotectants is underway and an effective delivery method may play an important role in the success of these medicines. Many of the drugs used are similar to those for AMD. Current studies with small populations involve intravitreal injections occurring every month for a period of six months or as necessary. Follow up and maintenance is a key to controlling the extent of the disease. A minimally invasive delivery method would allow for flexibility in dosing regimen as individual response to the drug may vary and will depend on the current extent of the disease. (Hughes et al 2005, Avery et al 2006, Chun et al 2006)

2.3 Ocular Drug Delivery Methods

2.3.1 Introduction

The eye is an intricate organ that can develop diseases that impact various structures or functions of the eye. As a result, drugs need to reach different portions of the eye depending on the disease and the mechanism of action of the drug. An effective drug delivery system for the back of the eye should embody four general characteristics. First, it should be minimally invasive and safe, so as to avoid complications caused by the procedure. Second, the drug should be administered in such a way that it is well targeted to the desired tissues and limit exposure to other regions of the eye. This would allow for high bioavailability while reducing adverse events and toxicity in surrounding tissues. Third, it should be capable of sustained delivery of the drug to reduce the frequency of administration and allow for better therapeutic control. Finally,

administration of the drug should be as simple as possible, requiring only a routine office visit or, ideally, permitting self administration. A simple, reliable procedure can help reduce errors and compliance problems. Current methods of drug delivery to the posterior segment cannot meet all of these requirements. Below is a short review of ocular delivery practices and current research aimed at increasing the effectiveness of these methods/technologies. Figure 2.3.1 shows some local ocular drug delivery methods for the back of the eye that are either currently practiced or under research.

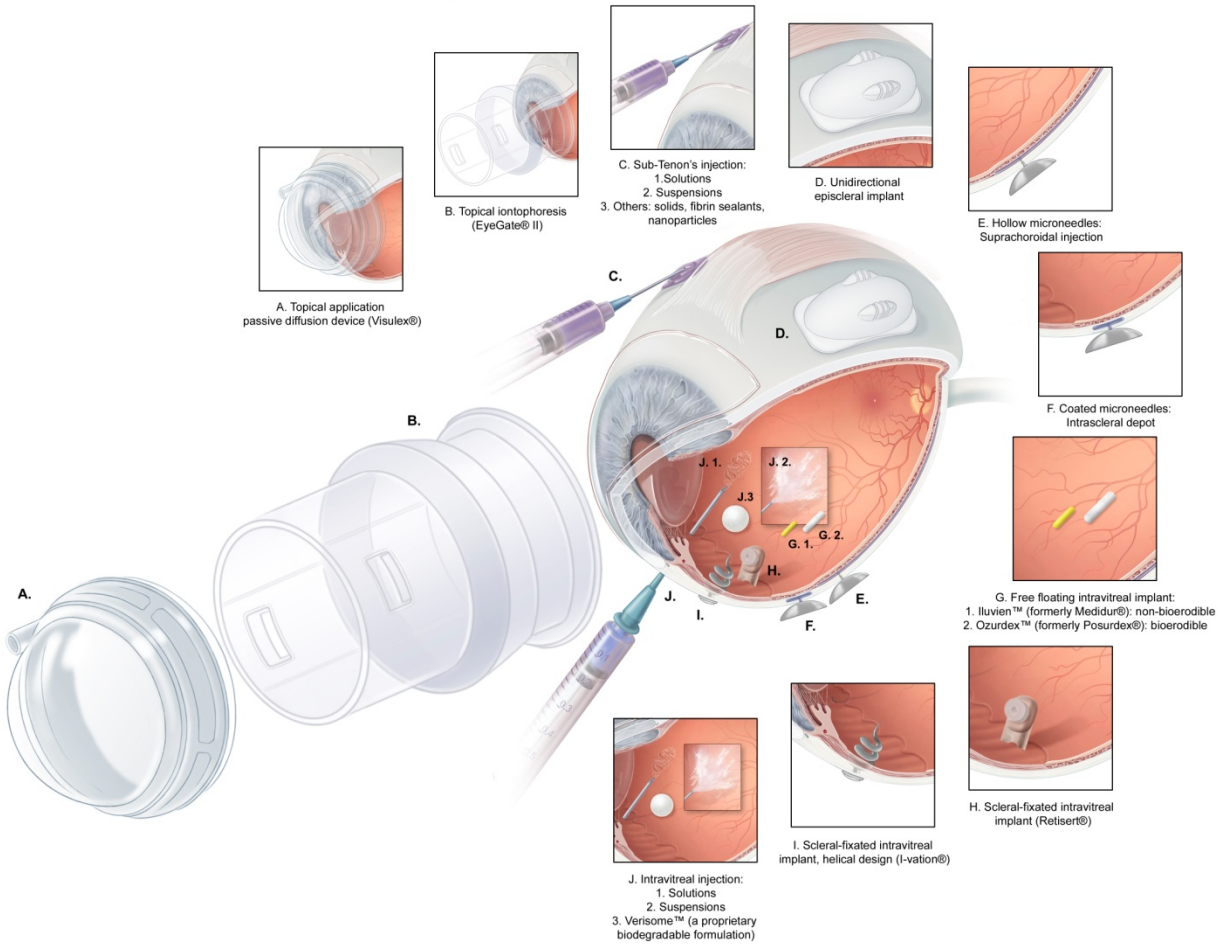

Figure 2.3.1 Local drug delivery methods to the back of the eye. There are a variety of ways to locally deliver drugs to the back of the eye. Some of these approaches are highlighted above: (a, b) topical, (c, j) injections, (d, g, h, i) implants, and (e, f) microneedles. (Edelhauser et al 2010)

2.3.2 Systemic

Systemic administration of drugs is one of the easiest ways to deliver a drug to the body. However, this method provides little room for targeting the drug to a specific region of the body. As a result, for targeted delivery to regions of the eye, systemic administration can be considered ineffective. Systemic administration often requires high doses of the drug to be taken and side effects are more common as tissues other than the eye will be exposed to the drug. In addition toxicity concerns can arise from periodic systemic administration as a drug may accumulate in an undesired part of the body. For example, carboplatin is a drug administered systemically for treatment of retinoblastoma. The target is in the eye, however the drug has a tendency to accumulate in other tissues in the body, raising toxicity issues. Often in systemic administration, more of the drug will reach unwanted areas of the body as opposed to the desired target. (Myles et al 2005)

A drug administered systemically has potential to reach the anterior portion of the eye through leaky vessels in the ciliary body. The drug can then diffuse through the iris and into the aqueous humor. Hydrophilic drugs are more likely to diffuse across the blood-aqueous barrier and reach the anterior chamber whereas lipophilic drugs are more likely to reach the posterior chamber of the aqueous humor. (Gaudana et al 2010)

Access to the posterior of the eye is limited by the blood-retinal barrier. Lipophilic molecules have some ability to move across both the outer and inner blood-retinal barriers. Examples include chloramphenicol and benzyl penicillin, which have been shown to achieve appreciable levels within the aqueous humor after systemic delivery. The tight junctions of the blood-retinal barrier prohibit much of the paracelluar transport that hydrophilic drugs rely upon. As a result hydrophilic drugs have little chance to reach the vitreous humor of the eye after systemic delivery without some active transport mechanism existing within the eye. (Hughes et al 2005)

2.3.3 Extraocular Approaches

2.3.3.1 Topical

One of the most common local methods of delivering a drug into the eye is to simply apply it topically, i.e. directly onto the surface of the eye. Topical application of the drug is often used because it is a noninvasive, convenient procedure and the surface of the eye is easily accessible. Topical administration of drugs on the surface of the eye has been around since the late 1800's in part because the method is fairly simple and can be performed by most patients without supervision. (Koevary 2003) However, there are many barriers preventing a drug that is applied to the surface of the eye from reaching the inner components of the eye. The natural reflex of blinking washes away much of the applied formulation from the surface of the eye. Tear flow on the surface of the eye also contributes to the removal of the drug from the eye surface. As a result, the drug formulation is rapidly eliminated through the nasolacrimal drainage system or simply from spilling out onto the face. In most cases little drug remains on the surface of the eye from a typical eye drop five minutes after application. (Eljarrat-Binstock et al 2010) The tear fluid itself is a dual layer system with an outer lipid layer and an inner aqueous-mucin layer. The mucin layer prevents many foreign particles from adhering to the surface of the eye to prevent infection and keep the vision pathway unobstructed. Unfortunately, from a drug delivery standpoint, this is a disadvantage because this means that drugs will not be able to reside on the surface of the eye for very long and frequent or multiple administration of drops is often necessary. (Koevary 2003)

Any amount of drug that is able to remain on the surface of the eye must then penetrate further into the eye by diffusing across the cornea and/or conjunctiva. A drug that penetrates through the corneal pathway can then reach the aqueous humor and be able to reach targets that are in the anterior portion of the eye. The cornea is however, composed of multiple layers and their barrier properties limit permeability of many compounds across its thickness. (Jarvinen et al 1995) This is particularly true for hydrophilic drugs. The conjunctiva, though,

may allow for higher permeability of these hydrophilic drugs as the tight junctions in the conjunctiva are not as tight as the cornea. Unfortunately many drugs get absorbed by the vasculature in the conjunctiva and the drug gets taken into systemic circulation. The bioavailability of drugs is not just dependant on the ability of the drug to reside on the surface but also dependant on the drug's ability to diffuse across these surface tissues. Various other barriers exist, preventing many drugs from reaching therapeutic concentrations further along the vision pathway. The combination of these barriers result on average to less than five percent ocular absorption of a drug applied in this manner. Practically speaking, topical drug delivery is then only effective for delivering drugs to the anterior portion of the eye. (Jarvinen et al 1995, Koevary 2003)

Current research in topical drug delivery has been aimed at countering the eye's barriers and increase the bioavailability of topically applied drugs. These efforts are aimed primarily at either increasing the permeability of the drug across the cornea or increasing the residence time of the drug.

Increasing permeability across the cornea can be done by adding penetration enhancers to the topically applied formulation. One class of penetration enhancers alters the structure of the cornea to allow for greater penetration of the drug. Examples include azone (laurocapam), hexamethylene lauramide, hexa-methylene octanamide, and decylmethyl sulfoxide. Use of these enhancers should however be done in caution as they can often cause irritation and permanent damage to the cornea can develop. Repeated use, from frequent application, can also lead to toxic levels of the enhancer with the eye. (Kaur and Kanwar 2002)

An alternative approach has been to increase the solubility of the drug at the cornea surface through the use of cyclodextrins. (Loftssona and Jarvinen 1999) Cyclodextrins increase the water solubility of lipophilic drugs providing a more stable environment in the tear film and are also shown to decrease irritation. Cyclodextrins have been shown to increase the permeability of steroids such as dexamethasone and hydrocortisone in addition to carbonic anhydrase inhibitors and cyclosporins when co-administered in a topical formulation.

Cyclodextrins may act as true carriers of lipophilic molecules in the hydrophilic tear film; i.e. they increase the amount of drug available at the tear film-corneal epithelium interface without actually causing any disruption of the corneal epithelium. (Loftssona and Jarvinen 1999, Stefansson and Loftsson 2002)

Another approach to increase absorption of topically applied drugs is to increase the residence time of the drug on the corneal surface. A formulation applied to the surface of the eye that has a high viscosity will not easily be washed away and thus will reside on the surface of the eye longer than traditional drops. This would allow more time for a drug to penetrate. (Kaur and Kanwar 2002) High viscosity solutions, however, can be hard to apply and may cause increased blinking and irritation, decreasing their effectiveness. Recently, formulations that can gel in-situ, i.e. form viscous gels upon application to the eye, are of interest. Gelling can be activated by the pH, temperature, or electrolytes present on the surface. (Ludwig 2005) These are advantageous because they can be easily administered and have minimal side-effects. (Zignani et al 1995) Products currently utilize the enhanced viscosity and in-situ gelling concepts are currently available. (Saettone and Salminen 1995)

An alternative way to increase the residence time is to use films or inserts. These can be placed on the surface of the eye to provide constant contact without being washed away. Films can come in the form of contact lenses with drugs loaded inside that can be released to the surface of the eye or drugs trapped between the lens and the surface of the eye. This introduces some versatility in design and can lead to a variety of sustained release scenarios. Inserts can be designed to sit under the lower eye-lid, so as not to obstruct vision and allow constant contact with the surface of the eye. However, films and inserts may not be properly applied by patients such as the elderly and may also result in non compliance. In addition continual use may introduce complications to the surface of the cornea. (Saettone and Salminen 1995)

2.3.3.2 Iontophoresis

Ocular iontophoresis has become a popular research area to combat the poor bioavailability of topically applied drugs. The basic idea is to apply a drug topically to the surface of the eye and hold it there using a cup like device while applying an electric field across the surface tissues, which is usually the cornea or conjunctiva/sclera. Iontophoresis can enhance transport using any of three possible mechanisms: electrophoresis, electroosmosis, and electroporation. The main attraction to this approach is that it is minimally invasive and locally applied. However high current densities may cause tissue damage. The development of a proper formulation is important for iontophoresis to be effective. Two commercial products have been developed with formulations specific to iontophoresis application to the eye: Ocuphor (Iomed Inc.) and Visulex (Aciont Inc). A variety of drugs have been tested for this delivery method including antibiotics, corticosteroids, and nanoparticles. (Eljarrat-Binstock et al 2010)

2.3.3.3 Periocular Routes

Periocular delivery usually refers to delivery into the eye across peripheral tissues of the eye. An injection can be one method of delivering periocularly. There are several different types of periocular injections, but the term refers in general to injection where the delivery site is on the periphery of the eye. Common periocular injections include posterior sub-tenon, retrobulbar, subconjunctival, and peribulbar. A sub-tenon or subconjunctival injection involves injecting in the sub-tenon space or just under the conjunctiva. Retrobulbar injections require injecting behind the eye, near the optic nerve. This is a fairly invasive procedure and requires inserting the needle fairly deep in order to reach the posterior of the eye. Peribulbar injections are injections that occur on the periphery of the eye and are similar to sub-tenon injections, except the delivery is not specific to the tenon space. The use of these injections is not a common way to deliver drugs to the body. Instead they find their use in specific cases. As an example, retrobulbar and periocular injections are often used for ocular anesthesia prior to surgery. (Raghava et al 2004, Lai et al 2005)

Periocular delivery can also occur with implants. The implanted device must be attached onto or through the periocular surface of the eye. The primary advantage of these systems is sustained delivery for an extended period of time. The drug release rate controlling material is often polymeric and these can be divided into degradable or non-degradable. Degradable implants offer the advantage of not having to go through a removal procedure. On the other hand, non-degradable implants offer better control of the release rate of the drug. Thin implants can be placed just under the surface of the eye between the conjunctiva and sclera. (Felt-Baeyens et al 2006) Implants can also be made to penetrate across the ocular tissues into the vitreous and deliver drugs directly into the vitreous. These implants are often placed on the surface of the sclera and so transport across the sclera and into the choroid and retina become important in determining the effectiveness of the implant. (Kuppermann 2007)

2.3.4 Intraocular

Even with these advancements, drugs applied topically exhibit very little absorption for drug delivery to the back of the eye. Many diseases affect the retina, choroid, macula, and other regions that are in the posterior portion of the eye. To treat these areas, the aforementioned delivery methods are usually ineffective and not targeted for this purpose. As a result intraocular approaches, approaches that try to place the drug directly within the eye, can be more efficient at getting drugs to intraocular tissues. Provided below are examples of methods specifically motivated at delivering drugs to areas in the posterior portion of the eye.

2.3.4.1 Intravitreal Injection

Intravitreal (IVT) injection is one of the most direct ways to deliver a drug to the posterior portion of the eye. The first reported use of an intravitreal injection was as early as 1911. Air was injected as an attempt to decrease the potential of retinal detachment. Injection of a pharmaceutically active compound however, took some time to come into practice. It wasn't until the late 1970's and

1980's that drugs were being tested on an individual basis in humans. Not until 1998 was a drug approved by the Food and Drug Administration (FDA) specifically for intravitreal injection. This drug was fomivirsen sodium used to treat cytomegalovirus and represented a breakthrough for this delivery method. (Jager et al 2004)

Currently IVT injections are being used for the treatment of AMD with the injection of Macugen, Avastin, and Lucentis. The procedure involves only local anesthesia such as lidocaine. The injection is performed with a 27 or 30 gauge needle approximately 3 mm from the limbus (i.e. where the cornea meets the sclera). The needle is inserted until it penetrates into the vitreous chamber, a small volume is injected into the vitreous and the needle is then retracted. The injected volume can range anywhere between 20-100 μL. (Maurice 2001, Avery et al 2006) Since the injection involves penetrating several tissues before reaching the vitreous and the injection of a relatively large volume of fluid into the eye, it is not without risks. The two most important safety concerns from IVT injections are the actual injection procedure and the toxicity of the drug in the vitreous. Ophthalmologists were reluctant at first to use this procedure for exactly these reasons. (Peyman and Ganiban 1995) It is also important to separate these two factors from each other when patients develop retinal detachment or endophthalmitis post injection.

A review of IVT injections was performed by Jager et. al. in an effort to determine how serious these risks are to the patient. They discovered by examining 14,866 IVT injections over 4,382 eyes resulted in a prevalence of endophthalmitis at a rate of 0.3% per injection and 0.9% per eye. Other complications such as retinal detachment, iritis, cataract formation, etc. were more commonly associated with the drug rather than the actual injection method. Nevertheless they caution that it is very important that the proper technique be followed because when complications do arise from this delivery method, they may lead to permanent vision loss. (Jager et al 2004) It is important to note, however, that the per eye rate is higher than the per injection rate, indicating that when multiple injections are necessary, the risks to damage can rise

considerably for any given patient. Since it is not uncommon to have monthly injections of the above mentioned drugs, one can imagine the risks for complications can become a serious concern and long term delivery by this method can prove to be dangerous.

2.3.4.2 Intravitreal Implants

In an effort to provide controlled or sustained release to the back of the eye, much of the research has focused on designing implants that release drug into the vitreous. A number of commercial products have recently been marketed that can provide drug delivery for a period of weeks to months. Examples include Medidur, Vitrasert, Retisert, Ozurdex (formerly Posurdex) etc. Many of these products are implants that are placed either directly in the vitreous or attached to the globe so that the drug formulation is released into the vitreous (Lee et al 2010, Yasukawa and Ogura 2010). These implants have shown well controlled release kinetics in-vitro and in some cases in animal models as well. Implants such as Medidur, Vitrasert and Retisert are nonbiodegradable and have to be removed once the drug formulation has been fully released from the device. Osurdex is a biodegradable implant that does not have to be removed at the end of the release of the drug (Kane et al 2008, Chang-Lin et al 2010, Kuno and Fujii 2010).

2.3.4.3 Suprachoroidal Delivery

In the past few years researchers have begun to explore administration into the suprachoroidal space. The first group of researchers to look at the suprachoroidal space from a drug delivery perspective showed that a transparent viscous gel made from a polymer, polyorthoester (POE), could be injected into the suprachoroidal space of pigmented rabbits. They examined the safety of their ‘tunneling’ procedure and of the POE in the space. The POE was present in the space for up to 3 weeks and the procedure and the material was well tolerated by the rabbits (Einmahl et al 2002). Others have shown that the space can be accessed by constantly infusing into the sclera. A commercially available

magnetic resonance imaging (MRI) contrast agent, Magnevist®, was infused into the eye. Magnevist consists of a Gd-DTPA which is a soluble gadolinium complex of diethylenetriamine pentaacetic acid of approximately 1 kDa in size. Magnetic resonance imaging imaging of Intrascleral infusions of Gd-DTPA showed that Gd-DTPA accumulated in the suprachoroidal space and was cleared within hours. (Kim et al 2007)

More recently a cannulation device has been developed that can be inserted into the suprachoroidal space after an incision into the sclera is made. The long cannula can be inserted from the site and slid to a more posterior site after which an injection can be made to deliver a formulation into the suprachoroidal space (Olsen et al 2006). Sustained release implants have also be inserted just underneath the sclera into horses to show treatment of uveitis for periods of up to 2 years. Sustained delivery of cyclosporine to suprachoroidal space showed drastic improvement in the visual acuity of the horses with minimal side effects, demonstrating the potential for treatment of choroidal and retinal diseases. (Gilger et al 2006)

2.4 Microneedles and Their Applications in Drug Delivery

2.4.1 Introduction

The term microneedle does not represent a singular device or design of a needle but is instead a term used to describe a class of micrometer scale needles that can be used in a variety of ways to deliver drugs locally to the body. Microneedles can be made from a variety of materials, such as metals, glass and plastics and they can be designed in various shapes. However, the overall purpose of all microneedles remains similar: microneedles pierce into a tissue to create micron scale pores or channels through which therapeutics can be transported more effectively into the body than without such pores or channels. We present in this section four general approaches to using various types of microneedles to deliver molecules into tissues. Microneedles were first envisioned for application to the skin and as a result many of these strategies

were developed with the skin in mind. However all of these approaches are applicable to the eye and may be advantageous depending on the target tissue and necessary delivery requirements. A summary of the approaches in a graphical format is shown in Figure 2.4.1 (Arora et al 2008).

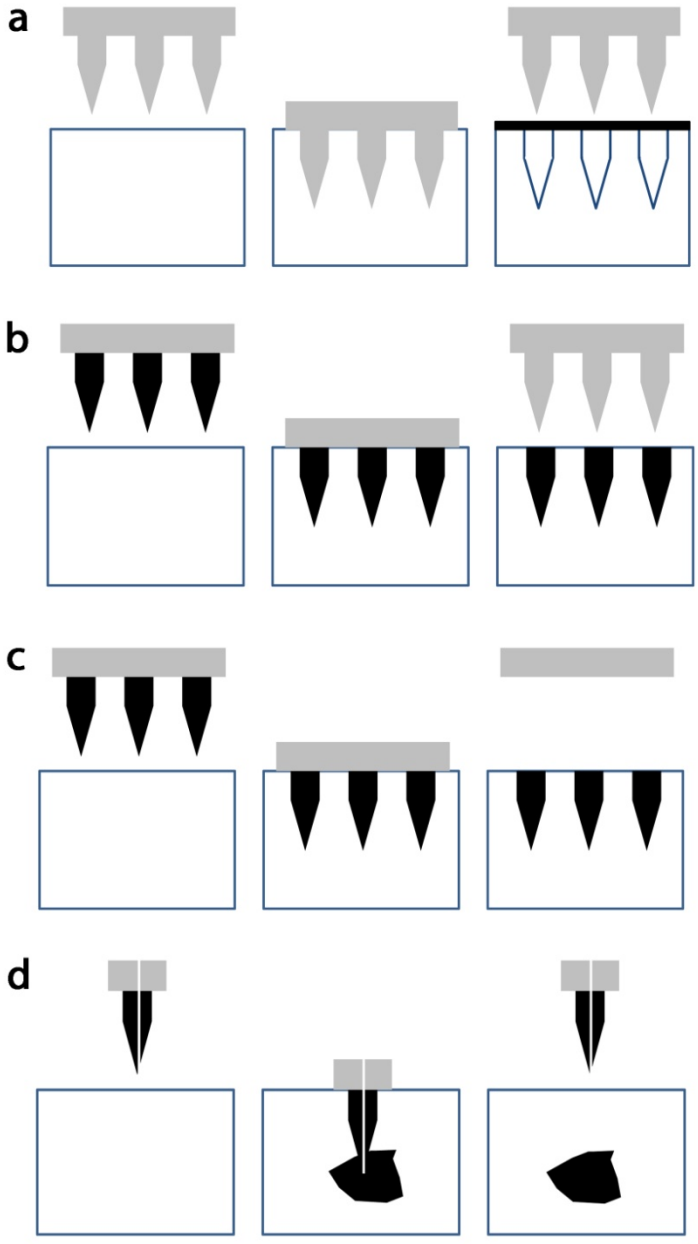

Figure 2.4.1 Microneedle strategies for drug delivery into tissues. (a) Poke and apply: Insert microneedles into the tissue to form pores, remove microneedles and then apply the drug formulation to the surface of the tissue. (b) Coat and poke: Coat microneedles with a drug formulation, insert microneedles into a

tissue to dissolve off the coating formulation within the tissue and remove microneedles to leave the deposited drug in the tissue. (c) Poke and release: Encapsulate drug in a biodegradable microneedle, insert microneedles into the tissue and leave them there, and as the microneedle degrades the drug is released into the surrounding tissue. (d) Poke and flow: Insert a hollow microneedle into a tissue, apply pressure to the fluid in the microneedle to flow the fluid into the tissue, and remove hollow microneedle after the desired volume has been injection, leaving behind fluid in the tissue. Adapted from Arora et al 2008.

2.4.2 Poke and Apply

One microneedle strategy is to simply insert solid microneedles into a tissue and remove the microneedles leaving behind channels or pores that make the tissue more permeable. A therapeutic agent can then be applied to the surface of the microneedle treated tissue. This makes the delivery a two step procedure; the first step is the creation of the channels followed by a second application of the formulation to be delivered. With this approach the microneedles serve primarily to create a transport pathway and do not come into contact with the drug formulation.

One of the first reported studies showed that microneedles made of silicon using microfabrication technologies borrowed from the microelectronics industry showed that holes created by microneedles could increase the permeability of human epidermis to calcein by four to five orders of magnitude (Henry et al 1999). Additional experiments using a similar strategy showed that pores created by microneedle could increase the permeability of larger compounds such as insulin, bovine serum albumin (BSA), vaccines and nanospheres up to 50 nm in radius (McAllister et al 2003, Martanto et al 2004, Ding et al 2009). Many of these early studies showed that microneedles could create pores to enhance the delivery of many compounds that would otherwise not be deliverable through the skin.

This strategy can be applied to the ocular tissues as well. Solid microneedles can be inserted into tissues such as the sclera, cornea, near the limbus, or near the target area and removed after creating pores. Solid microneedles have been shown to pierce the sclera tissue and create pores

within the sclera (Jiang et al 2007). Topical drops could then be applied to the surface of the eye. The pores would allow enhanced diffusion of the applied molecule and increase the bioavailability of the drug. However, unlike the skin, the residence time of most topical applications is on the order seconds to minutes (Zignani et al 1995). The short contact time makes this approach less advantageous.

2.4.3 Coat and Poke

A strategy that makes the delivery process a single step procedure is the coat-and-poke approach. This approach requires the drug formulation to be coated on the surface of a microneedle. Upon insertion of the coated microneedle into a wet tissue, the coating formulation dissolves off of the microneedle and the microneedle can be removed, leaving the coating formulation inside the tissue within the channels created by the microneedle. This allows for the drug to be localized just at the insertion site. Coated microneedles can provide targeted delivery to tissues such as the sclera, cornea, or any part of the eye that can be accessed directly for the exterior of the eye. This can be done with individual microneedle insertions or an array of microneedles inserted simultaneously into the desired tissue.

The cornea is often treated as a barrier to drug delivery. This is especially true when glaucoma is treated using drops on the surface of the eye and the drug needs to be delivered to tissues further within the eye. However, if drugs can be delivered directly to the corneal stroma, i.e., intrastromal delivery, it can be used advantageously for drug delivery. The approach is to coat the surface of the solid microneedle with a model compound, insert it into the wet cornea environment, allow the coating to dissolve off of the microneedle and then remove the microneedle leaving most of the coated formulation within the cornea. Figure 2.4.2 shows a solid stainless steel microneedle before and after a coating of a dye, sulforhodamine.

To test this approach, sodium fluorescein was used as a model molecule and coated on the microneedle. Jiang et al (2007) studied the intraocular

distribution of sodium fluorescein after intrastormal delivery using coated microneedles and showed that this held true. The work showed that microneedles can indeed deliver molecules directly within the corneal stroma in vivo in rabbits. A single solid stainless steel microneedle was coated with 280 ng of sodium fluorescein. The microneedle was inserted into the cornea and the concentration in the cornea, aqueous humor and lens was measured over time in vivo. As a comparison, experiments were also done applying a 3 µg dose of sodium fluorescein topically to the surface of the rabbit eye as a drop and identical measurements were made. (Jiang et al 2007)

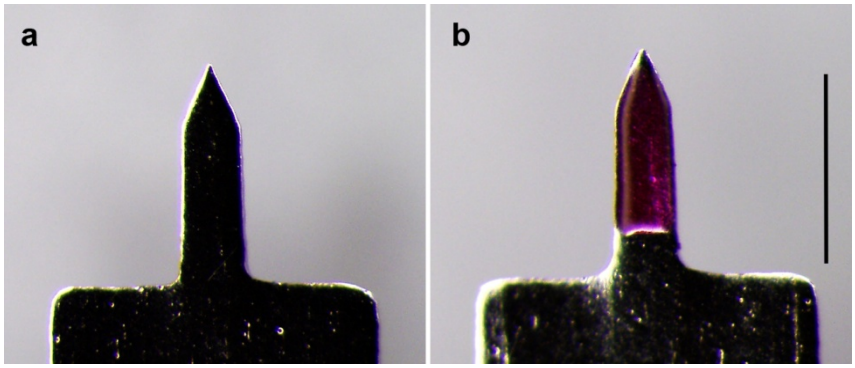

Figure 2.4.2 (a) A brightfield image of a single solid stainless steel microneedle. The surface of the microneedle can be coated with a liquid formulation. (b) As an example, it can be coated with an aqueous formulation of sulforhodamine B (red liquid). Scale bar: 500 µm

The coated microneedle experiment showed that microneedles could be inserted into the cornea and that sodium fluorescein dissolves off the needle creating a depot within the stroma. In addition, sodium fluorescein levels in the anterior ocular tissues were higher than a topical application of an equivalent dose. As an example at the three hour time point, fluorescein concentrations in the eye were about 60 times higher than a topical application of an equivalent dose. The kinetic data also demonstrated that microneedle based administration of fluorescein resulted in extended residence time of fluorescein as compared to topical application. In both cases fluorescein concentrations returned to near baseline levels in the anterior segment within 24 hours. The calculated bioavailability of coated sodium fluorescein delivered to the eye was 69 % with

microneedle administration versus only 1 % for topical administration (Jiang et al 2007). This shows that microneedle administration effectively targeted the cornea while the topical application resulted in nearly all of the fluorescein being washed away from the eye.

These results indicate that coated microneedles should be able to deliver a therapeutically relevant molecule to the cornea and anterior segment of the eye more effectively than topical administration. Furthermore, the targeting capability of microneedles should allow for a high bioavailability of the drug and an enhanced pharmacological effect. In order to test this pilocarpine, a drug used to treat glaucoma, was delivered intrastromally using microneedles. Solid stainless steel microneedles were coated with approximately 1.1 μg of pilocarpine and inserted in the peripheral cornea of New Zealand white rabbits in vivo (Jiang et al 2007). Microneedle based administration of pilocarpine caused the pupil to constrict 2.5 mm within 15 minutes after insertion. A similar dose of pilocarpine, 5 μg, delivered topically cause constriction of only 1 mm. Additionally the pupil began to constrict several minutes earlier when pilocaprine was administered using microneedles. This indicated that the kinetics of microneedle based delivery of pilocarpine is faster than topical. When 500 μg of pilocarpine were applied topically, the pupil constricted a total of 4 mm with kinetics similar to that of 5.5 μg administered using coated microneedles. These experiments showed that a drug can be administered using microneedles and can be targeted by inserting the microneedles within the peripheral cornea (Jiang et al 2007).

This approach relies heavily on the ability to coat a drug on the solid microneedle. As a result the coating formulation plays an important role in obtaining a sufficient amount of drug on a microneedle and having consistent coatings. In experiments studying the aqueous coating of riboflavin it has been shown that the viscosity and surface tension of the coating formulation are two critical parameters. Optimization of the viscosity enhancing agent, CMC, and the surfactant, Lutrol F-68, in the coating solution revealed that uniform and repeatable coatings were achievable (Gill and Prausnitz 2007aa). The coatings were performed using a micro-dip coating procedure that confined the coating to

the microneedle and prevented the substrate from being coated (Gill and Prausnitz 2007b). To confirm this, sulforhodamine was coated onto microneedles using sucrose and Tween 20 as a viscosity enhancer and surfactant respectively. Addition of sucrose to the coating solution increased the thickness of the coating and adding Tween 20 increased the uniformity of the coating. Further work showed that non-aqueous coating formulations can also be applied to microneedles in a similar fashion. However, if solvents, such as ethanol, have low surface tension, then a surfactant may not be necessary (Gill and Prausnitz 2007aa).

A variety of materials can be coated onto microneedles These range from small molecules, to large proteins, and even microparticles (Xie et al 2005, Gill and Prausnitz 2007b). Figure 2.4.3 shows the coating of calcein, vitamin B, bovine serum albumin, plasmid DNA, viruses, and latex microparticles onto solid microneedles (Gill and Prausnitz 2007b). Demopressin, a synthetic peptide hormone, has also been coated onto titanium microneedles (Cormier et al 2004). The ability to coat a wide array of molecules makes this attractive for drug delivery to the eye. Many ophthalmological drugs could be coated onto microneedles and delivered in this fashion for targeted delivery. Pilocarpine has been effectively delivered in this fashion within the stroma of the cornea, but many other drugs could similarly be coated and delivered (Jiang et al 2007). The key to this approach would be to coat a sufficient amount of drug on a microneedle or small array of microneedles to provide a therapeutic benefit.

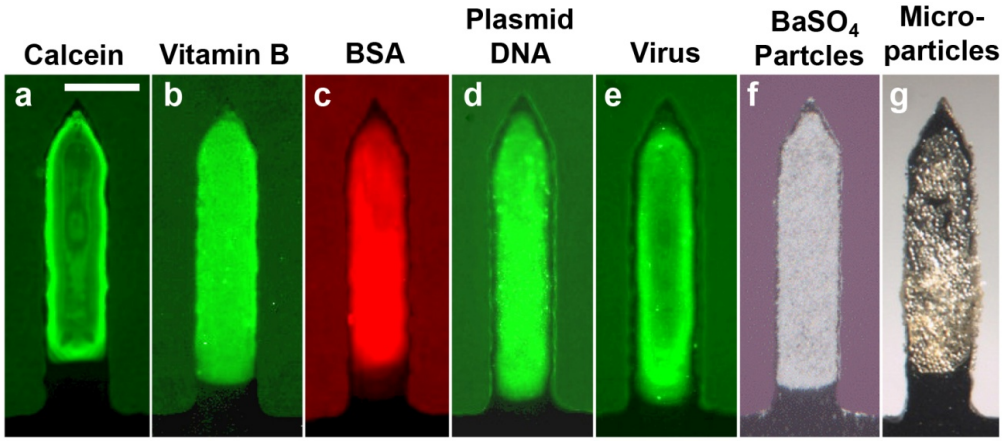

Figure 2.4.3 Brightfield and fluorescent images showing the variety of materials that can be coated onto solid stainless steel microneedles: (a) calcein, (b) vitamin B, (c) bovine serum albumin conjugated with Texas Red, (d) plasmid DNA conjugated with YOYO-1, (e) modified vaccinia virus - Ankara conjugated with YOYO-1, (f) 1-μm diameter barium sulfate particles and (g) 10-μm diameter latex particles. Scale bar: 200 μm. Adapted from Gill and Prausnitz 2007b.

2.4.4 Poke and Release

Instead of inserting a microneedle, depositing the drug and removing the microneedle, the microneedle itself could be left in the tissue. This approach, the poke-and-release approach, involves loading a drug formulation within a microneedle and leaving the microneedle in the tissue as it releases the loaded drug formulation into the tissue. These microneedles are usually made of biodegradable polymers or sugars that encapsulate a drug and as the polymer breaks down or sugar dissolves it releases the active within the tissue. The added benefit of this approach is that the polymer could control the release of the molecule that is encapsulated within the microneedle and provide sustained release. This would extend the time the drug is within the eye and allow for less frequent administration.

Microneedles made of biodegradable polymers have been shown to successfully insert and deliver molecules into the skin. Park et. al (2005) showed that an array of polymer microneedles can be fabricated using a micromolding technique. Mechanical testing of these microneedles made of biodegradable polylactic and polyglycolic acid copolymers (PLGA) were strong enough to insert into the skin and increase skin permeability of calcein and bovine serum albumin. (Park et al 2005) Microneedles encapsulating small molecules and proteins within PLGA have also been shown to deliver their payload over extended periods of times. As a result, controlled drug delivery is achievable with the microneedles for periods of hours to months depending on the formulation and encapsulation methods (Park et al 2006). It has also been shown that microneedles made of carboxymethylcellulose (CMC) could be designed to insert and degrade in the skin to deliver a drug. Figure 2.4.4 shows a polymer microneedle array made of CMC. A micromolding and encapsulating method was

developed to deliver a model protein, lysozyme into pig cadevar skin. The enzymatic activity of lysozyme after 2 months within the microneedle array was 96 % of the initial activity indicating the processing conditions and microneedle formulation were benign to the enzyme. By encapsulating drug into the backing layer in addition to the microneedle shaft, the microneedles and patch could be used to provide sustained drug delivery (Lee et al 2008). Although these microneedles have not been inserted or tested in eye tissues, they could conceivably be inserted in a similar fashion for ocular drug delivery.

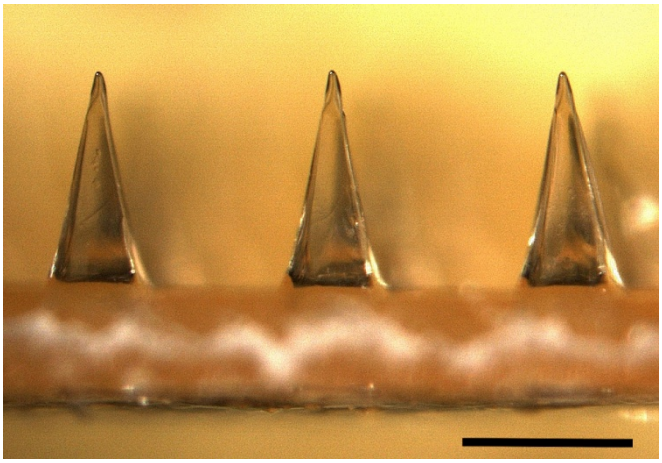

Figure 2.4.4 An array of carboxymethylcellulose (CMC) microneedles of 600 μm in length and a base of 300 μm. Scale bar: 500 μm. Adapted from Lee et al 2008.

2.4.5 Poke and Flow

The poke-and-flow approach to using a microneedle is analogous to the hypodermic needle. A hollow microneedle is inserted within a tissue and a liquid formulation can be injected through the hollow cannula in the microneedle for delivery within a tissue at depths of less than a millimeter. Hollow microneedles provide unique capabilities such as being able to inject formulations and to immediately spread the injected formulation within tissues. This is in contrast to other microneedle designs and approaches which deposit the drug only locally to the insertion site. This is advantageous from two aspects. The most important aspect for the eye is the ability to deliver a drug to a site that is not directly accessible. This is an important element in suprachoroidal delivery because the

microneedle is inserted at an accessible portion of the eye and the formulation is spread within the suprachoroidal space to an inaccessible region further back in the eye. The other important aspect is that a hollow microneedle allows more of a drug to be delivered in a single injection compared to other microneedle strategies. This is because a hollow microneedle simply serves as a conduit for delivery whereas in other scenarios the surface area or volume of the microneedle is limiting the amount of drug that can be delivered from a single insertion.

Fabrication of hollow microneedles can be challenging because an internal bore needs to be created within the structure and this may compromise the integrity of the microneedle. Hollow metal microneedles have been made from micromolding and etching techniques. These techniques can be used to make hollow silicon, nickel, and gold microneedles (Gardeniers et al 2003, McAllister et al 2003). Glass microneedles fabricated using a micropipette pulling techniques have been shown to effectively insert and deliver into skin. Figure 2.4.5 shows a hollow microneedle made from this process. Martanto et al (2006) showed that in addition to microneedle insertion and infusion parameters the tissue itself can be a limiting factor in how much volume can be delivered. Ex-vivo experiments showed that partial retraction of the hollow microneedle aided in infusing fluid into the skin and reducing the compaction of skin that occurs at the site of insertion (Martanto et al 2006). Hollow microneedles have also been shown to deliver insulin into human skin in vivo. Experiments on humans using hollow microneedles showed that delivering a bolus injection of insulin into the dermis were effective at reducing blood glucose levels with kinetics that were faster than equivalent delivery using a catheter (Gupta et al 2009).

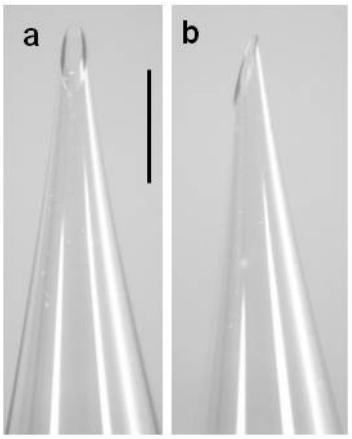

Figure 2.4.5 (a) Front and (b) side view of a single hollow glass microneedle. The microneedle has a beveled tip and an approximately elliptical orifice. Scale bar: 250 μm. Adapted from Jiang et al 2009.

Hollow microneedles may be able to spread a fluid within the sclera collagen matrix and accomplish intrascleral delivery of fluids. The first reported study to show that a hollow microneedle was capable of intrascleral injection demonstrated delivery of a sulforhodamine solution within the sclera of human eyes in vitro. Bare sclera was excised from human cadaver eyes and a hollow glass microneedle was inserted into the sclera and infused with a solution. The delivery and spread of sulforhodamine solution within the sclera showed that a hollow microneedle can inject a solution intrasclerally and target the sclera tissue (Jiang et al 2009).

In addition to injecting a solution intrasclerally, injection of nano or microparticles has also been demonstrated. Nanoparticles of 280 nm in diameter with up to 10 wt. % suspension were injected into the sclera with an applied pressure of 15 psi. Injections were performed in different region of the sclera tissue to determine if a hollow microneedle was capable of injecting nanoparticles into all regions. Hollow microneedles were capable of injecting into all regions of the sclera implying that a hollow microneedle can inject intrascelrally to any site that can be accessible on the eye. However, the spread in the posterior region of the sclera did appear to be over a larger area than the other regions. This showed that nanoparticles could be injected intrasclerally similarly to the way fluids were injected into the sclera (Jiang et al 2009).

However, administration of microparticle suspensions intrasclerally was not as straightforward. Suspensions of microparticles did not flow through the sclera tissue. This is in large part attributed to the spacing of the collagen fibers rather than a limitation on the microneedle capability. The collagen fiber spacing is on the order of several hundred nanometers, and as a result microparticles may not easily flow within this medium (Edwards and Prausnitz 1998). To test this hypothesis two approaches were employed to aid the movement of particles in the dense collagen matrix. One was the use of collagenase to break up the collagen structure and provide larger pathways for microparticles to flow through the sclera. The sclera tissue was either soaked in collagenase prior to injection or the collagenase was co-injected with the microparticle suspension. Both of these steps allowed infusion of the microparticle suspension demonstrating that disruption of the collagen structure allowed microparticle infusion within the sclera. The second approach involved coinjecting hylauronidase, a dispersive agent known to help injectable formulations flow through densely packed tissues such as the skin. Microparticles were also successfully administered using this approach. As a result, incorporation of hylauronidase into a suspension may be a feasible way to deliver controlled release microparticle formulations within the sclera for drug delivery to the back of the eye (Jiang et al 2009).

CHAPTER 3

MATERIALS AND METHODS

3.1 Feasibility of Suprachoroidal Delivery Using a Hollow Microneedle

3.1.1 Materials

Whole rabbit eyes (Pel-Freez Biologicals, Rogers, AR), pig eyes (Sioux-Preme Packing, Sioux Center, IA) and human eyes (Georgia Eye Bank, Atlanta, GA), all with the optic nerve attached, were shipped on ice and stored wet at 4 °C for up to 3 days. Prior to use, eyes were allowed to come to room temperature and any fat and conjunctiva were removed to expose the sclera.

Hollow microneedles were fabricated from borosilicate micropipette tubes (Sutter Instrument, Novato, CA), as described previously (Jiang et al 2009). A custom, pen-like device with a threaded cap was fabricated to position the microneedle and allow precise adjustment of its length. The device was made of aluminum and contained a threaded internal backside. An olive shaped gasket fit into this backside and was attached to a micropipette holder (MMP-KIT, World Precision Instruments, Sarasota, FL) with tubing that was connected to a carbon dioxide gas cylinder for application of infusion pressure. The olive gasket provided a seal between the hollow glass microneedle and the holder. The holder was attached to a micromanipulator (KITE, World Precision Instruments) which was used to control insertion of the microneedle into the sclera. Figure 3.1.1 shows a hollow microneedle held in the device compared to the tip of a 30 gauge hypodermic needle.

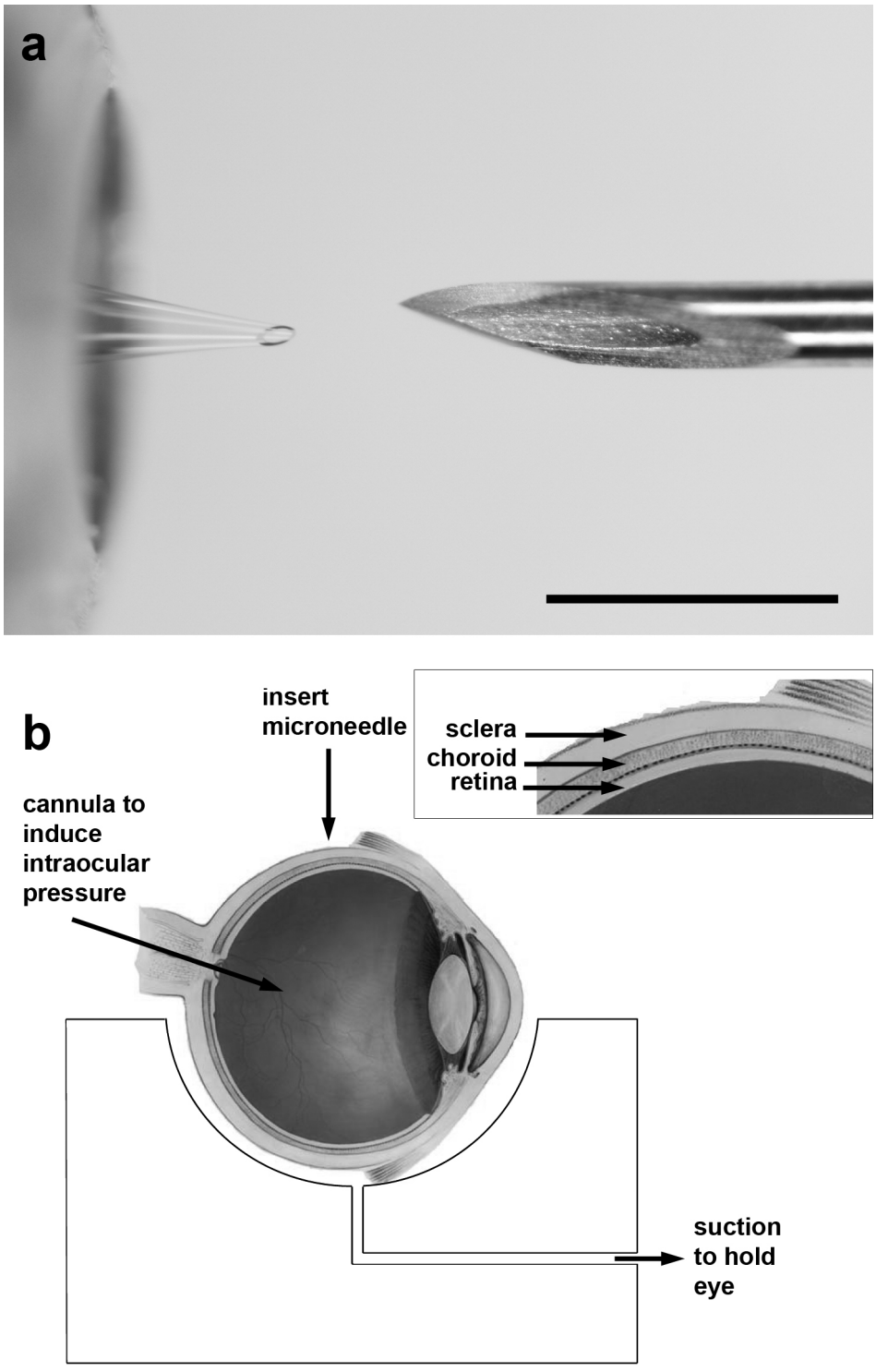

Figure 3.1.1 Experimental approach to microneedle infusion into the suprachoroidal space. (a) Comparison of a hollow microneedle mounted in an insertion device (above) and the tip of a 30 gauge hypodermic needle (below). Scale bar: 1mm. (b) Schematic diagram of the experimental set up used to study suprachoroidal injection. The eye was placed on a custom-made mold with a

channel through which suction was applied to hold the eye in place. A cannula inserted through the optic nerve of the eye allowed application of intraocular pressure. The microneedle was inserted into the sclera using the custom-made insertion device. Image of the eye was adapted from National Eye Institute, National Institutes of Health with permission.

Carboxylate-modified FluoSpheres (Invitrogen, Carlsbad, CA) were injected as 2 wt % solids suspension of 20 nm, 100 nm, 500 nm, and 1000 nm diameter particles. Tween 80 (Sigma-Aldrich, St. Louis, MO) at a final concentration of 0.5 wt %, was added to the suspension and sonicated prior to use. The fluospeheres were made of polystyrene and are not biodegradable. Sulforhodamine B (Sigma-Aldrich) was dissolved in Hanks' balanced salt solution (Mediatech, Manassas, VA) to make a sulforhodmine solution of 10^{-4} M. Barium sulfate particles (Fisher Scientific, Waltham, MA) measuring 1 μm in diameter were suspended in balanced salt solution (BSS Plus, Alcon, Fort Worth, TX) to form a 1.5 wt % suspension.

3.1.2 Experimental Procedure

A custom acrylic mold, shaped to fit a whole eye, was built to hold the eye steady and used for all experiments (Figure 3.1.1b). A catheter was inserted through the optic nerve into the vitreous and connected to a bottle of BSS Plus raised to a height to generate internal eye pressure of 18 mm Hg unless otherwise specified. Suction was applied to a channel within the mold to hold the external surface of the eye steady during microneedle insertion and manipulation. Each microneedle was pre-filled using flexible quartz tubing (World Precision Instruments) with a desired volume of the material to be injected. The

microneedle was placed in the device holder at a set microneedle length, attached to the micromanipulator and connected to the constant pressure source. Microneedles were then inserted perpendicular to the sclera tissue 5-7 mm posterior from the limbus. A set pressure was applied to induce infusion. Thirty seconds were allowed to see if infusion of the solution began. If infusion occurred, the pressure was stopped immediately upon injection of the specified volume. If visual observation of the injected material showed localization in the suprachoroidal space, the injection was considered a success. If infusion had not begun within that timeframe, then the applied pressure was stopped and the needle was retracted. This was considered an unsuccessful delivery.

Eyes to be imaged using microscopy were detached from the set-up within minutes after delivery was completed. The eyes were placed in acetone or isopentane which was kept on dry ice or liquid nitrogen causing the eye to freeze completely within minutes after placement. The frozen eye was removed from the liquid and portions of the eye were hand cut using a razor blade for imaging of injected material. Imaging was performed using a stereo microscope using brightfield and fluorescence optics (model SZX12, Olympus America, Center Valley, PA). The portions containing the sclera, choroid and retina were placed in Optimal Cutting Temperature media (Sakura Finetek, Torrance, CA) and frozen under dry ice or liquid nitrogen. These samples were cryosectioned 10-30 μm thick (Microm Cryo-Star HM 560MV, Walldorf, Germany) and imaged by brightfield and fluorescence microscopy (Nikon E600, Melville, NY) to determine

the location of injected material in the eye. Images were collaged as necessary using Adobe Photoshop software (Adobe Systems, San Jose, CA).

Pig eyes used for microcomputed tomography imaging were not frozen after injection. Instead pig eyes were injected with the barium sulfate suspension and stabilized in a 30 mm diameter sample tube and scanned in air using a Scanco μCT40 desktop conebeam system (Scanco Medical AG, Brüttisellen, Switzerland) at 30 μm isotropic voxel size, E = 55 kVp, I = 145 μA, and integration time = 200 ms. Through a convolution backprojection algorithm based on techniques from Feldkamp et. al. (Feldkamp et al 1984), raw data were automatically reconstructed to generate 2D grayscale tomograms. Global segmentation values (Gauss sigma, Gauss support, and threshold) were chosen for the contrast-enhanced region as well as general eye tissue. Grayscale tomograms were stacked, and 3D binarized images were produced by applying the optimal segmentation values (one image for the entire eye and another for the region injected with contrast agent). These images were overlayed using Scanco image processing language to demonstrate the relative 3D position of the contrast-enhanced region within the entire eye.

3.2 Spread of Injections in the Suprachoroidal Space

3.2.1 Hollow Glass Microneedle Device

Hollow microneedles were fabricated from borosilicate micropipette tubes (Sutter Instrument, Novato, CA), as described previously (Jiang et al 2009). A simple device was designed to hold a hollow glass microneedle that could be

inserted into the sclera of a rabbit eye in vivo and used to inject a fluid into the suprachoroidal space. Figure 3.2.1 shows the whole device. The main housing of the custom device (1-3) contains a shaft through which a hollow glass microneedle can be inserted. The tip of the microneedle extends from the tip of the cap on the housing (2). The cap can be rotated so as to allow the desired amount of the glass microneedle to protrude from the device. The microneedle length is adjusted using this rotatable cap. The back end of the device is connected to a metal luer adapter (S4J Mfg, Cape Coral FL) containing an olive shaped gasket (4). One end of the adapter is screwed onto to the device which tightens onto the glass microneedle and holds it in place. The other end of the luer adapter could be attached to any male luer tubing (5) or syringe (6). For these experiments a 7 inch extension tubing (Wolf Medical Supply, Sunrise FL) was used. The opposing end of the tubing is directly attached to a glass syringe (Hamilton Company, Reno NV).

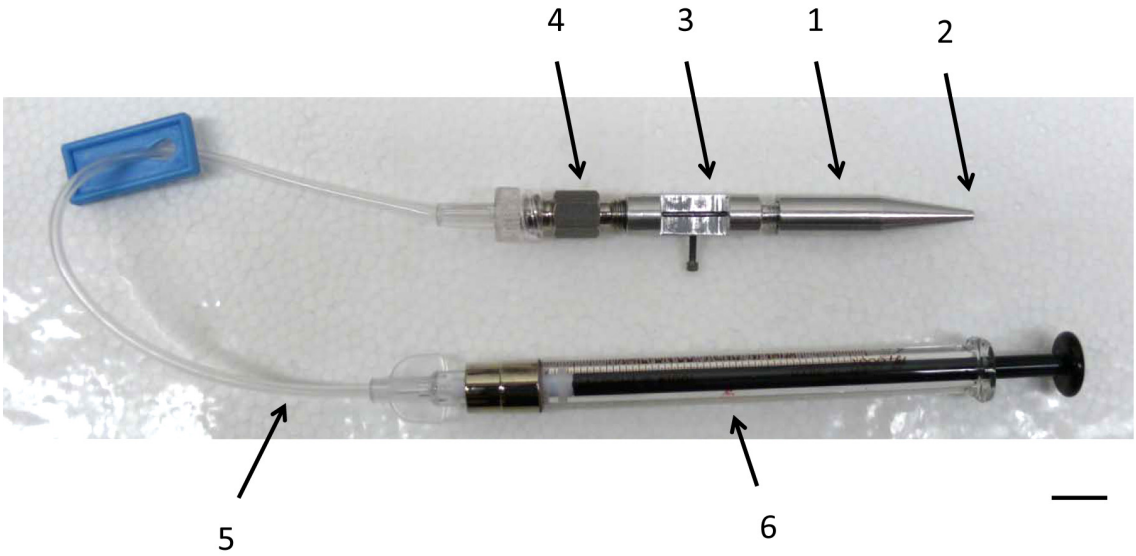

Figure 3.2.1 A custom hollow microneedle device for injection of fluids in vivo in to the rabbit suprachoroidal space. The main housing of the custom device (1-3) contains a shaft through which a hollow glass microneedle can be inserted through. The tip of the microneedle extends from the tip of the cap on the housing (2). The cap can be rotated so as to allow the desired amount of the glass microneedle to protrude from the device. The microneedle length is adjusted using this rotatable cap. The back end of the device is connected to a metal luer adapter containing an olive shaped gasket (4). One end of the adapter is screwed onto to the device which tightens onto the glass microneedle and holds it in place. The other end of the luer adapter is attached to extension tubing which is attached to a glass syringe. Scale bar: 1 cm.

3.2.2 Injection of India Ink

New Zealand white rabbits were used for all experiments in this study. All experiments were approved by the Emory Institutional Animal Care and Use Committee (IACUC) and complied with the ARVO statement for animal use. Animals were anesthetized with an intramuscular injection of ketamine (Hospira Inc, Lake Forest IL) and xylazine (Lloyd Inc, Shenandoah IA) prior to injection of a formulation within the eye. Black colored India ink (Speedball, Statesville NC) was diluted in deionized water to make a 1:20 India ink: water suspension.

While the rabbit was anesthetized, the eye was proctosed by pulling the eyelids back to expose the sclera of the rabbit eye. The cap on the microneedle device was set to the desired microneedle length (7-800 μm). The microneedle was inserted using the device into the superior temporal region of the eye approximately 3-4 mm posterior to the limbus. The desired amount of India ink was injected using the syringe. Approximately 20-30 seconds were allowed after injection to ensure complete injection of fluid and then the microneedle and device were removed from the eye. Any observation of leakage was noted and

the lids were pushed to normal position. Within minutes after injection the animal was euthanized with an overdose of pentobarbital and the eyes were enucleated.

3.2.3 Snap Freezing of the Eye

One way the delivery of India ink into the suprachoroidal space was confirmed was using the snap freeze method. Enucleated eyes were sutured at the limbus onto a plastic plate that contained an opening for the cornea along with tiny holes for the sutures around the cornea hole. The eye and plastic plate were dipped in isopentane which was kept under dry ice or liquid nitrogen. Within a few minutes eyes were frozen and removed from the isopentane bath. Using a surgical blade a cut was made across the sclera and into the vitreous, without penetrating into the vitreous, along the entire equator of the eye. This allowed the back half of the eye to be removed as a cup leaving behind the vitreous and other half of the eye on the plastic plate. The inside of the cup exposed the black India ink and the vitreous could then be examined for traces of India ink. During the whole process the eye was still frozen preventing any movement of the India ink or tissues.

3.2.4 Histological Analysis

For histological analysis of India ink injections the whole eye was fixed in 2.5% glutaraldehyde in 0.1 M cacodylate buffer overnight. A sample of the eye was cut from the injection site of the eye for analysis. The sample was rinsed, postfixed in 1% osmium tetroxide, en bloc stained with uranyl acetate and then

dehydrated in a graded series of ethanol baths. After a final wash in 100 % ethanol it was given 2 changes of propylene oxide and placed in a 1:1 mixture of propylene oxide and LX-112 resin (Ladd Research Industries, VT) overnight. The next day, tissue was transferred into pure resin, embedded in flat molds and placed in a 50-60 °C oven to polymerize. 1.5 um thick sections were cut and stained with 1% toluidine blue on a Leica ultracut UCT. Tissue blocks were trimmed down to the areas of interest and 70-80 nm thin sections were cut and placed on grids. Sections were stained with 2% uranyl acetate for 30 minutes followed by lead citrate.

3.2.5 Quantification of the Spread of India Ink

Enucleated eyes were placed in glycerol for 6-8 minutes causing the sclera to become transparent. The eye was removed when the India ink could clearly be seen. Images of the eye were taken using a Sony DSCH-50 digital macro camera (Sony Corporation, Tokyo Japan). Now that the India ink could clearly be seen measurements were also taken of the spread. Using the images and measurements a digital map of the spread was made for each injection. On this digital map the location of the limbus, the injection site, and the optic nerve were designated. Figure 3.2.2 shows a graphical representation of this process. The digital images were then used to quantify the area of the spread and distances

using Photoshop (Adobe Systems, San Jose CA) computer imaging software.

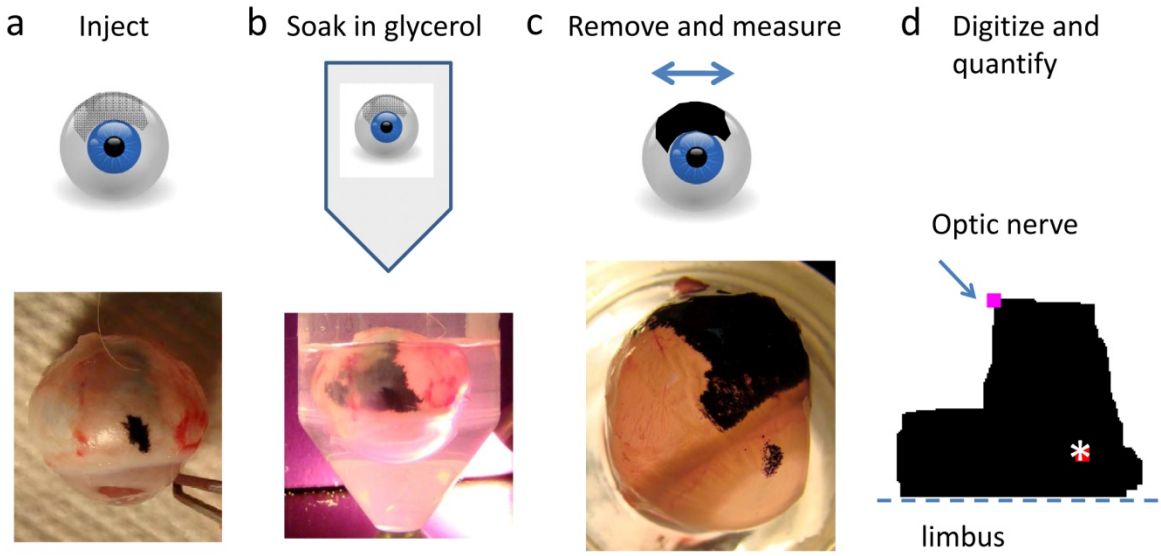

Figure 3.2.2 India ink surface area coverage quantification process. (a) Eyes were enucleated after injection of India ink. (b) Enucleated eyes were placed in glycerol for 6-8 minutes causing the sclera to become transparent. (c) The eye was removed when the India ink could clearly be seen. Images of the eye were taken using digital camera. The India ink could clearly be seen and measurements were taken of the spread. (d) Using the images and measurements a digital map of the spread was made for each injection. On this digital map the location of the limbus, the injection site (asterisk), and the optic nerve were designated.

3.2.6 Hollow Metal Microneedle Device

A hollow metal microneedle device was created for injection of latex into the suprachoroidal space of human eyes. The microneedles were made form 33 gauge stainless steel hollow hypodermic needles (TSK Laboratories, Tochigi, Japan). The hypodermic needles were fixed onto a custom plastic holder that kept the cannula flat on the surface and the luer adapater flush against the plastic end. The cannula was cut using an infrared laser (Resonetics Maestro, Nashua, NH) at a desired angle and length from the base of the luer adapter. The microneedle was electoropolished using an E399 electropolisher (ESMA,

South Holland IL) and cleaned with deionized water. Microneedles were sterilized as necessary using an AN74j anaprolene sterilizer (Anderson Products Inc, Haw River NC). An image of a finished microneedle is shown in Figure 3.2.4 in comparison to a 30 gauge hypodermic needle. The luer of the microneedle can be easily attached to any syringe for injection, just like a standard hypodermic needle.

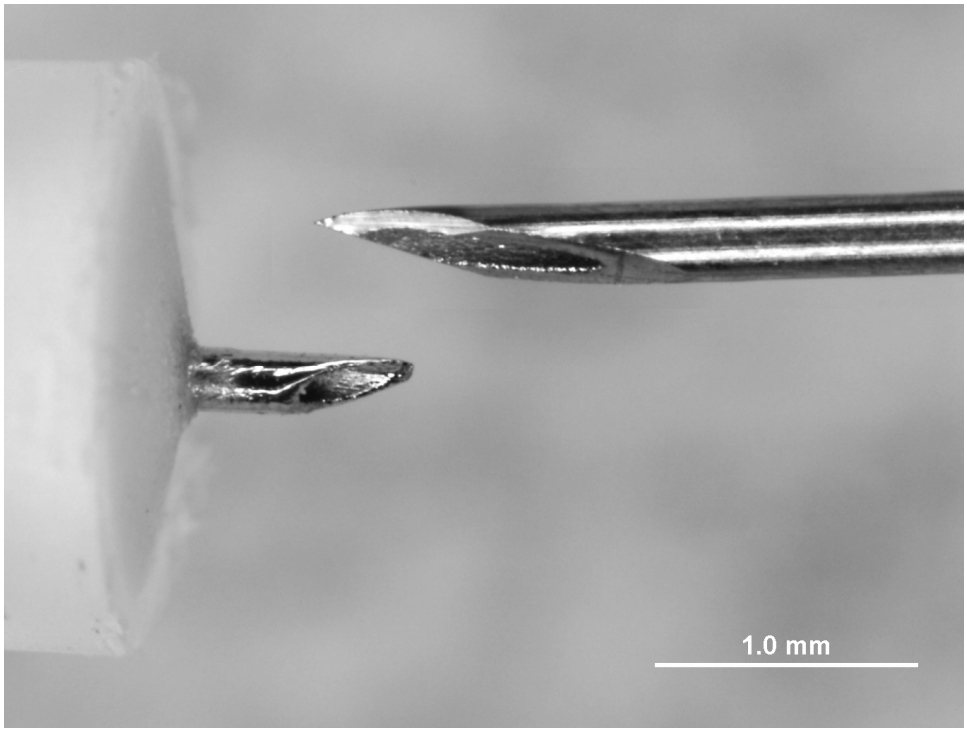

Figure 3.2.3 Comparison of hollow metal microneedle to a 30 gauge hypodermic needle. The hollow metal microneedle is on the left attached to a standard luer adapter (in white) which could be easily attached to any syringe. The total length of the microneedle is less than a millimeter which is similar to just the orifice opening of the 30 gauge hypodermic needle.

3.2.7 Injections of Latex into Human Eyes

Whole human eyes were obtained from Lions Eye Institute for Transplant Research (Tampa FL). A custom acrylic mold, shaped to fit a whole human eye,

was built to hold the eye steady and used for all experiments. A catheter was inserted through the optic nerve into the vitreous and connected to a column of BSS Plus raised to a specific height to generate internal eye pressure of 15 mm Hg. Red latex (Carolina Biological Supply Company, Burlington NC) was diluted to make a 1:4 Latex: BSS mixture. The mixture was sonicated for 3-5 minutes and made fresh before each injection. The desired volume of the mixture was loaded into a syringe and the microneedle was then attached to the syringe. The microneedle was inserted 8 mm posterior the limbus, across the sclera, and the latex mixture was injected. Thirty seconds were allowed after injection, and the microneedle was removed. The eye was then immediately snap frozen.

The optic nerve of the eye was attached to a suture or string and was dipped in isopentane which was kept under a dry ice bath. The eye was completely frozen within approximately 5 minutes. Once the whole eye was frozen the globe was dissected using a blade into “petals” starting from the optic nerve. The cuts were made up to the cornea leaving the cornea intact. The petals were opened up from the optic nerve. The petals contained the tissues of the globe (sclera, choroid and retina) and exposed the vitreous inside as a frozen white ball. The vitreous was removed carefully leaving the globe tissues and anterior segments of the eye. The petals were laid flat with the cornea in the center and the choroid and retina were slowly pulled away. This left behind latex (pink in color) on the sclera that could be easily distinguished from the white sclera with the transparent cornea in the center of the petals. Figure 3.2.4 shows a graphical representation of the procedure.

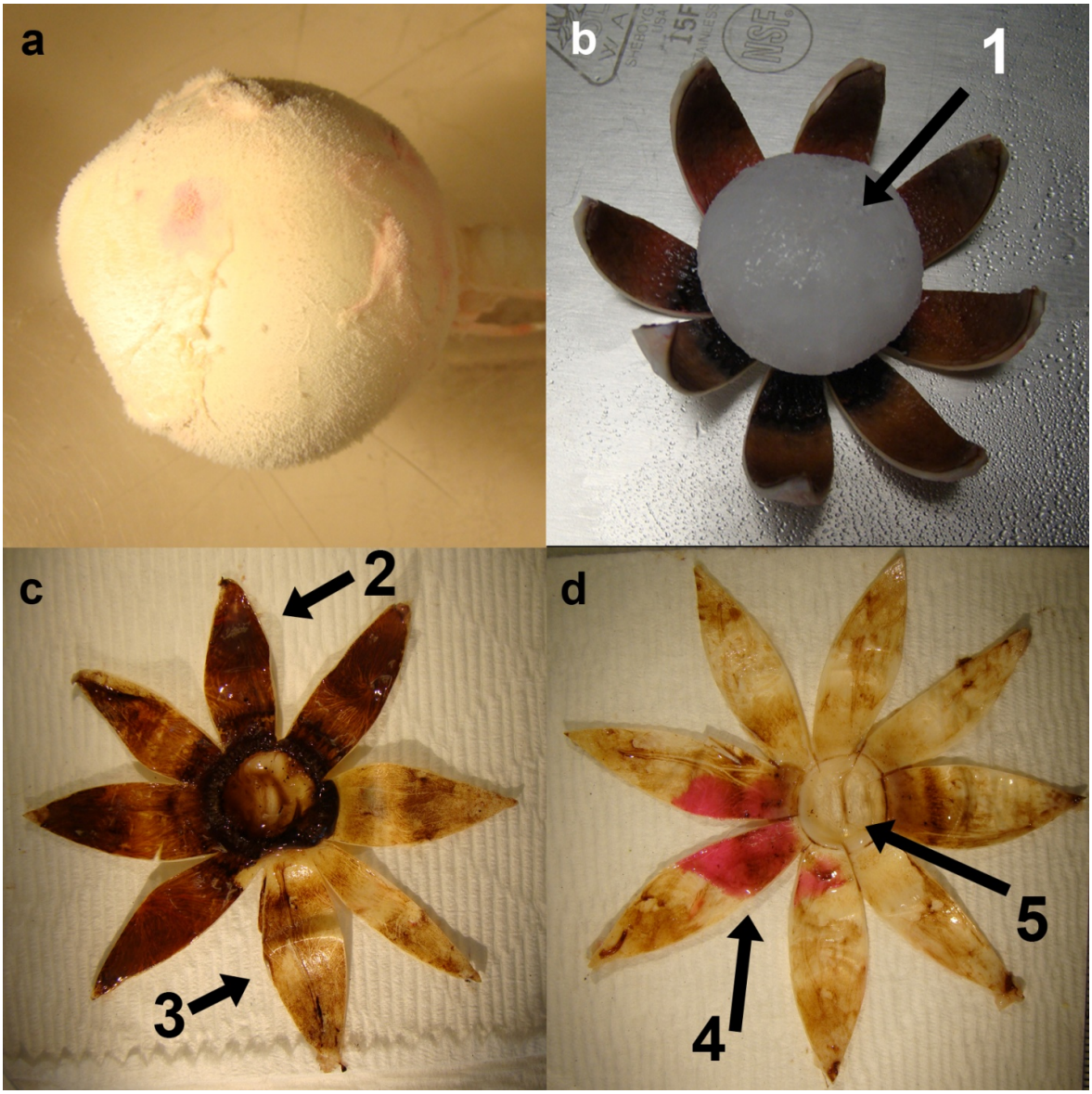

Figure 3.2.4 Latex surface area quantification procedure. (a) First the whole eye was frozen. The globe was dissected using a blade into “petals” starting from the optic nerve. (b) The cuts were made up to the cornea leaving the cornea intact. The petals were opened up from the optic nerve. The petals contained the tissues of the globe (sclera, choroid and retina) and exposed the vitreous (1) inside as a frozen white ball. (c) The vitreous was removed carefully leaving the globe tissues and anterior segments of the eye. The petals were laid flat with the cornea in the center and the choroid and retina (2) were slowly pulled away. Image (c) shows petals with choroid and retina still attached (2) and choroid and retina removed (3). (d) Once all the petals were removed the latex (4) on the sclera that could be easily distinguished from the white sclera with the transparent cornea (5) in the center of the petals.

Images of the latex spread, such as 3.2.4d were taken with a scale. The surface area could then be quantified from the images by determining the area that the pink latex covered. The total area could be determined by calculating the area of the white colored sclera plus the pink latex covered area. This was performed by scaling each image and using imaging software, Photoshop (Adobe Systems, San Jose CA). With these images additional measurements such as distances were also made.

3.3 In Vivo Ocular Distribution of Molecules and Particles

3.3.1 Materials

Hollow microneedles were fabricated from borosilicate micropipette tubes (Sutter Instrument, Novato, CA), as described previously (Jiang et al 2009). The custom device for hollow glass microneedles described in section 3.2.1 was used for injections of all molecules and nanoparticles within the suprachoroidal space. The hollow metal microneedle described in section 3.2.6 was used for injections of all microparticles within the suprachoroidal space. Microneedles were sterilized using an AN74j anaprolene sterilizer (Anderson Products Inc, Haw River NC) as necessary.

Several formulations were prepared for injection into the eye. Sodium fluorescein (Sigma-Aldrich, St. Louis, MO) and dextrans of 40 kDa and 250 kDa tagged with fluorescein isothiocyanate, FITC, (Sigma-Aldrich, St. Louis, MO) were dissolved in Hanks Balanced Salt Solution (Mediatech, Manassas, VA).

Avastin was tagged with a fluorophore, Alexa-Fluor 488, and was dissolved in Hanks Balanced Salt Solution (HBSS). The Avastin was provided courtesy of Dr. Uday Kompella's lab at the University of Colorado. Particles of 20 nm, 500 nm, 1 μm, and 10 μm (FluoSpheres) were purchased from Invitrogen (Carlsbad, CA). All particle suspensions were in an aqueous media at 2 wt. % solids except for the 10 μm suspension which contained approximately 0.2 wt. % solids.

New Zealand white rabbits were used for all experiments in this study. All experiments were approved by the Emory Institutional Animal Care and Use Committee (IACUC) and complied with the ARVO statement for animal use. Animals were anesthetized with an intramuscular injection of ketamine (Hospira Inc, Lake Forest IL) and xylazine (LLoyd Inc, Shenandoah IA) prior to injection of a formulation within the eye. Animals were sacrificed with an injection of pentobarbital through the ear vein as necessary for histology.

3.3.2 Injection Procedure

The custom metal device was used to insert a hollow glass microneedle into the rabbit eye across the conjunctiva and into the sclera several millimeters past the limbus. Hollow metal microneedles were inserted directly into the sclera in a similar fashion. The eye was exposed by pushing back the eyelids and exposing the eyeball from the socket. The injection site was in the superior temporal quadrant of the eye. Once the microneedle was inserted, the appropriate volume was injected by hand using a 1 mL syringe. After complete injection, approximately 30 seconds were allowed before removing the

microneedle and device from the surface of the eye. Hollow metal microneedles were used to inject 1 and 10 μm particles; all other materials were injected with a hollow glass microneedle. Intravitreal injections were performed using a 30 gauge needle and the needle was inserted transclerally and the formulation was injected near the mid-vitreous. The opposing eye was used as a control eye and nothing was injected into the eye.

3.3.3 Fluorescence Measurements

Measurement of fluorescence intensity within the rabbit eye was performed using an ocular fluorophotometer (Ocumetrics, Mountain View, CA). The system is tuned for measuring fluorescence measurements that are within the excitation and emission wavelengths of sodium fluorescein. No anesthesia was necessary for scanning and animals were awake for the entire process. The pupil was dilated using drops of a 2.5% solution of phenylephrine hydrochloride (Baush & Lomb, Tampa FL). The eye was aligned to allow light to pass through the anterior portion of the eye through the pupil and vitreous to the retina, choroid, and sclera in the back of the eye. A one dimensional scan of the fluorescence intensity from the front to the back of the eye was obtained from each scan. A baseline scan, a scan of the eye with no injection, was obtained for each eye prior to injection. Baseline scans provided details on location of tissues and background fluorescence within the eye. Figure 3.3.1 shows the results of a baseline fluorescence scan of the eye.

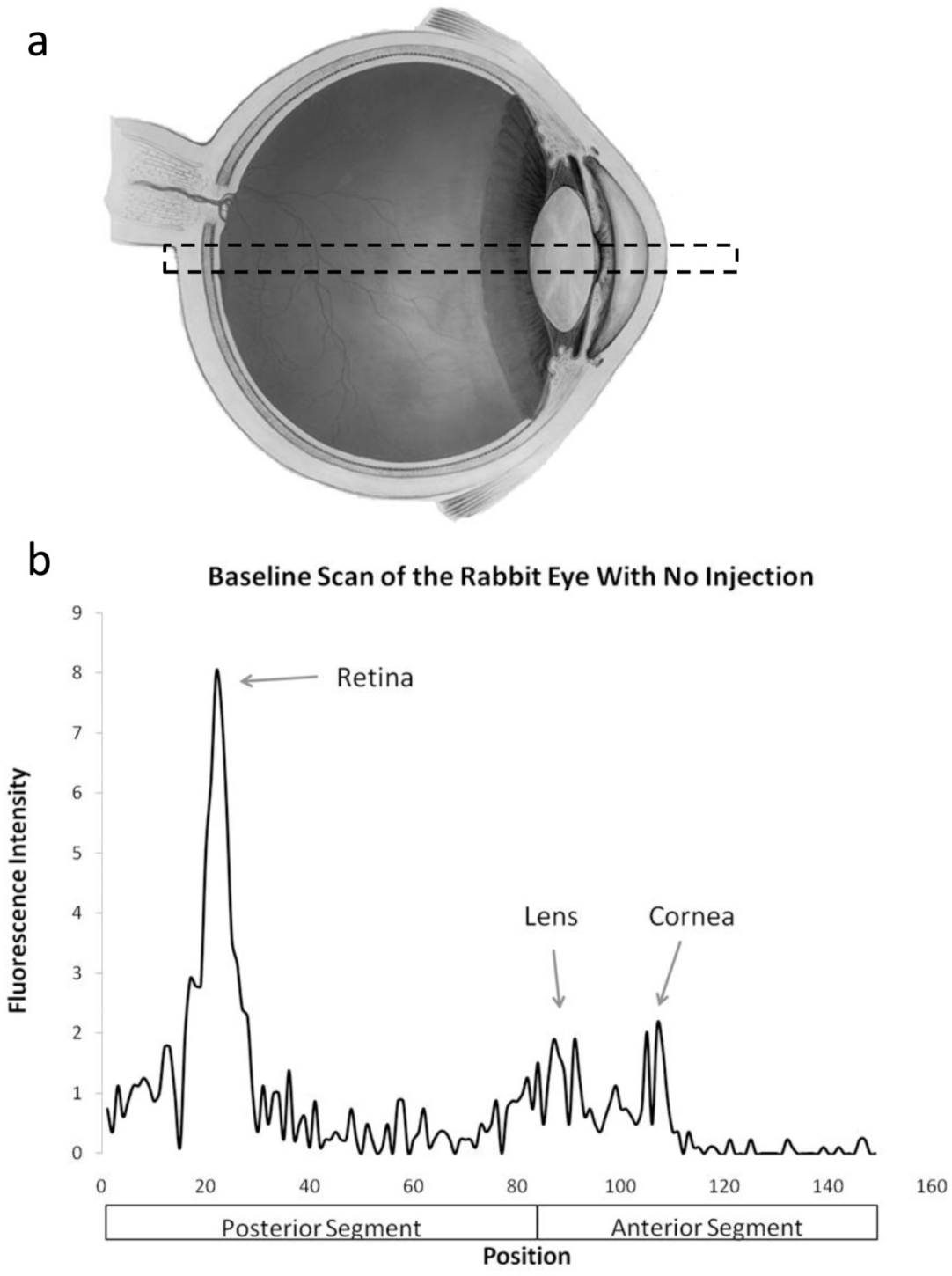

Figure 3.3.1 Representative baseline fluorescence scan of the rabbit eye in vivo. (a) The baseline scan is performed through the visual axis, dotted box area. (b) The scan of that region gives fluorescence measurements along this axis and assigns a relative position (x-axis). The fluorescence reading is plotted on the y-axis. The peaks provide an indication as to the position of key regions of the eye such as the retina, lens and cornea. The image of the eye is roughly scaled to

match the position axis of the scan for reference. Image of the eye was adapted from National Eye Institute, National Institutes of Health with permission.

3.3.4 Imaging Delivery into the Suprachoroidal Space

In order to image the fundus of the rabbit eye in-vivo, a Genesis-D handheld digital retina camera (Kowa Optimed Inc, Torrance CA) was used. Tropicamide (Baush & Lomb, Tampa FL) was applied topically to dilate the pupil and the animal was imaged while under anesthesia. A 90 diopter lens was used to allow for a wider field of view. Fundus images of the injected eye were taken through the pupil to evaluate any abnormalities compared to the uninjected eye. Using the fluorescence mode, images of the fundus were taken to confirm the presence of the particles in the eye.

Eyes to be imaged using microscopy were enucleated from the animal after sacrafice. The eyes were fixed in 2.5% glutaraldehyde in 0.1 M cacodylate buffer overnight. A tissue section of the eye near the injection site was removed for cryosectioning. The portions containing the sclera, choroid and retina were placed in Optimal Cutting Temperature media (Sakura Finetek, Torrance CA) and frozen under dry ice or liquid nitrogen. These samples were cryosectioned 10-30 μm thick (Microm Cryo-Star HM 560MV, Walldorf Germany) and imaged by brightfield and fluorescence microscopy (Nikon E600, Melville NY) to determine the location of injected material in the eye. Images were overlayed as necessary using Adobe Photoshop software (Adobe Systems, San Jose CA).

CHAPTER 4

RESULTS

4.1 Feasibility of Suprachoroidal Delivery Using a Hollow Microneedle

4.1.1 Introduction

In this study, we investigate the suprachoroidal space as a route to target delivery of drugs to the back of the eye. The suprachoroidal space is a potential space between the sclera and choroid that goes circumferentially around the eye (Krohn and Bertelsen 1998, Einmahl et al 2002). Previous studies employing surgical procedures to introduce catheters into this space have shown that drugs delivered into the suprachoroidal space can be targeted towards the choroid and retina because the suprachoroidal space is in direct contact with the choroid (Einmahl et al 2002, Gilger et al 2006, Olsen et al 2006, Kim et al 2007). Introduction of controlled release formulations into the suprachoroidal space could further enable long-term therapy. Access to the suprachoroidal space, however, is difficult and the methods that have previously been studied are invasive and too complex to be performed as a simple office procedure (Einmahl et al 2002, Gilger et al 2006, Olsen et al 2006, Kim et al 2007).

We hypothesize that hollow microneedles can provide a minimally invasive method to inject nanoparticles and microparticles into the suprachoroidal space for drug delivery to the back of the eye. Hollow microneedles are needles of micron dimensions that can infuse fluid into tissue with excellent spatial targeting. Fabrication and characterization of hollow microneedles has been

extensively studied for drug delivery to the skin (Brazzle et al 1999, Zahn et al 2000, Gardeniers et al 2003, McAllister et al 2003, Davis et al 2005), including recent human studies administering insulin (Gupta et al 2009) and influenza vaccine (Van Damme et al 2009). Another recent study showed that hollow microneedles can pierce hundreds of microns into the ocular tunic and inject small molecules and particles into the sclera and corneal stroma (Jiang et al 2009).

We seek to determine if microneedles can pierce to the base of the sclera and target the suprachoroidal space. Suprachoroidal delivery using microneedles has the promise to be simple, minimally invasive, targeted, and able to achieve sustained release by injecting nanoparticles and microparticles encapsulating drug for slow release.

More specifically, this study determines whether hollow microneedles can deliver small molecules and particles to the suprachoroidal space of pig, rabbit and human cadaver eyes. We further measure the effect of microneedle length, infusion pressure, and intraocular pressure on the delivery of particles ranging from 20 -1000 nm in diameter in pig eyes. Finally, we examine the role that particle size plays and the influence of ocular anatomical barriers on delivery to the suprachoroidal space. With this work, we show for the first time that microneedles are capable of delivering fluid and particles into the suprachoroidal space in a minimally invasive manner to deliver drugs to the back of the eye.

4.1.2 Imaging Delivery in to the Suprachoroidal Space

Because microneedles have not been used before to inject into the suprachoroidal space, we first wanted to determine if a liquid formulation could be delivered, what volume could be delivered, and over how large an area it would spread. We used red-fluorescent sulforhodamine B as a model compound and injected it into pig eyes ex vivo using a single hollow microneedle inserted just to the base of the sclera in order to target the suprachoroidal space. Using this approach, we found that it is possible to inject a liquid formulation into the suprachoroidal space and spread it circumferentially around the eye from a single microneedle injection, as discussed immediately below.

Figure 4.1.1a shows a saggital cross section of an untreated pig eye. The layers of the eye can be distinguished and the white colored sclera is in direct contact with the dark colored layer that represents the choroid and retinal pigment epithelium. Figure 4.1.1b shows a sagittal cross section of a pig eye frozen after injection of 35 µL of sulforhodamine. The pink sulforhodamine solution can be seen selectively delivered just below the sclera and above the choroid. This region represents the suprachoroidal space and confirms that the solution was injected and spread within the suprachoroidal space from the initial injection site. Examining the injection form the inside further confirms the location of the sulforhodamine.

Figure 4.1.2a shows a section of the pig globe with the vitreous removed and parts of the choroid and retina still attached to the sclera. Where the retina and choroid are missing the sulforhodamine solution is visible. When the choroid and retina are completely removed, Figure 4.1.2b, the sulforhodamine can clearly

be seen underneath where these tissues were. We were able to inject volumes up to 35 µL without leakage, but larger volumes leaked out from openings on the surface of the eye where vortex veins would be attached in vivo. However, subsequent experiments in pigs and rabbits in vivo have demonstrated suprachoroidal delivery of up to 100 µL without leakage through these openings.

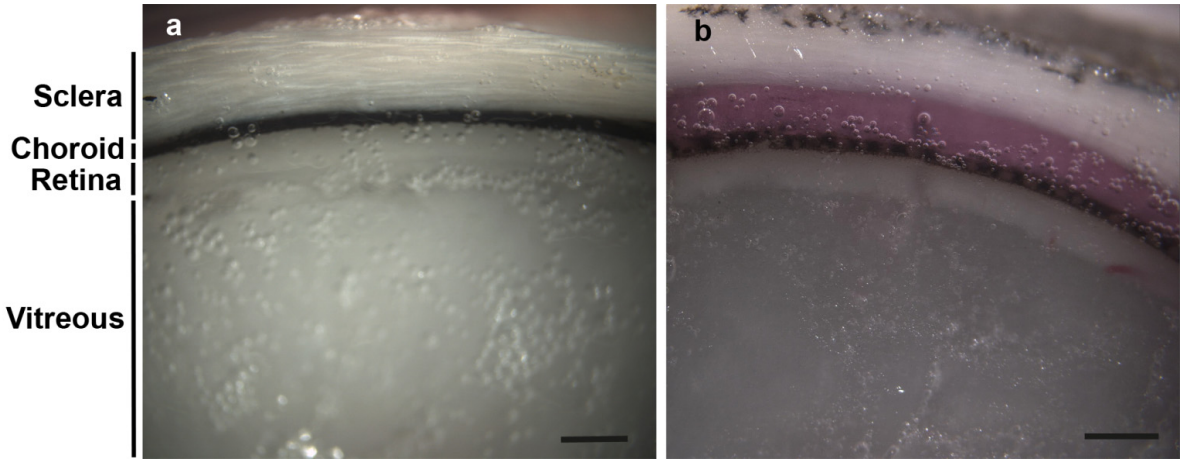

Figure 4.1.1 Imaging of fluid infusion into the suprachoroidal space. Brightfield microscopic images of a cross section of a frozen eye (a) showing normal ocular tissue (b) showing the delivery of sulforhodamine B (pink) between the sclera and choroid (i.e., in the suprachoroidal space) Scale bar: 500 µm.

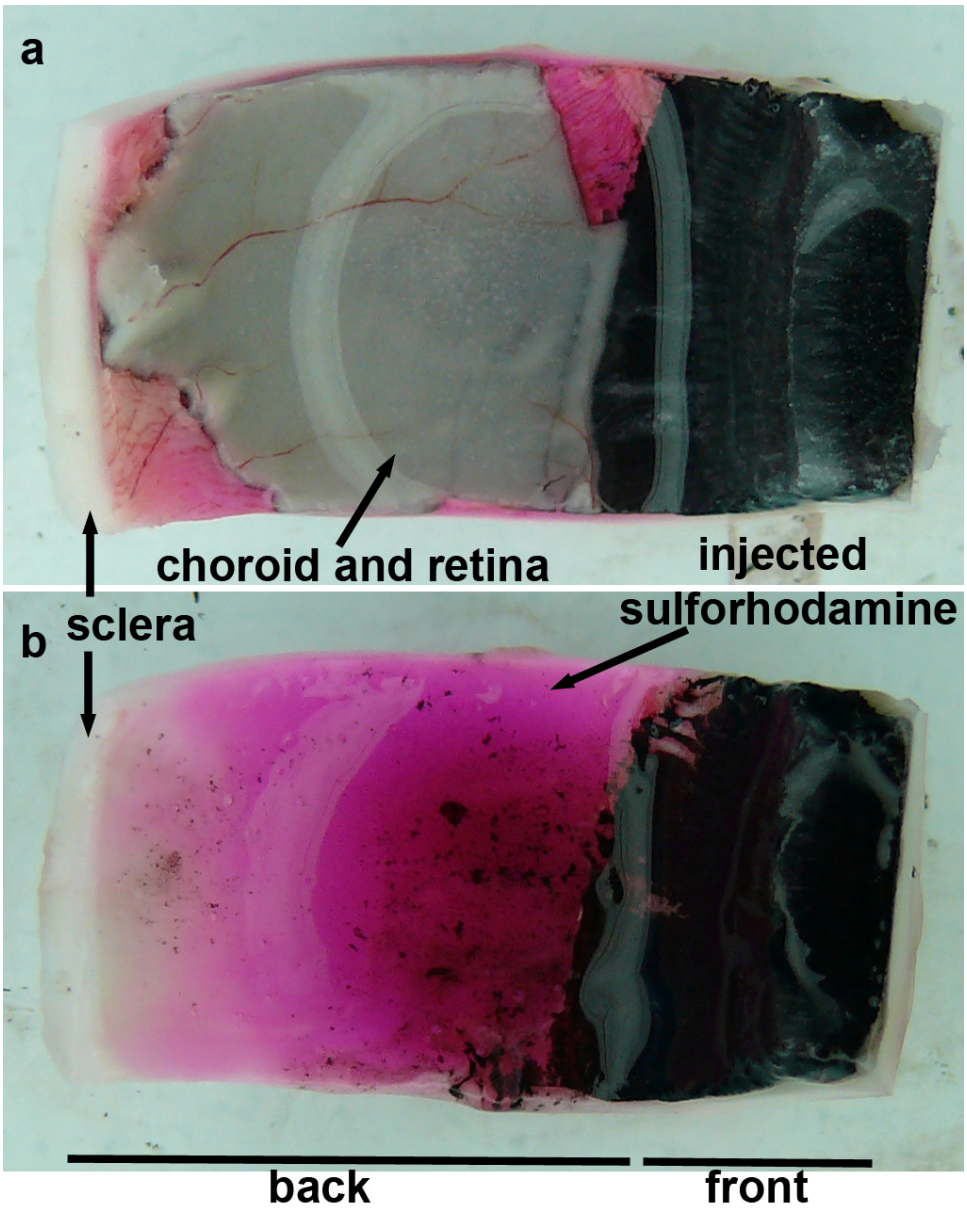

Figure 4.1.2 Imaging of sulforhodamine B (pink) infusion into the suprachoroidal space. Brightfield view of a frozen eye from the vitreous side (a) showing the sample with choroid and retina still attached in some locations and (b) with choroid and retina completely removed.

We next wanted to determine if microneedles can also deliver particles into the suprachoroidal space, which is of interest for sustained-release drug delivery scenarios. We therefore injected particles with diameters of 500 nm or 1000 nm into the suprachoroidal space of rabbit, pig and human eyes ex vivo

and imaged their distribution to confirm their localization just below the sclera. Cryosections of the rabbit eye were taken in the axial plane and images were collaged to form a panoramic view, as shown in Figure 4.1.3b. The images show the spread of the fluorescent (red/orange) particles along the equator of the eye in a thin sheath just below the sclera. In this experiment, a volume of 15 μL was injected and in this particular cross-section taken in the plane of the insertion site, the injection has spread approximately 20 mm, which corresponds to about 36% of the total circumference of the eye.

As shown in Figure 4.1.3c-d, cryosections of pig and human eyes were taken in the saggittal directions so that the images show the anterior of the eye to the right and the posterior of the eye to the left. These images show the ability of microinjected particles to spread in the suprachoroidal space both in the anterior and posterior direction of the eye from the injection site. In these experiments, a single microneedle delivered 30 μL of a 2 wt % particle suspension into the suprachoroidal space of both species. Leakage was observed at the vortex vein openings away from the injection site similar to what was observed with sulforhodamine injections.

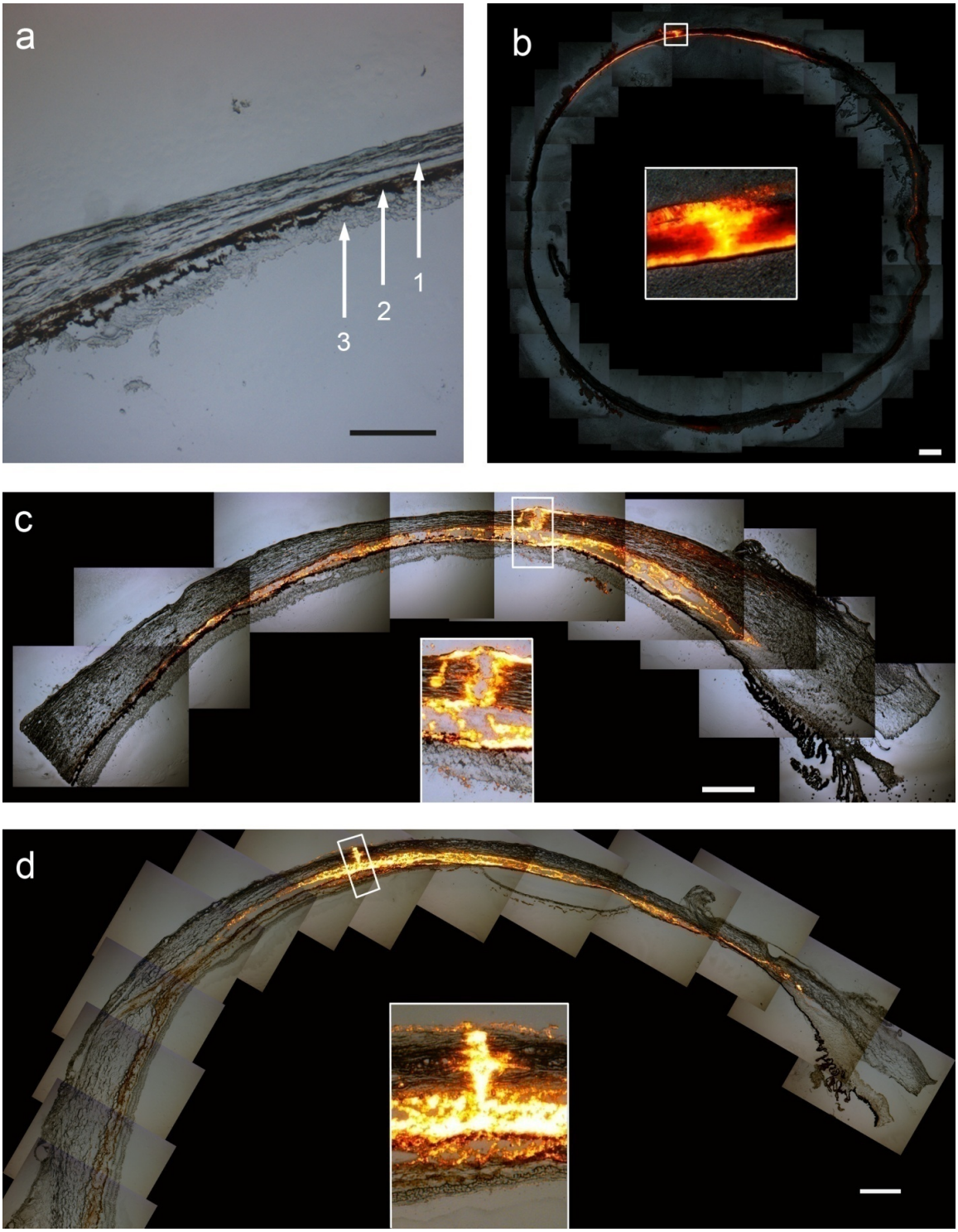

Figure 4.1.3 Imaging of particle infusion into the suprachoroidal space. Image of a cryosection of a pig eye with no infusin into the suprachoroidal space. (a) The layers of the eye are (1) sclera, (2) choroid, and (3) retina. Collaged fluorescence microscopy images of tissue cryosections show the delivery of (b) 500 nm particles into a rabbit eye, (c) 500 nm particles into a pig eye, and (d) 1000 nm

particles into a human eye, all ex vivo. Each image also displays an inset with a magnified view of the microneedle insertion site. These images show targeted delivery of particles into the suprachoroidal space and indicate that the microneedle did not penetrate into the choroid or retina. Scale bar: 500 μm.

The insets in these images show magnified views of the microneedle insertion site. In each case, the insertion site within the sclera is filled with particles. In the case of the pig and human, the retina is still attached and visible, and it is clear that the microneedle has not penetrated to the retina. The rabbit retina separated during the cryosectioning procedure and is not visible. These results confirmed that a microneedle was able to target the suprachoroidal space of rabbit, pig, and human eyes to deliver particles up to 1000 nm in diameter, which was the largest particle size used in this study. These particles spread from the injection site circumferentially in all directions within the suprachoroidal space.

To image the circumferential spread and localization of injected material in the suprachoroidal space in three dimensions using a noninvasive method, we utilized microcomputed tomography (μCT). After injecting 35 μL of 1 μm diameter barium sulfate contrast agent particles into the suprachoroidal space of a pig eye, cross sectional images showed the particles distributed as a thin white strip that circled just below the outer edge of the eye, i.e., just below the sclera (Figure 4.1.4a). This profile is characteristic of suprachoroidal delivery and similar to the results from fluorescence imaging. The three-dimensional reconstruction of these cross-sectional images shows the spread of the particles in the posterior segment of the eye (Figure 4.1.4b). The particle spread is approximately 5 mm

in radius, although asymmetrically distributed around the injection site, and covers an approximate area of 70 mm^2 which represents 7 % of the surface area of the back of the eye. This further confirms the ability of microneedles to spread particles over a significant portion of the posterior segment of the eye by targeting the suprachoroidal space.

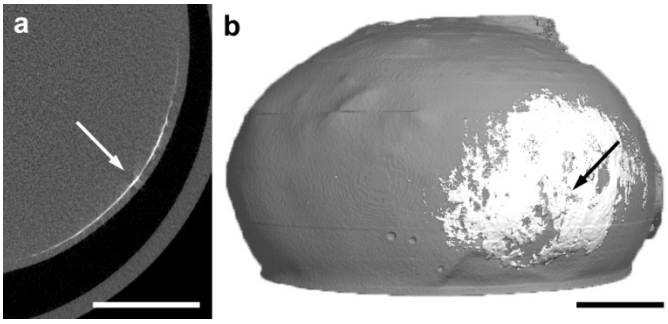

Figure 4.1.4 Microcomputed tomography images of suprachoroidal delivery of barium sulfate particles. (a) Two-dimensional axial cross section of a pig eye imaged after injection of 1 μm barium sulfate particles. The arrow points to the thin white strip of particles in the suprachoroidal space. (b) Two-dimensional cross sections were reconstructed to form a three-dimensional map showing the distribution of particles, which have spread circumferentially in all directions around the microneedle insertion site (arrow) in the suprachoroidal space. Scale bar: 5 mm.

4.1.3 Effect of Operating Parameters on Particle Delivery in to the Suprachoroidal Space of Pig Eyes

We hypothesize that injection into the suprachoroidal space is facilitated by the use of longer microneedles, greater infusion pressure and smaller particle size. To test this hypothesis, we injected particles of 20, 100, 500, and 1000 nm diameter into pig eyes ex vivo using a range of different microneedle lengths and infusion pressures to determine the success rate of suprachoroidal delivery. Our

observation was that an attempted injection is either fully successful, as defined as complete injection of the 25 μL particle suspension into the suprachoroidal space, or fully unsuccessful, as defined as an inability to inject at all. Partial injections were not observed. The success rates after five injection attempts at each condition are shown in Figure 4.1.5.

In each of the graphs, the success rate increased with greater infusion pressure and with greater microneedle length (ANOVA, $p<0.05$). For the smallest particles (20 nm), 100% successful injections were achieved using a pressure of 250 kPa at all microneedle lengths. For 100 nm particles, the effects of pressure similarly plateaued at 250 kPa and 100% success was achieved at all but the shortest microneedle length (700 μm). For the larger particles (500 and 1000 nm), the effects of pressure generally plateaued at 300 kPa and success rate significantly decreased for shorter microneedles.

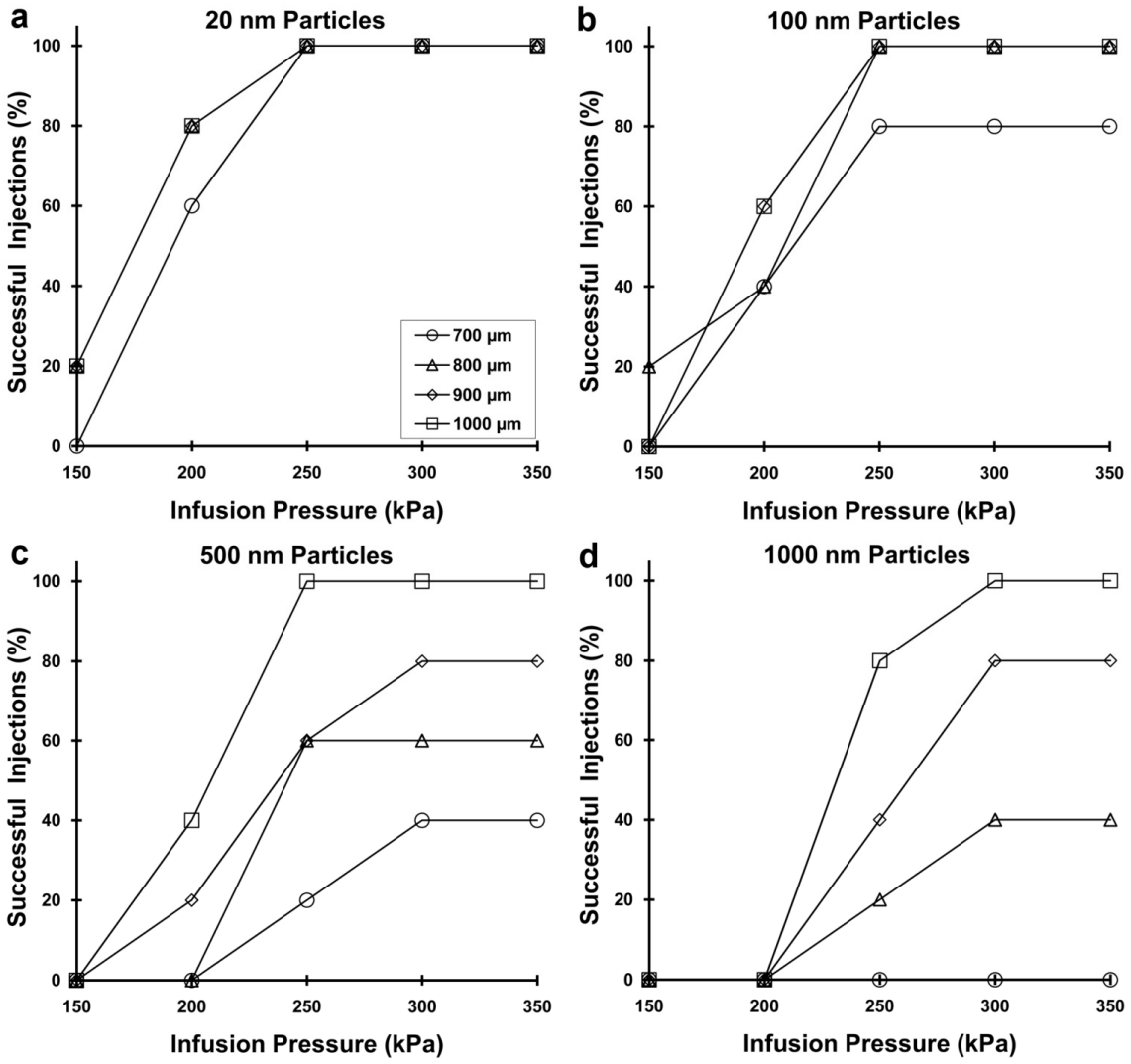

Figure 4.1.5 The effect of infusion pressure and microneedle length on the success rate of suprachoroidal delivery for (a) 20 nm, (b) 100 nm, (c) 500 nm and (d) 1000 nm particles into pig eyes. A total of five infusions were attempted at each condition studied. Increasing microneedle length and increasing infusion pressure increased the delivery success rate for all particle sizes (ANOVA $p<0.05$).

We interpret these data in the following way. Short microneedles lengths inject within the sclera, such that particles must be forced through a portion of the sclera to reach the suprachoroidal space. Smaller particles (20 and 100 nm) can do this more easily, because the spacing of collagen fiber bundles in the sclera is

on the order of 300 nm (Edwards and Prausnitz 1998, Meek and Fullwood 2001). The ground substance between the collagen fibers, which has a much smaller pore size (Edwards and Prausnitz 1998, Meek and Fullwood 2001), appears not to be rate limiting. However, larger particles (500 and 1000 nm) have more difficulty crossing this anatomical barrier, such that infusion pressure becomes an important parameter and injection success rate decrease significantly.

Consistent with this hypothesis, statistical analysis in Table 1 shows that at a microneedle length of 700 μm, where the most scleral tissue must be traversed to reach the suprachoroidal space, success rate depended strongly on particle size. Using 800 and 900 μm microneedles, particles smaller than the collagen fiber spacing (20 and 100 nm) behaved similarly and particles larger than the collagen fiber spacing (500 and 1000 nm) also behaved similarly, but there was a significant difference between 100 nm and 500 nm particles. The longest microneedles (1000 μm), which probably reach the base of the sclera, showed no significant dependence on particle size, suggesting that overcoming the collagen barrier in the sclera was no longer needed.

Table 4.1.1 Statistical comparison of injection success rates of particles of different sizes at different microneedle lengths. Values in the table are p values determined using ANOVA. Statistical significance between particle sizes at a given microneedle length was considered to be $p<0.05$ and indicated by an asterisk (*).

Microneedle Length	20 vs 100 nm	100 vs 500 nm	500 vs 1000 nm	20 vs 1000 nm
700 μm	0.02*	0.02*	0.09	0.02*
800 μm	0.37	0.00*	0.10	0.01*
900 μm	0.18	0.03*	0.18	0.03*
1000 μm	0.18	0.37	0.21	0.18

Our hypothesis further suggests that particles of 20 and 100 nm can spread within the sclera as well as the suprachoroidal space, whereas particles of 500 and 1000 nm should localize exclusively in the suprachoroidal space. In Figure 4.1.6, we compare the spread of 20 nm particles to 1000 nm particles under identical conditions. As expected, the smaller particles exhibited significant spread in the sclera as well as the suprachoroidal space (Figure 4.1.6a). In contrast, the larger particles are relegated primarily to the suprachoroidal space and are largely excluded from the sclera (Figure 4.1.6b). This localization of large particles is also consistent with results shown in Figure 4.1.2, which includes additional data for 500 and 1000 nm particles.

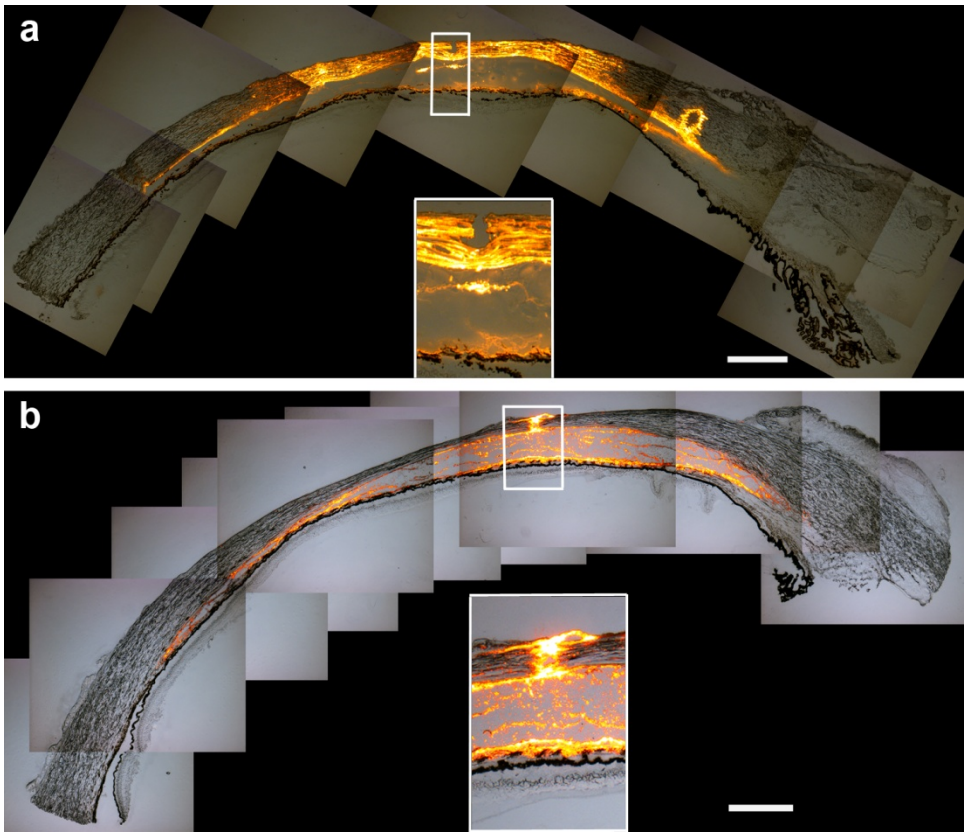

Figure 4.1.6 Effect of particle size on particle distribution in the eye. Collaged fluorescence microscopy images of tissue cryosections show the delivery of (a) 20 nm particles and (b) 1000 nm particles into the suprachoroidal space of pig eyes ex vivo. The images show that 20 nm particles spread in the suprachoroidal space and within the sclera. However, the 1000 nm particles are primarily in the suprachoroidal space. The insertion sites are magnified in the insets. Scale bar: 500 μm.

In summary, 20 and 100 nm particles were reliably injected using a minimum microneedle length of 800 μm and a minimum pressure of 250 kPa. To deliver 500 and 1000 nm particles, a minimum microneedle length of 1000 μm and a minimum pressure of 250 – 300 kPa was necessary.

4.1.4 Effect of Intraocular Pressure

We predict that an increase in intraocular pressure (IOP) should increase the success rate of particle delivery into the suprachoroidal space. To clarify, IOP is the internal pressure within the eye that keeps the eye inflated. It provides a back pressure that can counteract the infusion pressure. However, our infusion pressures of 150 – 300 kPa are two orders of magnitude greater than the mean IOP in a normal adult of 15-16 mmHg (~2 kPa) (Klein et al 1992), which means that IOP should contribute insignificant back pressure. Instead, we hypothesize that the main effect of elevated IOP is to make the sclera surface more firm, which reduces tissue surface deflection during microneedle insertion and thereby increases the depth of penetration into sclera for a microneedle of a given length. In a previous study, we similarly found that tissue deformation in the skin limited microneedle insertion depth (Martanto et al 2006).

To test this hypothesis, we injected 1000 nm particles at two different levels of IOP, 18 and 36 mmHg. Consistent with our hypothesis, delivery success rate increased at elevated IOP, as shown in Figure 4.1.7 (ANOVA, $p<0.05$). Notably, at normal IOP, no particles were delivered at the lowest infusion pressure (150 kPa) or using the shortest microneedles (700 μm) and only the longest microneedles (1000 μm) achieved 100% success rate at the highest infusion pressure (300 kPa) (Figure 4.1.7a). In contrast, at elevated IOP, particles were sometimes delivered at the lowest infusion pressure and using the shortest microneedles, and a 100% success rate was achieved using both 900 and 1000 μm microneedles at the highest infusion pressure (Figure 4.1.7b). Although we did not measure microneedle insertion depth directly, these results suggest that microneedle insertion may be more effective at elevated IOP because they insert deeper into the sclera and thereby increase infusion success rate.

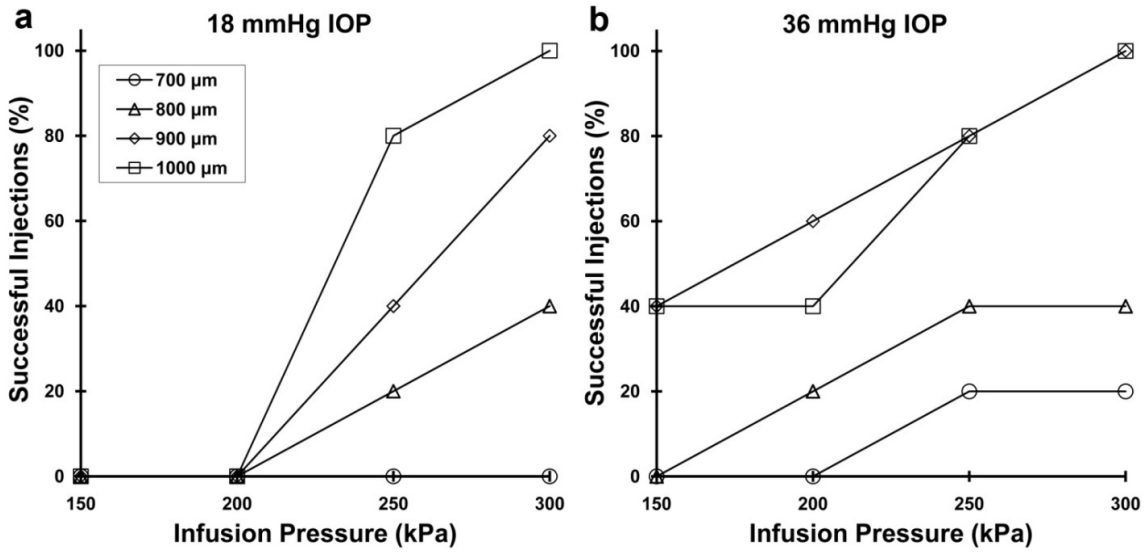

Figure 4.1.7 The effect of infusion pressure and microneedle length on the success rate of suprachoroidal delivery of 1000 nm particles at simulated IOP

levels of (a) 18 mmHg and (b) 36 mmHg. A total of five infusions were attempted at each condition studied. The delivery success rate generally increased with an increase in IOP. IOP significantly affected delivery success rate as a function of infusion pressure when using 800, 900, and 1000 μm long microneedles ($p<0.05$).

4.1.5 Discussion

This work introduced a minimally invasive strategy for drug delivery to the back of the eye. It showed that a hollow microneedle can inject liquid solution and suspensions of particles into the suprachoroidal space of rabbit, pig and human eyes ex vivo. Suprachoroidal delivery represents an improvement over current periocular and intravitreal delivery methods, both of which are poorly targeted to the retinochoroidal sites of most posterior segment diseases. Rather than injecting drug outside the eye or in the vitreous humor, microneedle technology enables precisely targeted injection within the suprachoroidal space of the ocular tunic, which bathes the chorioretinal surface with the drug formulation. Moreover, by taking advantage of the unique features of ocular anatomy, microneedle injection does not infuse the drug formulation in all directions from the injection site as in conventional injections. Instead, by targeting the suprachoroidal space, the drug formulation infuses circumferentially within the suprachoroidal space to cover a significant area of the back of the eye via a single injection.

This method of delivery has four important attributes of an effective drug delivery system for the posterior segment. First, the use of a hollow microneedle allows the delivery method to be minimally invasive, because the microneedle

only penetrates hundreds of micrometers into the eye, which should protect the retina from mechanical damage and reduce the risk of infection. This is a significant improvement over past studies that have accessed the suprachoroidal space using much more invasive procedures (Einmahl et al 2002, Gilger et al 2006, Olsen et al 2006, Kim et al 2007) and may offer a safety profile similar to that of conventional intravitreal injection. Second, the suprachoroidal space offers the ability to target the choroid and retina by localizing the injection immediately adjacent to these tissues. Third, we showed the potential for sustained delivery by demonstrating injection of particles up to 1000 nm in diameter into the suprachoroidal space. The ability of the suprachoroidal space to accommodate particles has not been previously reported. This finding suggests the possibility of injecting drug-loaded biodegradable particles into the suprachoroidal space for sustained drug release over a period of weeks to months, which could reduce the frequency of drug administration. Finally, the inherent safety and simplicity of microneedle injection suggest that suprachoroidal delivery could be carried out as a straightforward office procedure, rather than the surgical procedures required in previous suprachoroidal delivery studies (Einmahl et al 2002, Gilger et al 2006, Olsen et al 2006, Kim et al 2007).

This study further showed that microneedle length, particle size and infusion pressure all affect the success rate of particle delivery to the suprachoroidal space. Notably, suprachoroidal injection was found to either occur fully or not to occur at all for any given injection attempt. This binary (i.e., all or nothing) response suggests that a critical event must occur to enable infusion,

and we believe that critical event is formation of a pathway from the microneedle tip to the suprachoroidal space through the sclera. Because microneedles appear to be inserted into, but not fully across the sclera, particles must find a path through the remaining scleral tissue to reach the suprachoroidal space. This approach is advantageous, because it minimizes mechanical damage to the eye and isolates the choroid and retina from the microneedle.

Our data indicates that smaller particles (20 - 100 nm) can more easily flow through scleral tissue because the sieving effect of the sclera's collagen fibers (Jiang et al 2009) allows smaller particles through, but blocks larger particles (500 – 1000 nm). The success rate is therefore increased by increasing microneedle length, which reduces the amount of scleral tissue between the microneedle and suprachoroidal space, and by increasing infusion pressure, which provides a greater driving force to push particles through the sclera. Increased microneedle length and infusion pressure were especially important for larger particles. Although an elevated IOP is not necessary for injection and neither is it desirable in patients, we found that elevated IOP also increased infusion success rate. We believe that elevated IOP reduced scleral surface deflection, which increased microneedle insertion depth and thereby reduced the amount of scleral tissue between the microneedle tip and the suprachoroidal space.

In this ex vivo study, we were able to inject volumes of 15 – 35 μL into the suprachoroidal space. Larger volumes led to leakage through vortex veins cut during excision of the eye from the animal, which we believe is an artifact of the

ex vivo model. These volumes are somewhat lower than typical intravitreal injections of 50 – 100 µL (Peyman et al 2009). However, previous studies on rabbits have shown that the suprachoroidal space can accommodate fluid up to several hundred microliters in vivo (Mittl and Tiwari 1987), which is supported by our preliminary data using microneedles in rabbits in vivo too (data not shown). We therefore conclude that volumes suitable to administer drug doses of use for ophthalmic applications can probably be administered using microneedle injection into the suprachoroidal space.

All experiments in this study were conducted on freshly excised animal and human cadaver eyes, which is an imperfect model for drug delivery in vivo. For example, the conjunctiva was not present on the eyes tested here, because the conjunctiva generally detaches once the eye is removed from the orbit. The presence of conjunctiva and tear fluid may affect microneedle insertion as additional layers the microneedle must penetrate to reach the suprachoroidal space. Additionally, the spread of solution and particles in the suprachoroidal space may be influenced by choroidal blood flow, which was not present during our experiments. For reference, Kim et al. showed that Gd-DTPA, with a molecular mass of ~1 kDa, is cleared from the suprachoroidal space within hours (Kim et al 2007), which constrains the possibility of sustained drug delivery. However, particles are expected to be cleared much more slowly due to their much larger size than soluble molecules. Spread of a formulation within the suprachoroidal space will also be influenced by the viscosity of the formulation. Formulations that are more viscous than the water-like formulation used in these

studies will most likely spread less within the suprachoroidal space. Detailed in vivo studies are needed to better understand the spread and clearance mechanisms from the suprachoroidal space.

4.1.6 Conclusions

This work provides the first study to evaluate injection into the suprachoroidal space using a microneedle. It shows that this approach offers an attractive route to target the posterior segment of the eye in a simple, minimally invasive way. Delivery of particle formulations into the suprachoroidal space was facilitated by increasing infusion pressure, increasing microneedle length, increasing IOP, and decreasing particle size. Injecting particles in this way could enable sustained drug delivery from the suprachoroidal space and thereby reduce dosing frequency. Finally, this work determined the effect of operating parameters on particle infusion, coupled with mechanistic insight into the injection process that can be used to design microneedle-based drug delivery systems for the suprachoroidal space.

4.2 Spread of Injections in the Suprachoroidal Space

4.2.1 Introduction

Earlier work has shown that small molecules, particles and even gel formulations can be injected into the suprachoroidal space of the eye (Einmahl et al 2002, Patel et al 2011). However, the spread and distribution of injected materials within the suprachoroidal space has not previously been studied. Furthermore, no hollow microneedle device exists which can reliably inject within this space in vivo. A reliable microneedle device may provide a minimally invasive way to access the suprachoroidal space as compared to other injection procedures (Einmahl et al 2002, Kim et al 2007). A demonstration of such a device in an in vivo scenario would provide a valuable tool characterize the spread of materials as well as the capabilities of a microneedle based administration system.

In these studies we seek to design a device to reliably inject into the suprachoroidal space in vivo and understand the spread of materials injected into the suprachoroidal space of rabbit and human eyes. We design the first in vivo hollow microneedle device aimed at injecting into the suprachoroidal space of rabbit eyes and show that the device can reliably inject into the suprachoroidal space of live rabbits in a minimally invasive way. We do so by injecting India ink into rabbits, imaging the delivery in multiple ways and quantifying the number of successful injections. We show that volumes up to 100 μL can reliably be delivered. Furthermore, we quantify the spread of the injected material in the suprachoroidal space and demonstrate the spread as a function of volume. The

data is further characterized to determine the directionality of the spread within the eye.

The second half of the study examines the ability of a simple hollow metal microneedle device to inject into the suprachoroidal space of fresh human eyes ex-vivo. We demonstrate that a microneedle can deliver volumes up to 150 μL into the suprachoroidal space of human eyes. The experiments in this study simulate in vivo conditions and demonstrate the spread of latex within the suprachoroidal space as a function of volume. The study shows that the spread is not radial and there is a definite directionality to the spread. This work represents the first study to examine spread within the suprachoroidal space of human eyes.

4.2.2 India Ink Spread in the Suprachoroidal Space of Rabbit Eyes In Vivo

4.2.2.1 Imaging Spread and Hollow Glass Microneedle Device Reliability

In order to inject into the suprachoroidal space of rabbit eyes in vivo a new hollow glass microneedle prototype device was designed. The effectiveness of the device was tested by attempting to inject India ink into the suprachoroidal space. Of the thirty seven individual injections only two needed to be repeated, resulting in a 95 % success rate. The two injections that were not successful resulted in no injection at all. There was no accidental delivery into another region of the eye. At no point did the microneedle penetrate further into the ocular globe and inject within the vitreous. The two failures can be attributed to improper insertion that did not allow the microneedle to insert properly into the

sclera. Upon repositioning the microneedle and reinserting into the same eye, both injections were successful. In some cases where the pupil was large, the suprachoroidal injection could be observed visually after enucleating the eye from the animal. Figure 4.2.1a shows that by looking through the pupil away from the site of injection (arrow). If you look through the pupil away from the injection site, the India ink is not visible. As the viewing angle is rotated towards the site of injection some dark regions can be viewed (Figure 4.2.1b) and the back of the eye looks partially dark and partially light. The dark black color signifies the presence of India ink while the light color is without. Looking directly towards the site of injection, (Figure 4.2.1c) the whole back of the eye looks dark.

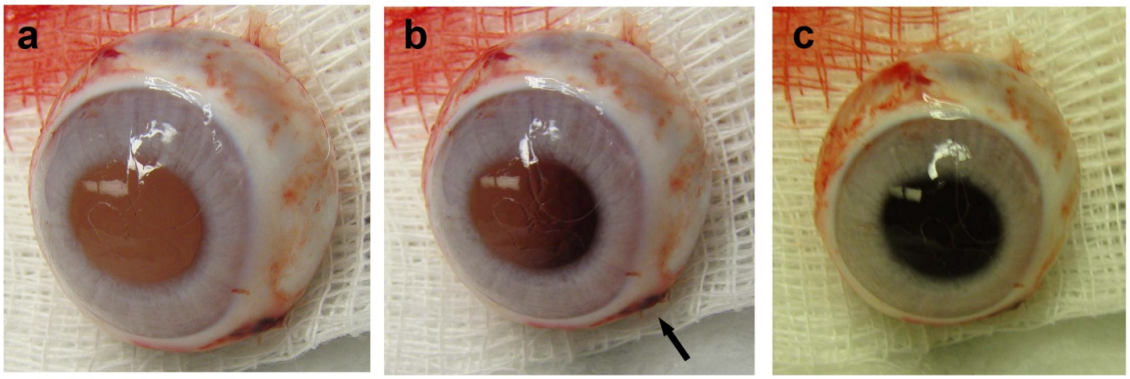

Figure 4.2.1 Images showing a view of an India ink injection into the suprachoroidal space through the pupil. (a) India ink (black) is not visible in the back of the eye when looking away from the injection site (arrow) and as you look towards the injection site (b) more India ink can be seen until the back of the eye looks completely black (c) In this eye, a hollow glass microneedle, 700 µm in length, was used to inject 50 µL into the suprachoroidal space.

Out of all injections, eight (22%) exhibited some amount of reflux through the insertion site upon removal of the microneedle. The amount refluxed was not quantified but in all cases where there was some reflux, less than 10 µL was

refluxed and a significant amount of India ink was still evident in the suprachoroidal space eye of the eye. This is in part due to an increase in intraocular pressure during the injection. This may be from both the injection of the fluid into the suprachoroidal space as well as the pressure applied on the eye while the eye is exposed from the socket. The pressure applied on the eye can be reduced with a different approach to positioning the eye during injection. This may in turn reduce the occurrence of reflux. A summary of these data is provided in Table 4.2.1. All injections took less than 1 minute from time of insertion to removal of the microneedle from the eye. The actual injection time took less than 20 seconds.

Table 4.2.1 Table of statistics from injections of India ink within the suprachoroidal space of live rabbits.

Volume injected	Number of injections	Number of injections successful on first attempt	Number of injections without any reflux
30 µL	8	8 (100%)	7 (88%)
50 µL	23	21 (91%)	17 (74%)
100 µL	6	6 (100%)	5 (83%)
Totals	37	35 (95%)	29 (78%)

Suprachoroidal injection success was imaged at two different levels. The first was from a macroscopic perspective done by freezing the eye using the snap freeze technique. The results showed that the India ink was indeed limited to the suprachoroidal space and the spread of the India ink could be clearly seen.

Figure 4.2.2a shows the back of the whole eye with the optic nerve in the center. The India ink has clearly spread all the way to the back of the eye near the optic nerve. The spread of the India ink appears to be confined between the sclera and retinal tissues. This is observed by removing the sclera, choroid and retina out of the eye as one whole piece and looking at the inside of the back of the eye (Figure 4.2.2b). The 'cup' of the back of the eye shows that the India ink has covered a specific surface area in these tissues. By examining the remaining frozen part of the eye, Figure 4.2.c, it is clear that the India ink has not penetrated into the vitreous as it is completely clear and free of any black pigmentation from the India ink. A thin strip of India ink (II) can be seen around the equator within the remaining tissues of the globe. An arrow marks the injection site (IS) on the sclera.

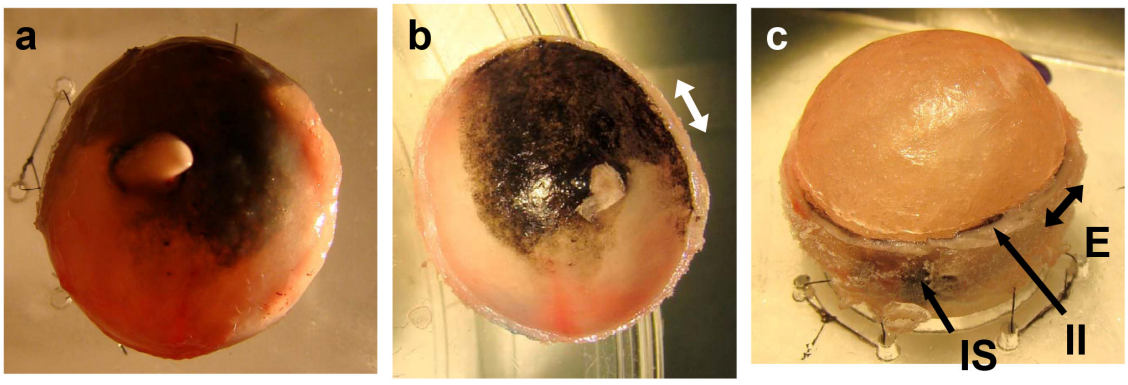

Figure 4.2.2 Images of a frozen rabbit eye after India ink injections into the suprachoroidal space. (a) A view from the back of the whole eye shows the India ink has reached all the way to the optic nerve, (b) A view of the sclera, choroid and retina tissues after they are removed as a cup from the equator. The equator (E) is marked with double arrows. This view shows the back of the eye from the inside and the India ink within those layers. (c) The vitreous is free from the India ink and the injection site (IS) is marked. The India ink (II) can also be seen as a ring near the equator (E) in the portion of the eye that is left after removing the posterior cup (b).

In order to confirm delivery into the suprachoroidal space at a microscopic scale some of the eyes were fixed, cut into sections and stained for histological examination. After fixation a section of the eye was easily cut from the eye including the sclera choroid and retina just below the injection site. Viewing the tissues from the inside the eye clearly shows the India ink within these layers. Figure 4.2.3 shows the spread of the India ink in the removed sample and also the globe. The sample is nearly all black and the India ink has reached all the way to the optic nerve of the eye. Looking in the globe clearly shows a region of the eye where there is India ink (dark black region) and where there isn't (clear white region). There is no India ink in the vitreous further confirming that the microneedle did not penetrate into the vitreous.

The histological cross sections also confirmed the localization of the India ink to the suprachoroidal space (Figure 4.2.4). The India ink is selectively located just between the sclera and choroid layers of the globe. There is no evidence of India ink in the retina indicating no penetration of the microneedle deeper than the suprachoroidal space. This data indicates this microneedle device is a reliable device to use for injection into the suprachoroidal space of rabbit eyes in vivo.

Figure 4.2.3 A whole rabbit eye after fixation in glutaraldehyde. A section of the globe removed near the injection site is flipped over to reveal the Inida ink (black) within the tissues of the globe. A view of the inside of the eye shows that no India ink appears in the vitreous but some can be seen in the remaining tissues of the globe.

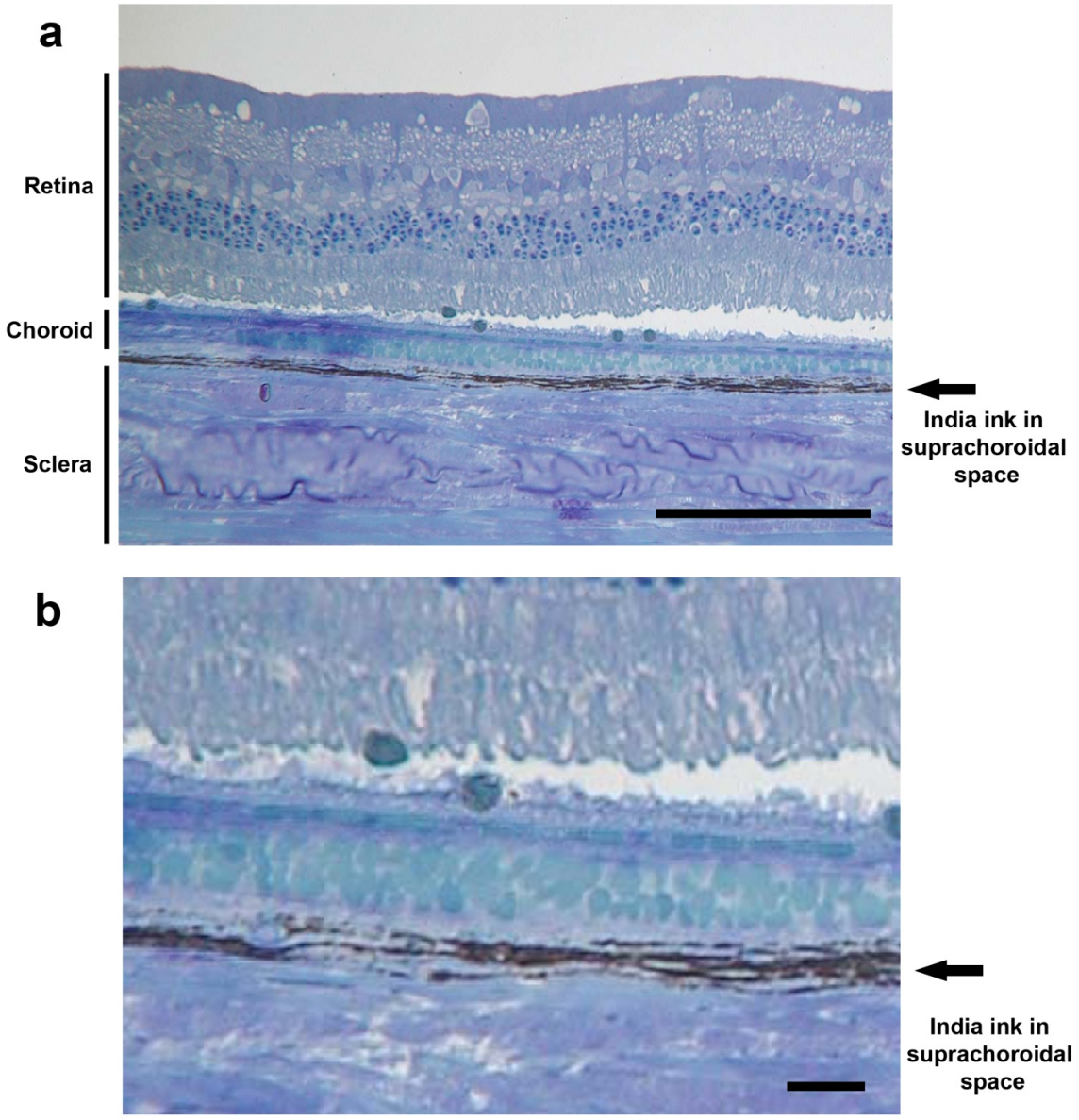

Figure 4.2.4 Histological cross section of the rabbit eye showing India ink within the suprachoroidal space. (a) The India ink can be seen in black located between the sclera and choroid layers of the eye tissue. Scale bar: 200 μm. (b) A magnified view of the India ink in the suprachoroidal space. Scale bar: 25 μm.

4.2.2.2 Quantifying Spread of India Ink in the Suprachoroidal Space

We hypothesize that India ink could be spread in the suprachoroidal space so as to cover a large area of the chorioretinal surface. In order to determine the coverage we injected 30, 50 and 100 μL into the suprachoroidal space and

quantified the spread within the space. We also hypothesize that the spread would increase with increased volume rather than simply expanding the suprachoroidal space and causing increased separation between the sclera and choroid layers. In order to test these theories and understand the spread within the suprachoroidal space of live rabbit eyes we injected material and characterized the delivery in a variety of ways.

Suprachoroidal injections were performed in the superior temporal quadrant of the rabbit eye in vivo. Figure 4.2.5 shows an example of the orientation of the rabbit eye relative to the injection site. An asterisk indicates the injection site in the right eye of the rabbit and an arrow indicates the direction downwards towards the nose. After injection of India ink, the eyes were enucleated and the spread of the India ink injected into each eye was digitized. Figure 4.2.6 displays all the digitized images of the injections. Each digitized image contains an asterisk to indicate the injection site, an arrow pointing to the optic nerve, and the letter N indicating the direction downwards towards the nose. In both right and left eyes the direction from the injection site to the nose is analogous to the direction indicated in Figure 4.2.5.

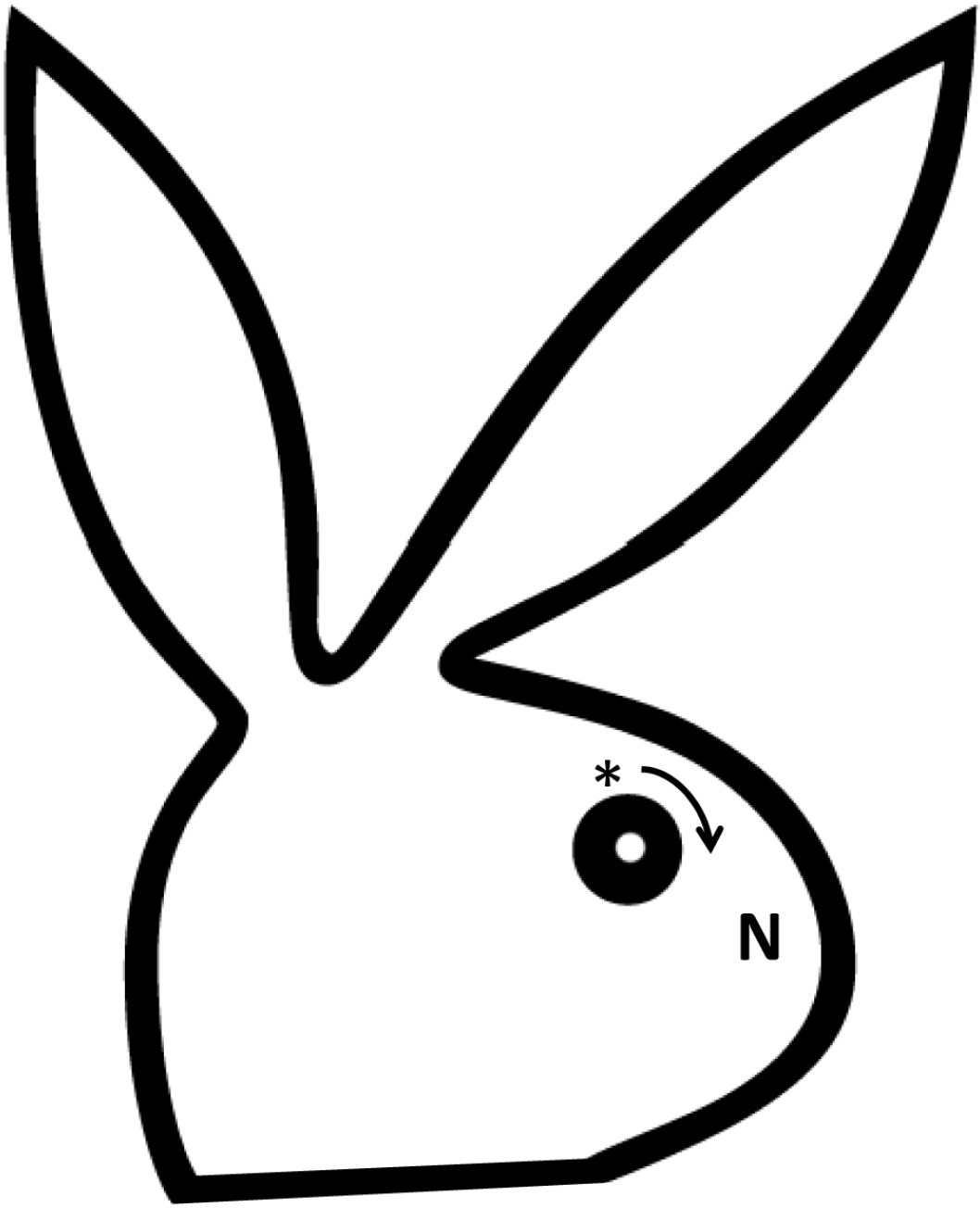

Figure 4.2.5 Injections of India ink were done on live rabbits in the superior temporal quadrant of the eye. The eyelids were pushed back to access the insertion site (*) more clearly. The image shows the approximate location of the injection site (*). It also shows the direction towards the nose (N) indicated by the arrow for reference and orientation of future images.

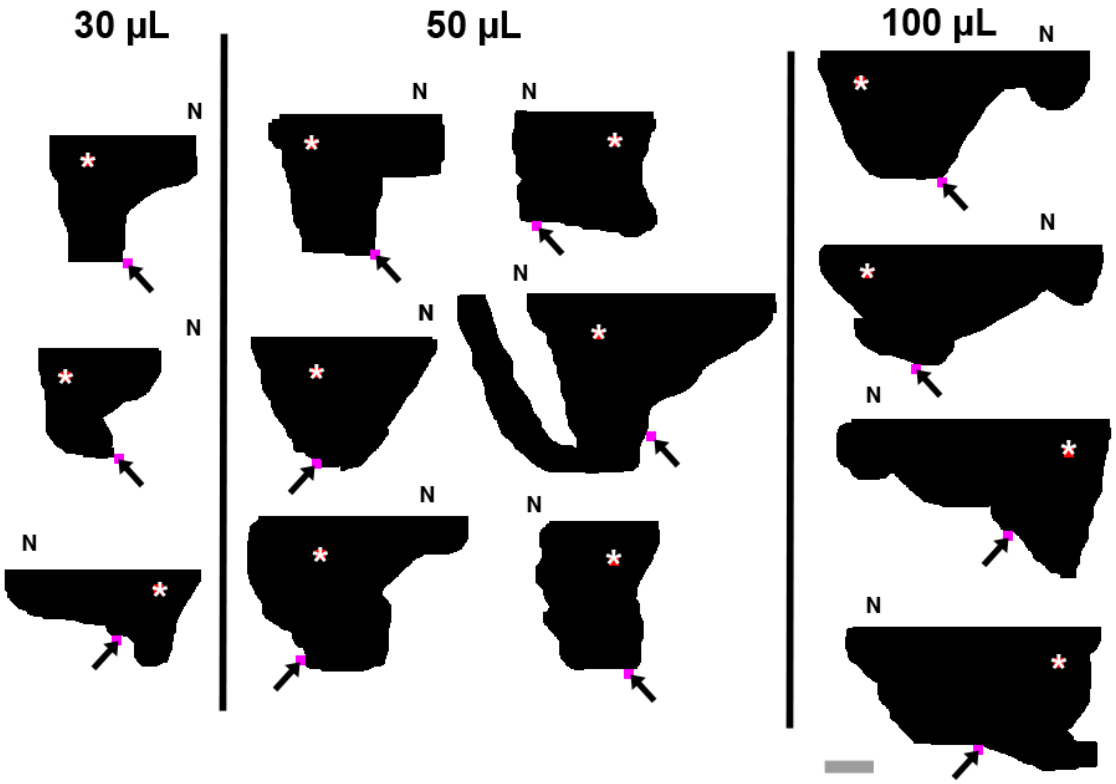

Figure 4.2.6 Digitized distribution of India ink within the suprachoroidal space of rabbit eyes. An asterisk indicates the injection site, the arrow points to the location of the optic nerve, and the letter N indicates the direction towards the nose. Scale bar: 5 mm.

Qualitative analysis of the spread from these images shows the India ink does not flow uniformly from the injection site; i.e. it does not spread in a radial fashion from the site and there appears to be some directionality to the flow. We hypothesize this directionality is not dependant on the microneedle but instead on the anatomy of the eye. The injection was done in the same quadrant of the rabbit eye, superior temporal, on both right and left eyes. Overall the India ink travels laterally towards the nasal direction along the limbus more than the opposing direction. This is more dramatic in the 100 µL injection images since the large volume causes the discrepancy between the two directions to be more

obvious. This is also confirmed quantitatively by calculating the ratio of the max distance towards the nose versus the opposing direction from the injection site. The ratios are 3.4±0.4, 2.3±1.1, 6.2±0.7 for 30, 50 and 100 µL respectively. The images also reveal that the injection stops abruptly at the limbus and does not move further towards the anterior segment of the eye. The injection site was chosen to be approximately 3-4 mm posterior to the limbus and calculations of the furthest distance the India ink traveled towards the anterior segment shows that it does not move beyond the limbus. The maximum distance anterior is 2.2±0.4, 2.8±0.4, 2.7±0.3 for 30, 50 and 100 µL respectively. This phenomenon is clearly seen after the eye is enucleated (Figure 4.2.3). This may be due to the dense cilliary processes and muscles present near the limbus that prevent expansion of the tissues. As a result, the limbus serves as a natural barrier that does not allow fluid within the suprachoroidal space to flow into the anterior segment. In addition since the limbus region is facilitates uveal scleral outflow of aqueous humor from the anterior chamber of the eye into the suprachoroidal space it may not allow flow in the opposing direction.

We hypothesize that volumes up to 100 µL of India ink injected into the suprachoroidal space will not simply accumulate in a confined area within the suprachoroidal space but spread further into unoccupied areas as more volume is injected. This appears to be true qualitatively (Figure 4.2.8) but in order to prove this we calculated and compared the choroiretinal surface area covered by each injection. The total area covered was calculated from each injection's digitized image. Figure 4.2.7 shows that as the volume of India ink injected

increases the surface area covered increases as well. On average the delivery of 30, 50 and 100 µL resulted in coverage of 113±15, 175±26 and 249±25 mm^2 of the choroiretinal surface, respectively. These values are statistically different from each other (ANOVA $p<0.05$) indicating that the India ink is spreading into uncovered portions of the suprachoroidal space as more volume is injected.

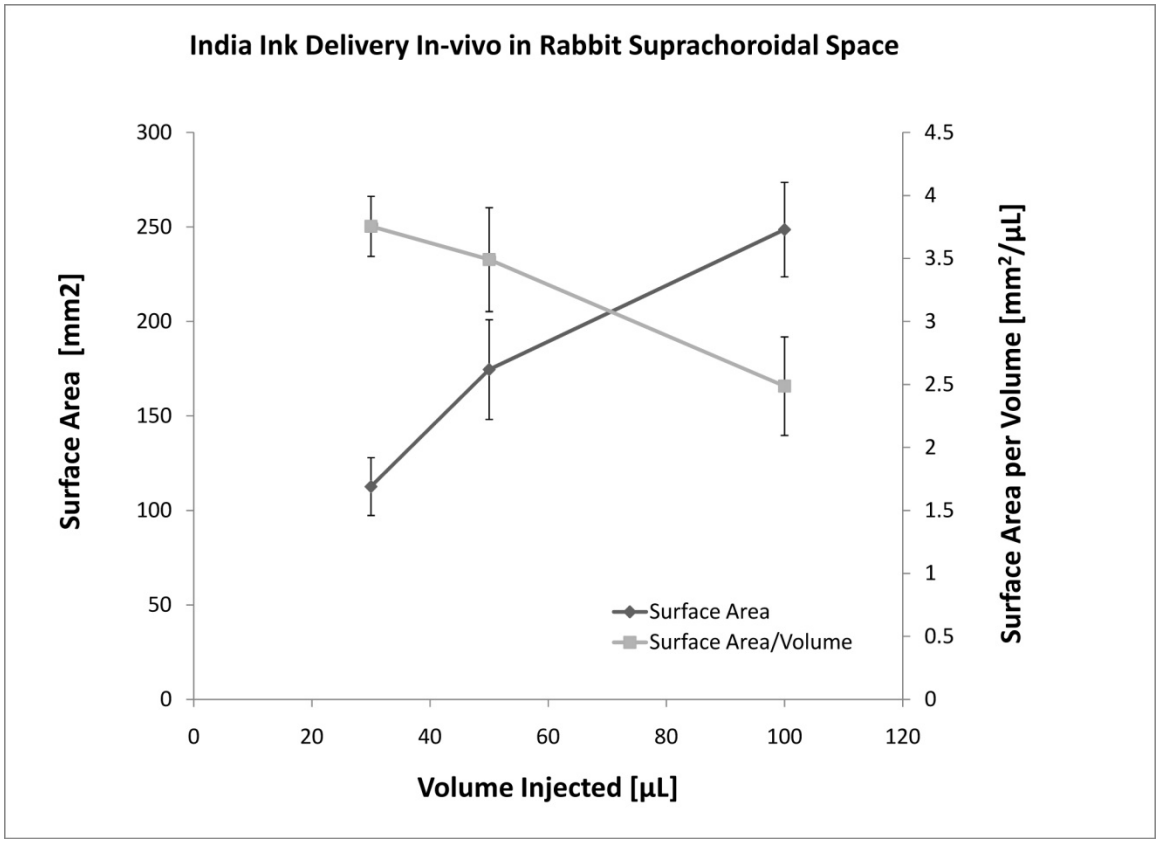

Figure 4.2.7 A graph showing the surface area covered from 30, 50 or 100 µL (x-axis) of India ink injected in the suprachoroidal space in vivo in rabbits using a glass microneedle. The chorioretinal surface area (left y-axis) covered increases with increasing volume. The surface area per volume of India ink (right y-axis) injected decreases as the volume injected increases. A minimum of n=3 injections were performed for each volume and standard deviations are shown.

We further hypothesize that as the volume of an injected fluid within the suprachoroidal space increases it will not only spread within unoccupied regions

of the suprachoroidal space but it will also cause an expansion of the suprachoroidal space. Our theory is that since this is a virtual space, it will allow the sclera and choroid to separate further from each other to accommodate the additional fluid. In order to show this was occurring with our India ink injections we further characterized the spread of India ink by normalizing the chorioretinal surface area covered by the volume injected. Figure 4.2.7 shows the surface area covered per volume is 3.8±0.2, 3.5±0.2 and 2.5±0.4 mm^2/ µL for 30, 50 and 100 µL respectively. The graph shows this normalized value drops as the volume is increased.

If the additional volume injected was simply expanding into unoccupied regions of the suprachoroidal space, then the surface area per volume would remain constant. If however, the additional volume was causing an expansion of the suprachoroidal space then this value should drop because the fluid is incompressible. Statistical analysis shows that the normalized values for 30 and 50 µL are the same but the value for 100 µL is statistically different from both 30 and 50 µL (ANOVA $p<0.05$). This implies that an increase in injected volume from 30 to 50 µL does not cause the suprachoroidal space to expand much more. Instead the additional 20 µL spreads into new unoccupied regions of the suprachoroidal space. However, when the injected volume is increased from 50 to 100 µL the suprachoroidal space does expand to hold the additional 50 µL. In order to make this more explicit the approximate thickness of the expanded suprachoroidal space for each of these normalized values was determined to be 270±38, 291±38 and 405±40 µm for 30, 50 and 100 µL respectively.

We hypothesize that since the suprachoroidal space is a virtual space in the posterior segment of the eye that can easily expand to hold fluid, suprachoroidal injections should be able to cover a large percentage of the choroiretinal surface area of the eye. To determine what fraction of the available surface area a single microneedle injection could cover we assumed the maximum surface area available in the back of the eye as the area of the sclera. The percentage area covered by injections of India ink was calculated by dividing the area of the India ink injections by the maximum surface area available. Figure 4.2.6 shows the percentage of the back of the eye that was covered by 30, 50 and 100 µL was 17±2, 26±4 and 36±4 %, respectively. The graph shows that the percent covered increases with increasing volume (ANOVA $p<0.05$) and a single injection of 100 µL can cover nearly 36 % of the available area. The suprachoroidal space of the rabbit eye may be able to accommodate even more than 100 µL. However, additional volume may cause the space to expand in thickness and limit the additional volume of fluid from spreading into new regions of the suprachoroidal space that are not already occupied by the injected formulation.

.

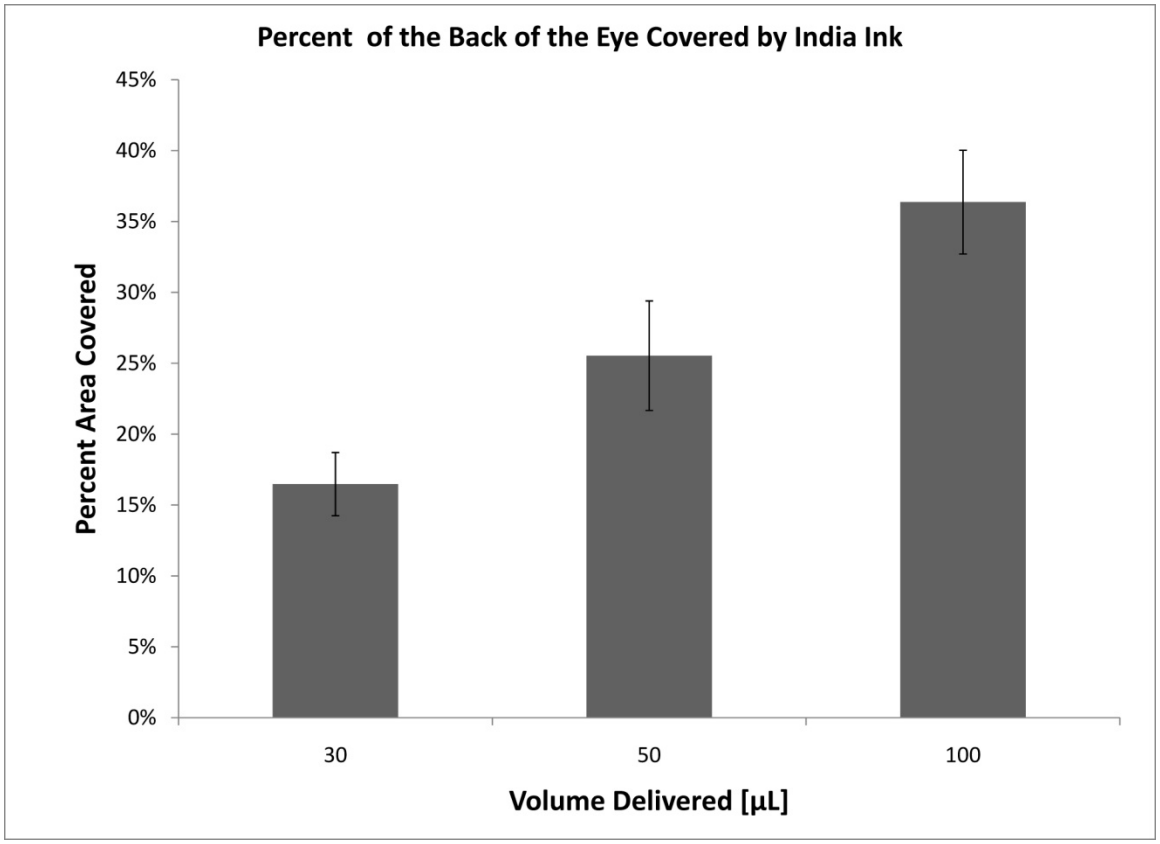

Figure 4.2.8 A graph showing the percentage surface area covered from a microneedle injection of India ink in the suprachoroidal space in vivo in rabbits. The percent area is on the y-axis and the volumes injected on the left. Error bars represent standard deviations. Each value is statistically different (ANOVA $p<0.05$) from each other indicating that the percent covered is increasing with increasing volumes.

In order to characterize the directionality of the injections we determined the maximum spread of India ink in two directions: (1) distance from the limbus towards the optic nerve and (2) the total lateral distance parallel to the limbus. The first represents the ability of the India ink to move further to the back of the eye and the second represents the ability of the India ink to spread around the eye along the equator. In all thirteen injections the India ink was able to reach the back of the eye, i.e. the optic nerve as shown in Figure 4.2.6. Even at the smallest injection volume, 30 µL, the India ink reached the optic nerve. Figure

4.2.9 summarizes the analysis of the directionality of the spread. The y-axis represents the maximum distance traveled in the two directions and the x-axis shows the two directions measured. The asterisks indicate the distances that are statistically significant between the different injection volumes (ANOVA $p<0.05$). On average the maximum distance the India ink traveled towards the optic nerve and the back of the eye was 11±1.6, 15±2.0, and 13±2.1 mm for 30, 50 and 100 µL injections, respectively. There was only a statistical difference between 30 and 50 µL indicating that the additional volume after 50 µL did not really cause the India ink to spread further in the back of the eye. The average distance covered laterally in parallel to the limbus was 16 ± 3.8, 19 ± 5.5, and 27 ± 1.2 mm for 30, 50 and 100 µL injections, respectively. The lateral distances for 30 and 50 µL injections were not statistically different but for the 100 µL injection the lateral distance was statistically different from the other two. This is indicates that after 50 µL there is significant spread in the lateral direction. Putting these two pieces of information together implies that Injecting 30 and then 50 µL causes the India ink to spread towards the back of the eye and does not spread much further since it has reached the optic nerve. The additional volume injected, up to 100 µL total, causes the spread to occur around the eye and also expands the suprachoroidal space thickness.

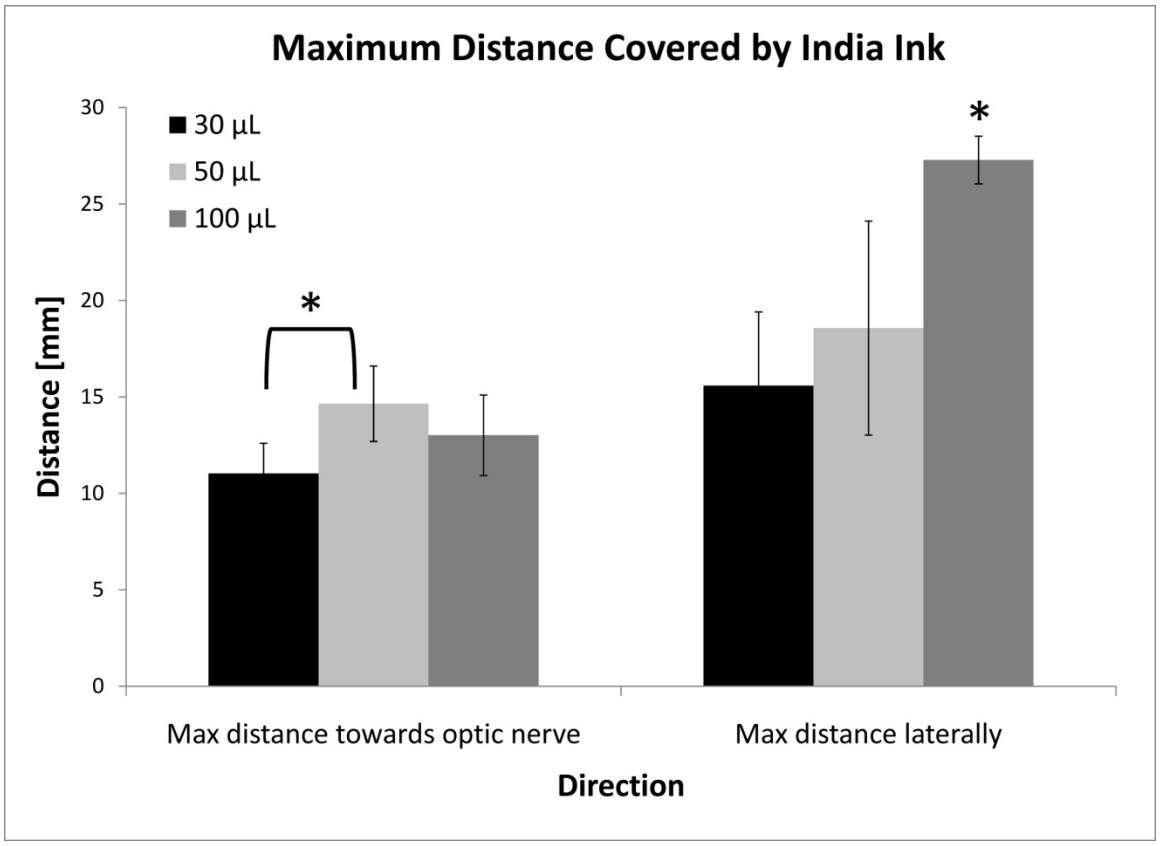

Figure 4.2.9 Graph showing the distance covered from a microneedle injection of different volumes of India ink in the suprachoroidal space of rabbit eyes in vivo. The y-axis represents the maximum distance traveled in the two directions and the x-axis shows the two directions measured. The max distance towards the optic nerve is the maximum distance the India ink covers from the limbus to the back of the eye. The max lateral distance is the maximum total distance the India ink covers parallel to the limbus (i.e. around the eye) The asterisks indicate the distances that are statistically significant between the different injection volumes (ANOVA $p<0.05$).

4.2.3 Spread of Latex in Human Eyes Using Hollow Metal Microneedles

We hypothesize that our hollow metal microneedles would be able to inject formulations into the suprachoroidal space of human eyes in a simulated in vivo experimental setup. We further hypothesize that the microneedles would be able to reliably inject volumes up to 150 μL and be able to cover a significant portion of the back of the eye. In order to test this we developed a procedure to visualize the spread of a formulation delivered within the suprachoroidal space. The procedure involved injecting latex into human eyes, snap freezing the whole eye and dissecting it in a way so as to preserve the injected latex on the inside part of the sclera where it could be imaged and quantified. We used this procedure to inject human eyes with a latex formulation and quantified the spread of the latex in the suprachoroidal space. We chose to perform these experiments on eyes that were freshly enucleated from humans. The reason for choosing this condition was to preserve as much as possible the structure and arrangement of the layers of the eye. In addition, we induced an intraocular pressure of 15 mm Hg to simulate the pressure in a living eye. The insertion site was located 8 mm posterior to the limbus. This distance was chosen since it would be accessible on an actual patient using a microneedle. A summary of the eyes used and injection parameters are listed in Table 4.2.2.

Table 4.2.2 Table showing the characteristics of the human eyes used and the experimental parameters tested. The eyes were obtained as quickly as possible from the time of death. The longest time between death and injection was less than 8 hours.

Globe #	Time of Death	Injection Time	Time Difference [HH:MM]	Injection Volume [µL]
1	9:20	14:57	5:37	50
2	7:31	15:23	7:52	50
3	12:17	17:15	4:58	50
4	9:20	15:07	5:47	100
5	7:31	15:17	7:46	100
6	12:17	17:20	5:03	100
7	2:49	10:04	7:15	150
8	12:29	16:23	3:54	150
9	12:29	16:24	3:55	150

A single hollow metal microneedle was able to inject volumes up to 150 µL into the suprachoroidal space. The eye was frozen and the globe was dissected using a blade, into “petals” starting from the optic nerve. The cuts were made up to the cornea leaving the cornea intact. The petals were opened up from the optic nerve. The petals contained the tissues of the globe (sclera, choroid and retina) and exposed the vitreous inside as a frozen white ball. The vitreous was removed carefully leaving the globe tissues and anterior segments of the eye. The petals were laid flat with the cornea in the center and the choroid and retina were slowly pulled away. This left behind latex (pink in color) on the sclera that could be easily distinguished from the white sclera with the transparent cornea in the center of the petals. Figure 4.2.3 shows representative images of the different volumes injected after this procedure has been performed. The surface area could then be quantified from the images by determining the area that the pink latex covered. The total area could be determined by calculating the area of the white colored sclera plus the pink latex covered area.

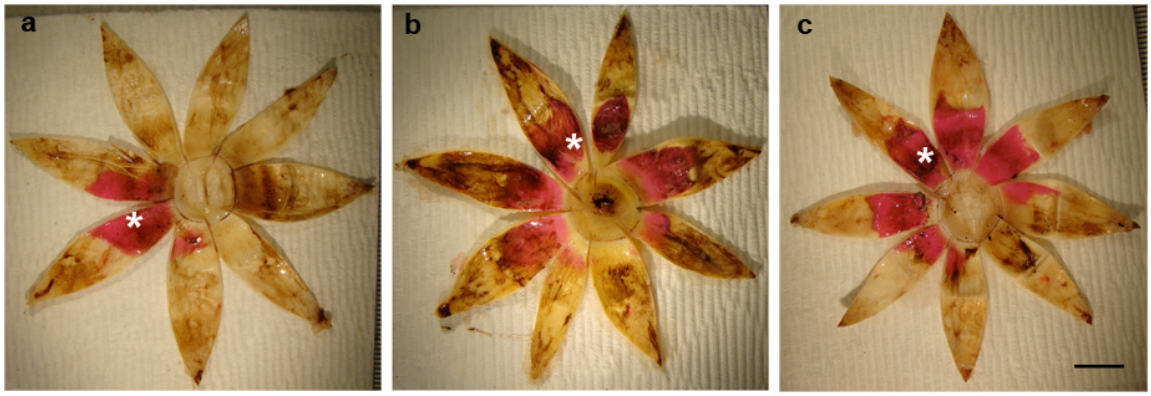

Figure 4.2.10 Representative images of the spread of latex in the suprachoroidal space after injection of (a) 50 µL, (b) 100 µL, and (c) 150 µL using a hollow metal microneedle. The white petals are the sclera with pink latex on top of them. Some of the sclera is pigmented (b) and is darker than others. The choroid and retina have been removed and the cornea is in the center. The injection site is marked with an asterisk. Scale bar: 10 mm.

We hypothesize that there may be a maximum chorioretinal surface area that a single microneedle injection of latex can cover. In order to determine this we determined the surface area coverage from injections of up to 150 µL of latex. The injections resulted in coverage of 257 ± 50, 432 ± 105 and 439 ± 6 mm^2 area of the back of the eye for from 50, 100, and 150 µL respectively. The data suggest that the spread of latex increases with an increase in volume from 50 to 100 µL however, further increase in volume does not result in a substantial increase in area. Statistical analysis (ANOVA $p<0.1$) confirmed that the areas corresponding to 50 and 100 µL were different but there was no difference in 100 and 150 µL areas. In order to confirm that this was not simply a result of a difference in the sizes of the eyes or available area, the percent coverage was calculated by normalizing the areas to the total available area for injection. These areas correspond to 17 ± 4, 39 ± 10 and 40 ± 1 % of the total area available in

the back of the eye. Statistical analysis (ANOVA $p<0.1$) confirmed that the percentages corresponding to 50 and 100 µL were different but there was no difference in 100 and 150 µL percent areas (Figure 4.2.11). However, these data do show that a single microneedle injection of 100 or 150 µL could cover approximately 40 % of the back of the eye.

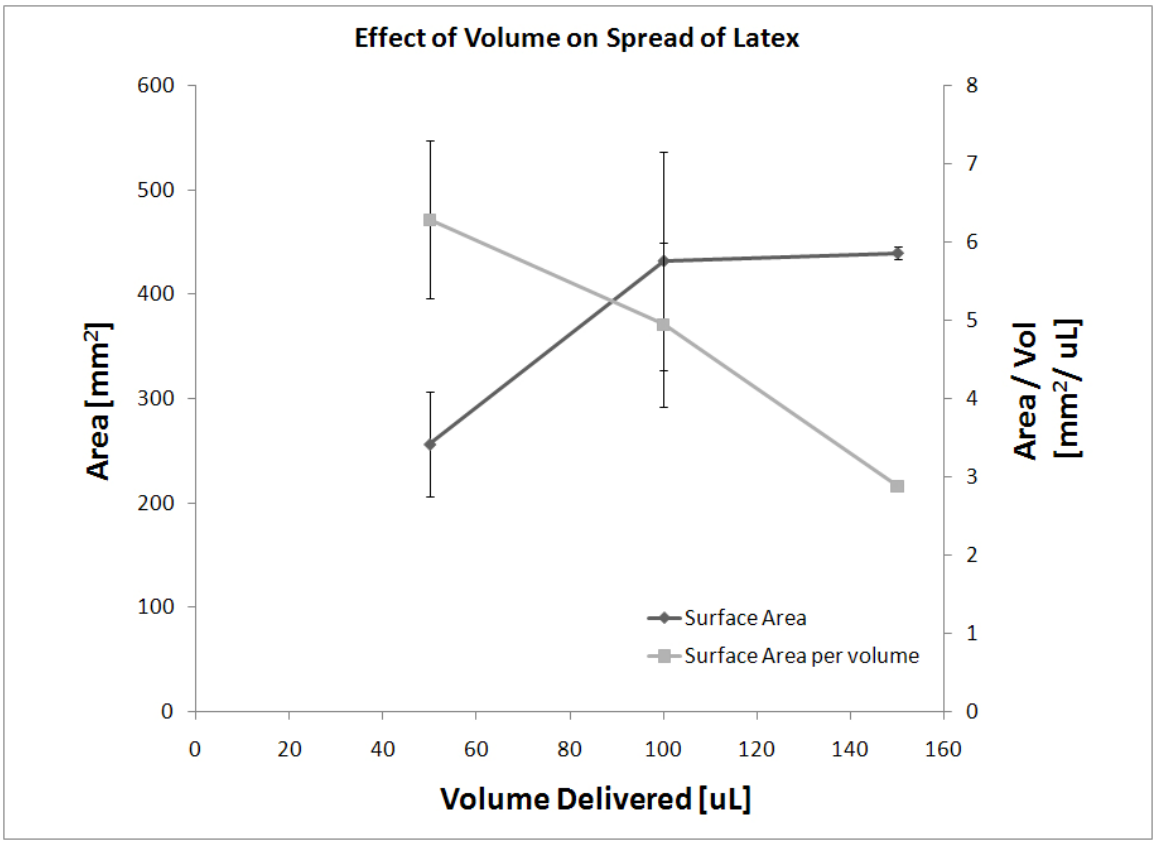

Figure 4.2.11 Graph showing the surface area covered from a single microneedle injection of latex in the suprachoroidal space of fresh human cadaver eyes The x-axis displays the volume delivered. The surface area covered (diamond markers) show the surface area covered using the left y-axis. The surface area per volume of fluid (square markers) is plotted against the right y-axis. Error bars are standard deviations.

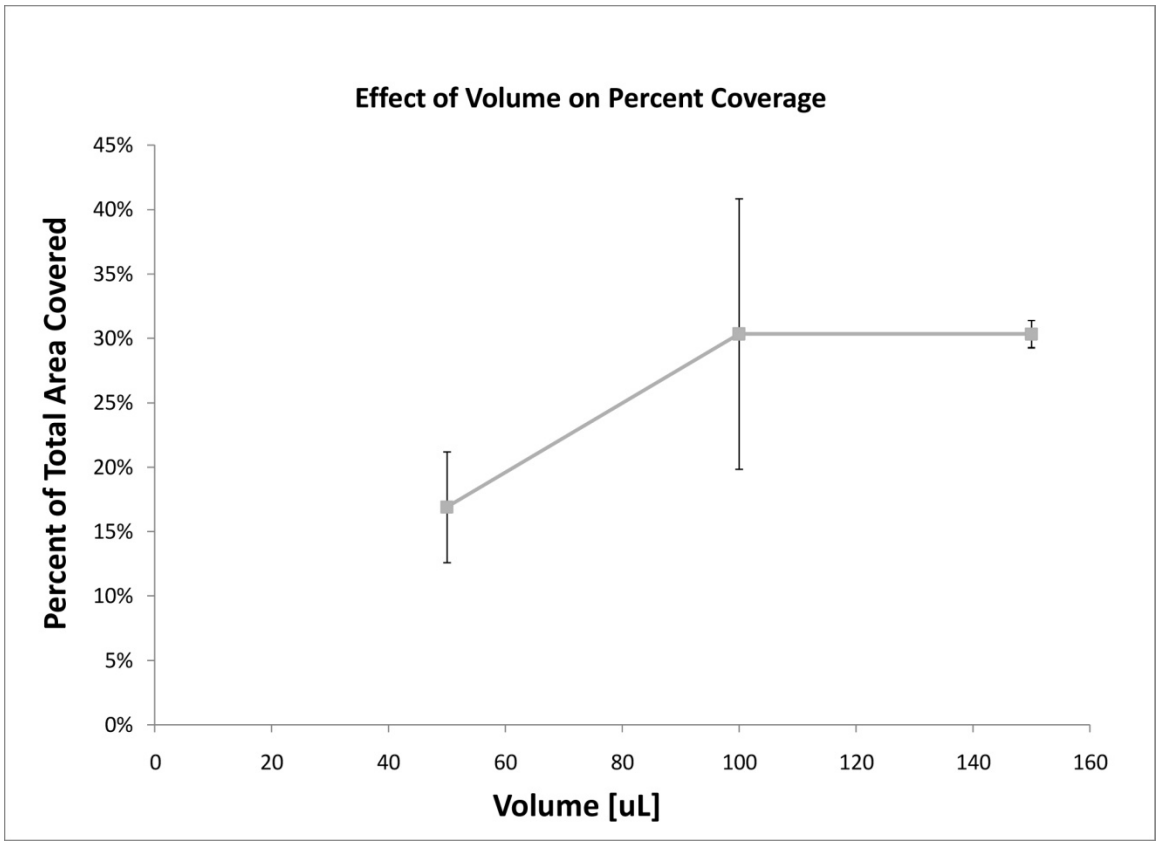

Figure 4.2.12 Graph showing the percent area covered from a microneedle injection of latex in the suprachoroidal space of fresh human cadaver eyes. Error bars are standard deviations.

We further hypothesize that as the volume of latex injected within the suprachoroidal space increases it will not only spread within unoccupied regions of the suprachoroidal space but it will also cause an expansion of the suprachoroidal space. Our theory is that since this is a virtual space, after some threshold volume the suprachoroidal space may expand in thickness significantly. In order to determine this value with latex injections we further characterized the spread of India ink by normalizing the chorioretinal surface area covered by the volume injected. Figure 4.2.11 shows the surface area covered per volume is 6.3 ± 1.0, 4.9 ± 1.1 and 2.9 ± 0.1 $mm^2/\mu L$ for 50, 100 and

150 μL respectively. The graph shows this normalized value drops as the volume is increased.

If the additional volume injected was simply expanding into unoccupied regions of the suprachoroidal space, then the surface area per volume would remain constant. If however, the additional volume was causing an expansion of the suprachoroidal space then this value should drop because the fluid is incompressible. Statistical analysis shows that the normalized values for 50 and 100 μL are the same but the value for 150 μL is statistically different from both 50 and 100 μL (ANOVA $p<0.1$). This implies that an increase in injected volume from 50 to 100 μL does not cause the suprachoroidal space to expand more. Instead the additional 50 μL spreads into new unoccupied regions of the suprachoroidal space. However, when the injected volume is increased from 100 to 150 μL the suprachoroidal space does expand to hold the additional 50 μL. In order to make this more explicit the approximate thickness of the expanded suprachoroidal space for each of these normalized values was determined to be 200±35, 243±69 and 341±5 μm for 50, 100 and 150 μL respectively.

In order to characterize the directionality of the injections we determined the maximum spread of latex in two directions: (1) distance from the limbus towards the optic nerve and (2) the total lateral distance parallel to the limbus. The first represents the ability of the India ink to move further to the back of the eye and the second represents the ability of the India ink to spread around the eye along the equator. Figure 4.2.13 summarizes the analysis of the directionality of the spread. The y-axis represents the maximum distance traveled in the two

directions and the x-axis shows the different volumes injected. The asterisks indicate the distances that are statistically significant between the different injection volumes (ANOVA $p<0.1$). On average the maximum distance the latex traveled towards the optic nerve and the back of the eye was 15±2.0, 17±1.3, and 15±0.3 mm for 50, 100 and 150 µL injections, respectively. There was a statistical difference between 50 and 100 µL injections as well as 100 and 150 µL injections but not between 50 and 150 µL injections. This indicates that there may be some variability in the distance the latex traveled towards the back of the eye but delivering as much as 150 µL did not cause the latex to spread further back than a 50 µL injection. The average distance covered laterally in parallel to the limbus was 15 ± 3.8, 20 ± 8, and 24 ± 1.5 mm for 50, 100 and 150 µL injections, respectively. On average there was an increase in the lateral distance spread around the limbus but neither 50 nor 150 µL injection distances were statistically different from 100 µL injections. This may be due to the high degree of variability in the 100 µL injections. However there was a difference between 50 and 150 µL injections indicating a significant increase in spread in the lateral direction by increasing the volume from 50 to 100 µL. Putting these two pieces of information together implies that injecting volumes in excess of 50 µL may not cause the spread of latex towards the back of the eye to increase much, but does cause the spread around the eye to increase.

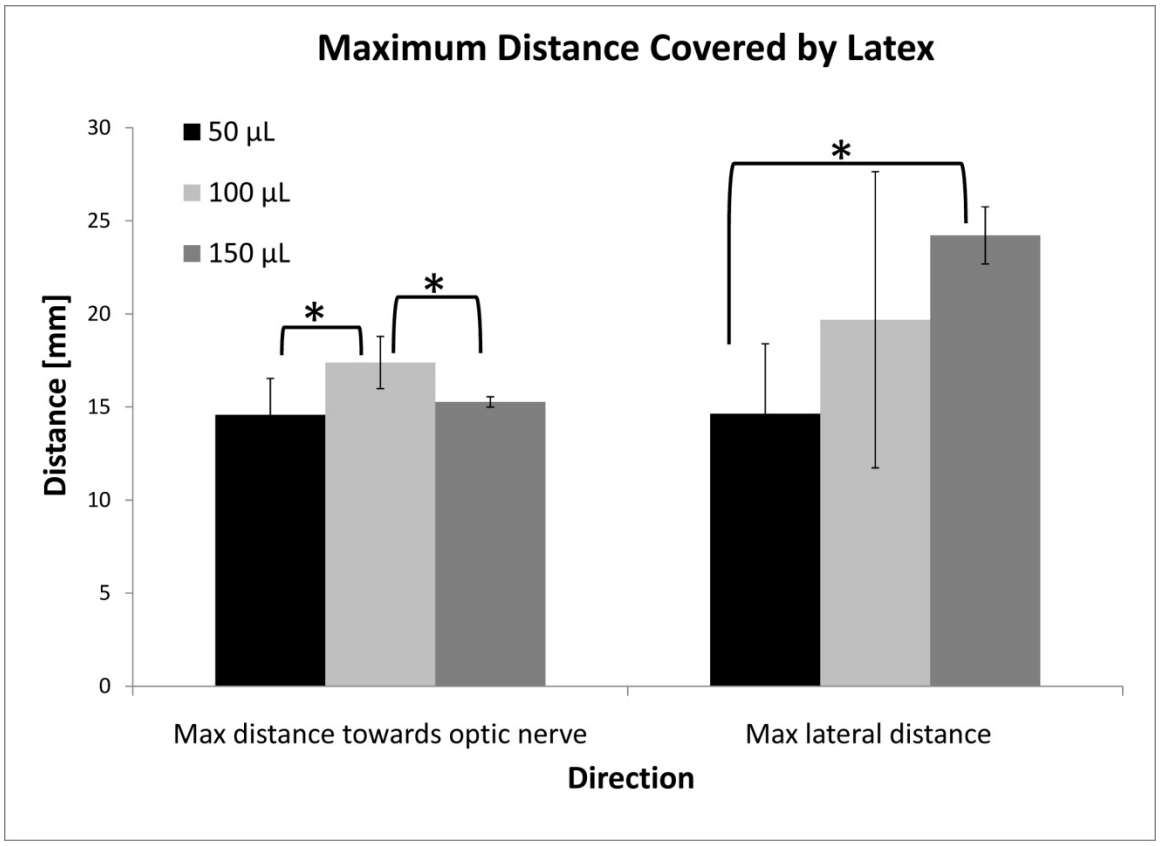

Figure 4.2.13 Graph showing the distance covered from a microneedle injection of latex in the suprachoroidal space of human cadaver eyes. The y-axis represents the maximum distance traveled in the two directions and the x-axis shows the two directions measured. The max distance towards the optic nerve is the maximum distance the latex covers from the limbus to the back of the eye. The max lateral distance is the maximum total distance the latex covers parallel to the limbus (i.e. around the eye). The asterisks indicate the distances that are statistically significant between the different injection volumes (ANOVA $p<0.1$).

4.2.4 Discussion

This study represents the first study to examine the capability of a hollow microneedle to inject within the suprachoroidal space of a live animal eye. The first part of the study showed that a prototype hollow glass microneedle device could reliably inject India ink into the suprachoroidal space of rabbits in vivo. The India ink study showed that volumes up to 100 µL could be delivered into the rabbit eye and the India ink is well localized to the suprachoroidal space. The

coverage of the chorioretinal surface from suprachoroidal injections of India ink was determined and this data showed that up to 36 % of the available surface could be covered from a single microneedle injection of 100 μL. Further characterization of the spread showed the India ink reaches the optic nerve in the back of the eye with a volume as small as 30 μL and further injections do not cause the spread to occur further back but instead in the lateral direction around the eye. In addition, the analysis showed that volumes in excess of 50 μL can cause the suprachoroidal space to expand in thickness and these thicknesses are on the order of several hundred micrometers.

The second half of the study examined the ability of a metal hollow microneedle device to inject latex within the suprachoroidal space of fresh human cadaver eyes. The work showed that it was possible to inject up to 150 μL of latex in to the suprachoroidal space and cover up to 40 % of the chorioretinal surface. In addition, the injections were performed at a site that would be accessible on a human (8 mm posterior to the limbus) and the results show that it is possible to inject in the suprachoroidal space from such a site. In addition the volumes injected represent volumes that are currently being injected into the vitreous for treatment of diseases such as AMD. As a result, this shows that it would be theoretically possibly to inject a comparable dose into the suprachoroidal space.

The latex study implies that there may be a maximum available surface area that a single microneedle injection can cover. The available surface area covered by 100 and 150 μL was nearly identical, 40 %, but the variability for the

two volumes was quite different. For 100 μL the standard deviation was 10 % while for 150 μL it was only 1 %. This suggests that a sufficient volume is needed to fill out the maximum available area after which the additional volume causes the thickness of the suprachoroidal space to expand. In the case of latex in these human cadaver eyes that area may be near the 40 % of the available area, approximately 440 mm^2. Until that area if properly filled the variability may be high, as is the case with 100 μL, and as it gets filled out, this variability decreases. Somewhere between 100 and 150 μL the maximum available surface area may be sufficiently filled and as a result the 150 μL variability is low. This is also consistent with the variability seen in the calculation of the thickness of the suprachoroidal space. The standard deviation for 50 and 100 μL thicknesses was 35 and 67 μm while for 150 μL it was only 5 μm. In the case of the India ink study in rabbit eyes this limit may not have been reached and as a result a similar trend is less explicit.

What this further implies is that a single microneedle injection may not be able to fill all of the available suprachoroidal space. The resistance to flow further into unoccupied regions of the suprachoroidal space versus the resistance to expand the thickness of the suprachoroidal space may be too large. The primary force to overcome for expansion of the space may simply be the intraocular pressure. However it is unclear if the connections of the between the suprachoroidal space and its neighboring tissues, the sclera and choroid, vary significantly in location in the eye. As a result, in order to properly understand if this limit exists and if it is dependent on the anatomy of the eye further studies

need to be done to explore the makeup of the suprachoroidal space, variations in location and the balance of forces in the eye that control the expansion of the suprachoroidal space.

The prototype devices tested for injecting into the suprachoroidal space in this study showed consistent delivery into the suprachoroidal space. Both the hollow glass and metal microneedle devices performed well under the laboratory conditions, however additional modifications need to be made for this method to be applicable for human clinical practice. During the initial tests of the metal microneedle injection, one insertion (out of a total of 16) resulted in an intravitreal injection. This may have occurred because of a combination of a thin sclera and long microneedle. The microneedle may have been longer than was needed to be to reach the base of the sclera and as a result penetrated into the vitreous. Since human sclera thickness can vary between patients and location on the eye, it would be convenient to measure tissue thickness at the site of injection and adjust microneedle length or select and appropriately sized microneedle to ensure successful delivery. An automated insertion and infusion method may also increase the chances of successful deliveries. An insertion method incorporating a feedback system when the needle has inserted properly into the sclera and that infuses the fluid slowly into the suprachoroidal space may also reduce the occurrence of reflux from the eye. The current design shows promise in a research setting and improvements such as these may make the device more reliable and safe for human testing.

The spread of latex within the suprachoroidal space of fresh human eyes revealed some valuable information about what to expect from an injection using a hollow microneedle. Although the latex formulation is not the ideal material to inject within the suprachoroidal space, it did demonstrate that it is possible to inject volumes up to 150 μL. Since most intravitreal injections are either 50 to 100 μL in volume, this shows that a suprachoroidal injection is capable of administering a dose similar to that of an intravitreal injection (Peyman et al 2009). It also showed that injections of 50 μL resulted in the latex moving back a maximum distance of approximately 15 mm from the limbus and this value did not change much with additional volumes up to 150 μL. Instead the additional spread was around the eye; i.e parallel to the limbus and equator. It seemed apparent that the resistance for latex to move in the suprachoroidal space is less around the equator than it is towards the posterior direction. These results imply that in order to get a drug all the way to the optic nerve or macula of a human eye it will be important to study the anatomy and physiology of the suprachoroidal space, the effects of formulation properties on spread within the space and also how injections and device design influence the spread.

Both the rabbit and human eye study only examined the immediate spread from an injection into the suprachoroidal space. In an in-vivo situation the injected formulation may spread further in the suprachoroidal space over time. Dynamic transport mechanisms and flow may alter the spread of injected formulations from within the suprachoroidal space causing them to spread in different directions or may actually clear material from within the space. As an

example, the uveoscleral drainage routes for the aqueous humor may cause flow to occur from the anterior of the eye towards the posterior through the suprachoroidal space. This bulk flow may also cause an injected drug to be transported out of the suprachoroidal space. .

4.2.5 Conclusion

This study showed that it is possible to inject up to 100 µL in vivo in rabbits and 150 µL ex vivo in human eyes targeting the suprachoroidal space. The work also showed that the prototype devices used to inject into the suprachoroidal space could do so reliably. These injections also showed that the spread of the material increases in the lateral direction as more volume is injected rather than the posterior direction. Furthermore, a single injection can cover up to 40 % of the back of the human eye. Overall this work showed that a single hollow microneedle can reliably deliver therapeutically relevant volumes of fluid into the suprachoroidal space and cover a large percentage of the chorioretinal surface.

4.3 In Vivo Ocular Clearance of Molecules and Particles

4.3.1 Introduction

An effective ocular drug delivery system for the back of the eye should be able to provide targeted and sustained delivery to its target tissues, the choroid and retina, in a minimally invasive way. In our initial work we have shown that a hollow microneedle has the ability to inject a variety of materials into the suprachoroidal space. The ability to inject particles shows the potential to provide sustained delivery. However, the in-vivo kinetics of molecules and particles in the suprachoroidal space have not been studied. In this work we examine the ability of a hollow microneedle to inject a variety of materials into the suprachoroidal space and examine the clearance kinetics of these materials.

We aim to test two things: (1) determine if suprachoroidal delivery is more targeted to the choroid and retina tissues than currently practiced intravitreal delivery and (2) determine if particles delivered into this space have long residence times so they can provide sustained delivery to the choroid and retina. To address these questions, this work shows that sodium fluorescein injected into the suprachoroidal space is well localized to the back of the eye and does not expose the lens to the drug, whereas an intravitreal injection shows no apparent targeting to the chorioretinal tissues in the back of the eye. This study examines small molecule and macromolecule residence times and shows that both clear the suprachoroidal space on a timescale that is on the order of hours. As a result proper formulations are necessary for controlled or sustained delivery from this space. We demonstrate that if particles are injected into the

suprachoroidal space, they can remain in this space on the time scale of months. This could enable sustained or controlled drug delivery from within the suprachoroidal space. This is the first study to examine the capability of suprachoroidal delivery to provide targeted delivery to the eye and examine the kinetics of particles within the suprachoroidal space.

4.3.2 Comparison of Suprachoroidal and Intravitreal Injections

In order to compare the intraocular distribution profile of suprachoroidal and intravitreal injections, sodium fluorescein was injected into both locations and the fluorescence intensity in the eye was monitored over time. A 600 μg/mL solution was used for suprachoroidal injection with a 700-800 μm length hollow microneedle, and a 6 μg/mL solution was injected into the vitreous using a standard 30 gauge needle. Identical volumes, 50 μL, were injected in both scenarios. The difference in concentration of the sodium fluorescein is due to the sensitivity of the machine to detect the fluorescence within and between tissues versus what it can detect in transparent media such as vitreous and aqueous humor in the eye. The goal of this experiment was to compare the distribution profile of sodium fluorescein in the eye, determine the half life of the fluorescein in each injection site, and the ability to target the choroid and retina (chorioretinal) layers of the eye from each type of injection.

An initial baseline scan was performed on all eyes prior to injecting any formulation (Figure 4.3.1). A baseline scan provided the fluorescence intensity within the visual axis of the eye. The position of eye tissues are estimated from

peaks observed in the baseline scan. The peak to the furthest left, near position 20, is the retina while the two peaks at the furthest right, near position 110, are the cornea. Just to the left of the cornea are two additional peaks, near position 90, which demarcate the lens. The positions in between the lens and the retina can be approximated to be the vitreous. The position of these tissues may not be exactly the same with each scan, even among the same eye, but will be relatively in the same position. As a result the baseline scan provides the reference point for future scans about the location of these tissues.

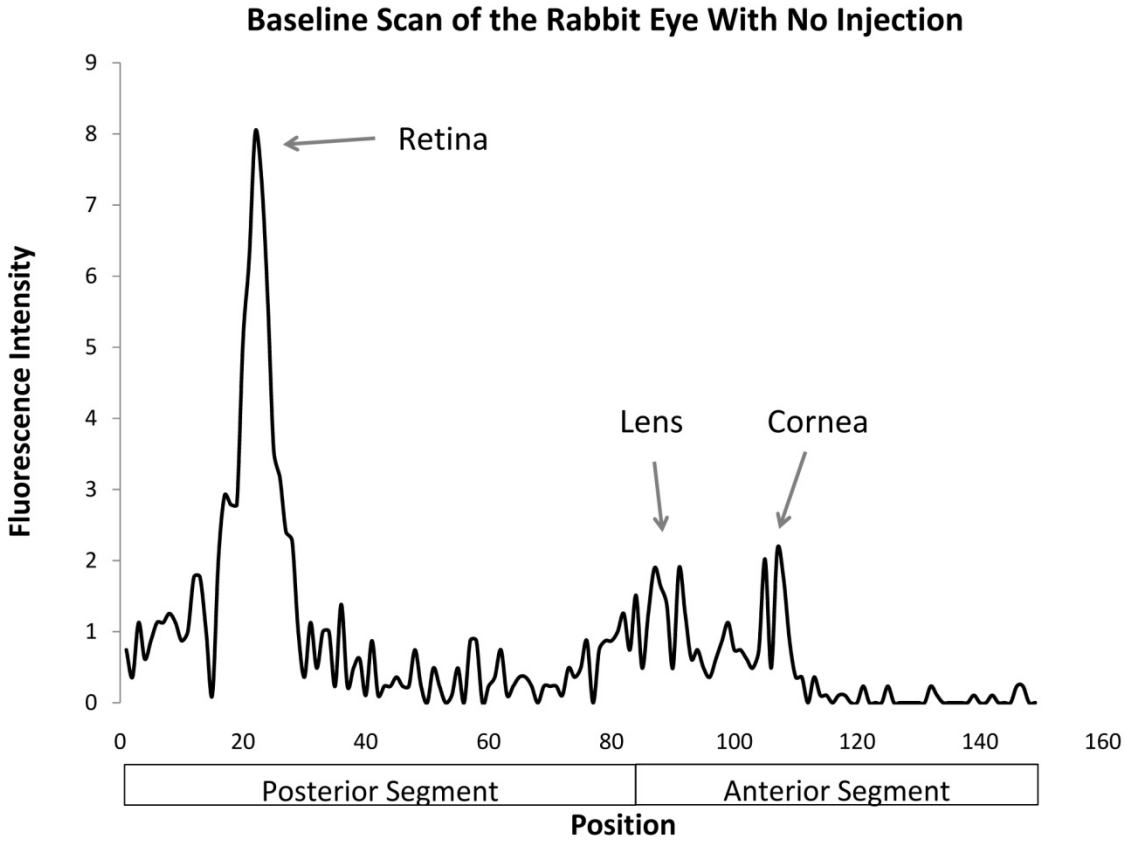

Figure 4.3.1 Representative baseline scan of the rabbit eye in vivo with no injection. The baseline profile was obtained from a single scan of the eye along the visual axis. The x-axis, position, represents the visual axis of the eye while the y-axis shows the measurement of the fluorescent intensity at that position.

The position of eye tissues are estimated from peaks observed in the baseline scan. The peak to the furthest left is the retina while the two peaks at the furthest right are the cornea. Just to the left of the cornea are two additional peaks which demarcate the lens.

Intravitreal injection profiles showed that the sodium fluorescein distributes itself fairly uniformly within the vitreous and remains primarily in the vitreous (Figure 4.3.2). Within 30 minutes after injection a broad peak is seen throughout the vitreous and within 1 hour the maximum concentration is reached within the vitreous as it distributes itself throughout the vitreous chamber. After the 1 hour time point the concentration profile is fairly uniform within the vitreous. These levels drop off uniformly in the subsequent hours. Within 24 hours the levels in the eye have returned to baseline levels indicating the fluorescein was no longer detectable in the eye (Figure 4.3.2). The calculated half life of fluorescein based on a first order kinetic fit to the concentration within the midvitreous for each eye was 2.4±0.2 hours. The average concentration in the midviterous for all injections over time is shown in Figure 4.3.3.

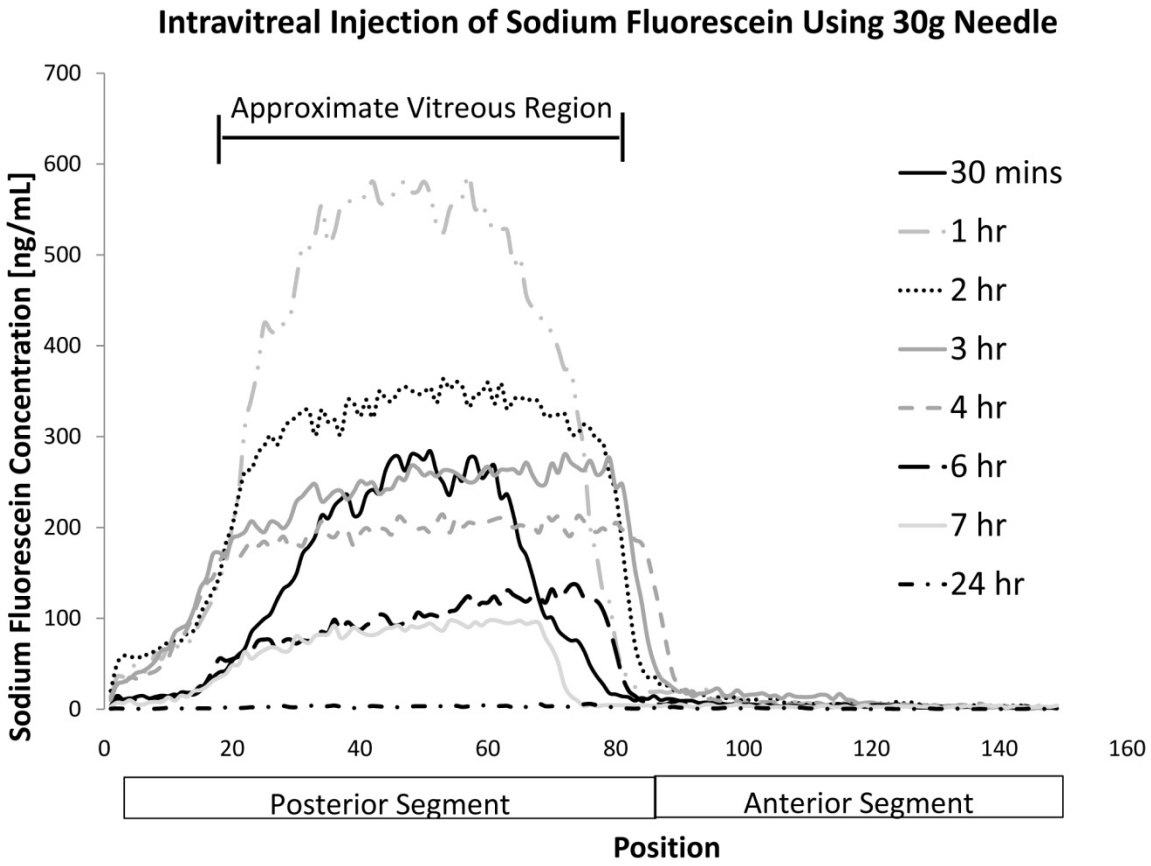

Figure 4.3.2 Representative concentration profiles of sodium fluorescein in the rabbit eye in vivo over time after an intravitreal injection of 50 µL using a 30 g needle. Each profile was created from a single scan of the eye along the visual axis. The x-axisx-axis, position, represents the visual axis of the eye with the cornea located to the right of the x-axis in the anterior segment. The approximate position of eye tissues is estimated from baseline scans of the eye.

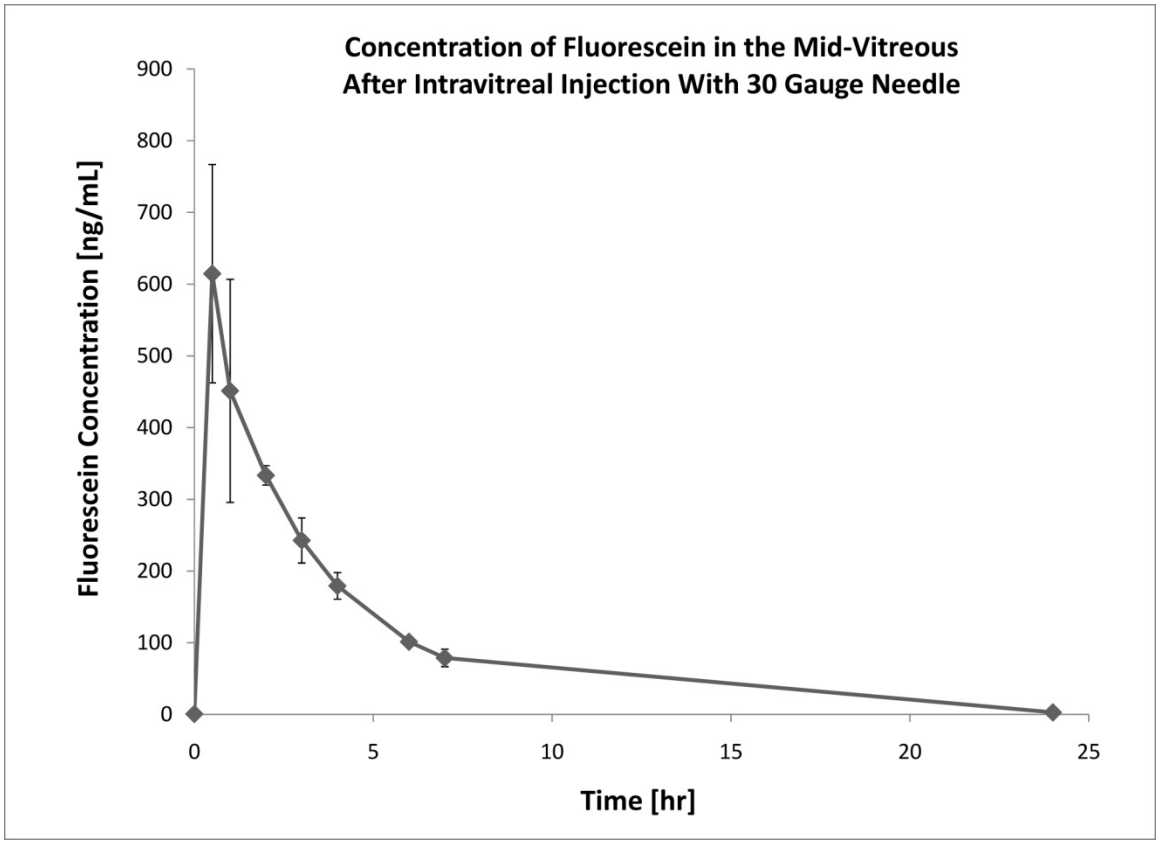

Figure 4.3.3 Average concentration of sodium fluorescein in the vitreous over time after an intravitreal injection of 50 µL (6 µg/mL) using a 30g needle. The concentration drops over time and the fluorescein is cleared from the vitreous within 24 hours after injection. (n=3 and error bars are standard deviations).

The distribution profile for a suprachoroidal injection of sodium fluorescein showed a dramatically different result than the intravitreal injection profile (Figure 4.3.4). Within 5 minutes after injection a sharp peak developed in the suprachoroidal space that dropped off quickly in the surrounding tissues. Over time this peak remained in the suprachoroidal space with significantly lower levels in the vitreous. The concentration dropped quickly within the first few hours but still remained lower in the vitreous than in the suprachoroidal space. The profiles indicate no significant transport of sodium fluorescein into the vitreous or anterior segment. Similar to an intravitreal injection, within 24 hours the sodium

fluorescein concentration returned to baseline levels indicating the fluorescein had cleared the suprachoroidal space (Figure 4.3.4). The calculated half life of fluorescein based on a first order kinetic fit to the concentration within the suprachoroidal space for each eye was 1.2±0.1 hours. Figure 4.3.5 shows the average concentration of sodium fluorescein in the suprachoroidal space over time.

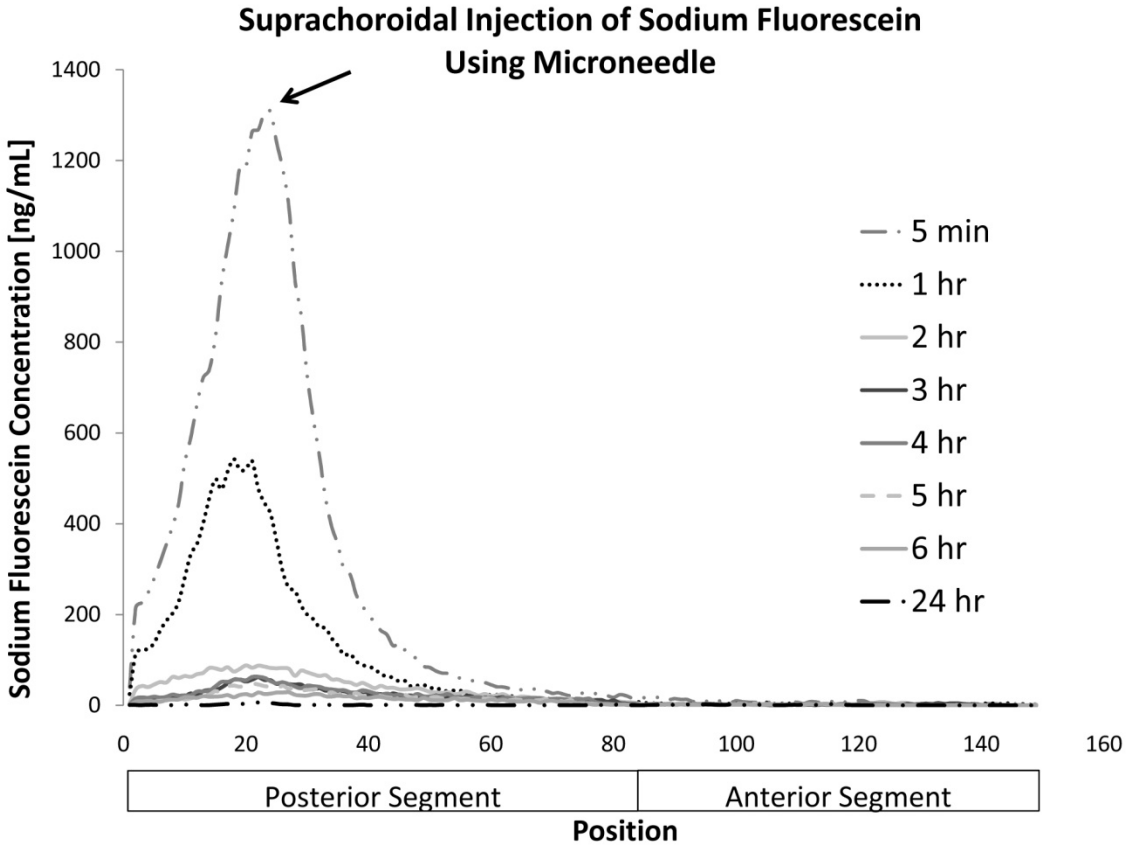

Figure 4.3.4 Representative concentration profiles of sodium fluorescein in the rabbit eye in vivo over time after a suprachoroidal injection of 50 µL using a microneedle. Each profile was created from a single scan of the eye along the visual axis. The x-axis, position, represents the visual axis of the eye with the cornea located to the right of the x-axis in the anterior segment. The approximate position of eye tissues is estimated from baseline scans of the eye. The arrow points to the peak of the concentration profile occurring in the suprachoroidal space.

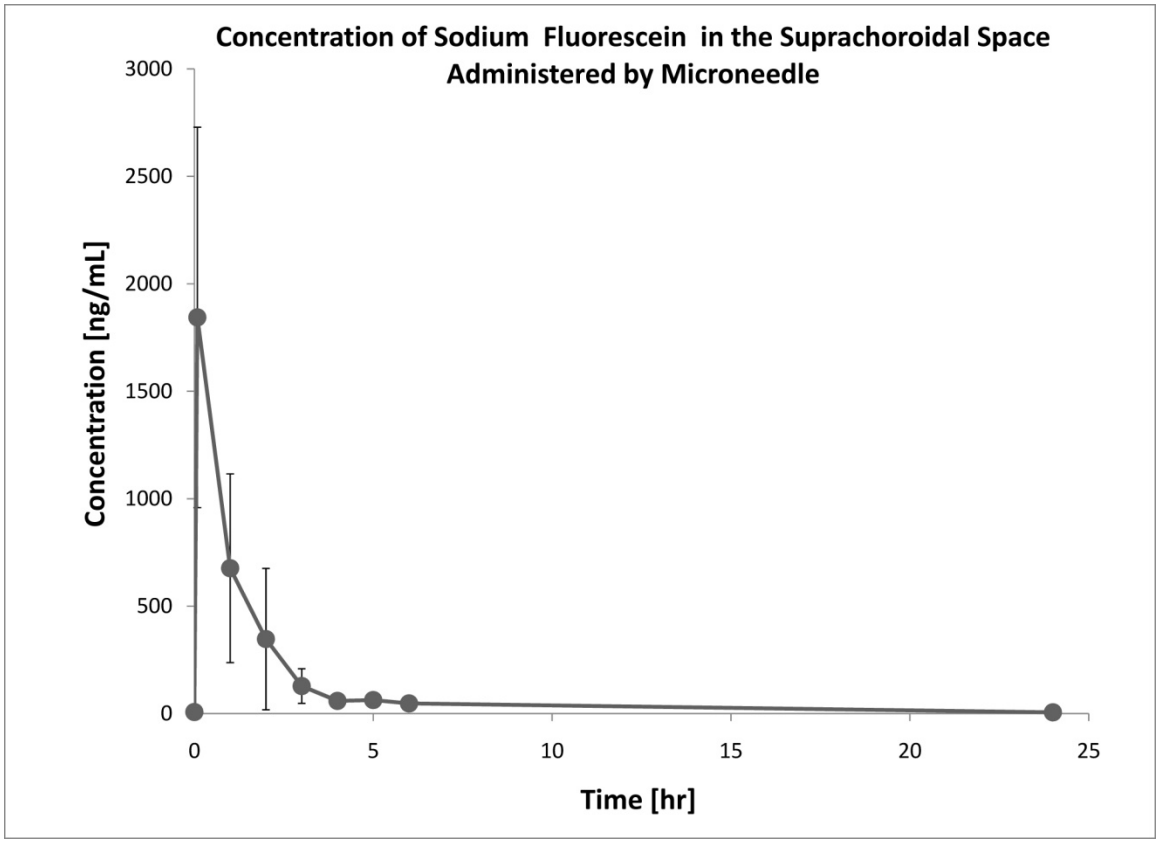

Figure 4.3.5 Average concentration of sodium fluorescein in the suprachoroidal space over time after a suprachoroidal injection of 50 µL (600 µg/mL) using a microneedle. The concentration drops over time and the fluorescein is cleared from the vitreous within 24 hours after injection. (n=3 and error bars are standard deviations).

We hypothesize that suprachoroidal delivery can target the chorioretinal tissues in the back of the eye more effectively than an intravitreal injection. In order to quantify this we compared levels of fluorescein near the target choroid/retina tissues to the level at the lens. For intravitreal injections, the ratio of fluorescence intensity at the vitreous/retina interface to the vitreous/lens interface was determined. For a suprachoroidal injection we calculated the ratio of the fluorescence intensity in the suprachoroidal space to the intensity at the

lens. With these definitions, a large ratio indicates more effective targeting to the chorioretinal tissues in the back of the eye. The values were then plotted over time and compared in Figure 4.3.6. The ratio for an intravitreal injection hovers near 1 for all times post injection and for most time points is actually below 1. This indicates that the fluorescein distributes throughout the vitreous fairly evenly and there is no selectivity towards the back of the eye where the retina is located. In contrast, the ratio for suprachoroidal injections at baseline is 4.2 ± 0.8 and immediately after injection this ratio jumps to 214 ± 116 since the injection spreads the formulation within the suprachoroidal space to the back of the eye within minutes. This ratio falls as time goes on but always remains above 10. The ratio is higher for all time points post injection from a suprachoroidal injection as compared to an intravitreal injection (ANOVA $p<0.05$). As a result, a suprachoroidal injection is better at targeting the fluorescein to the chorioretinal tissues in the back of the eye as compared to an intravitreal injection.

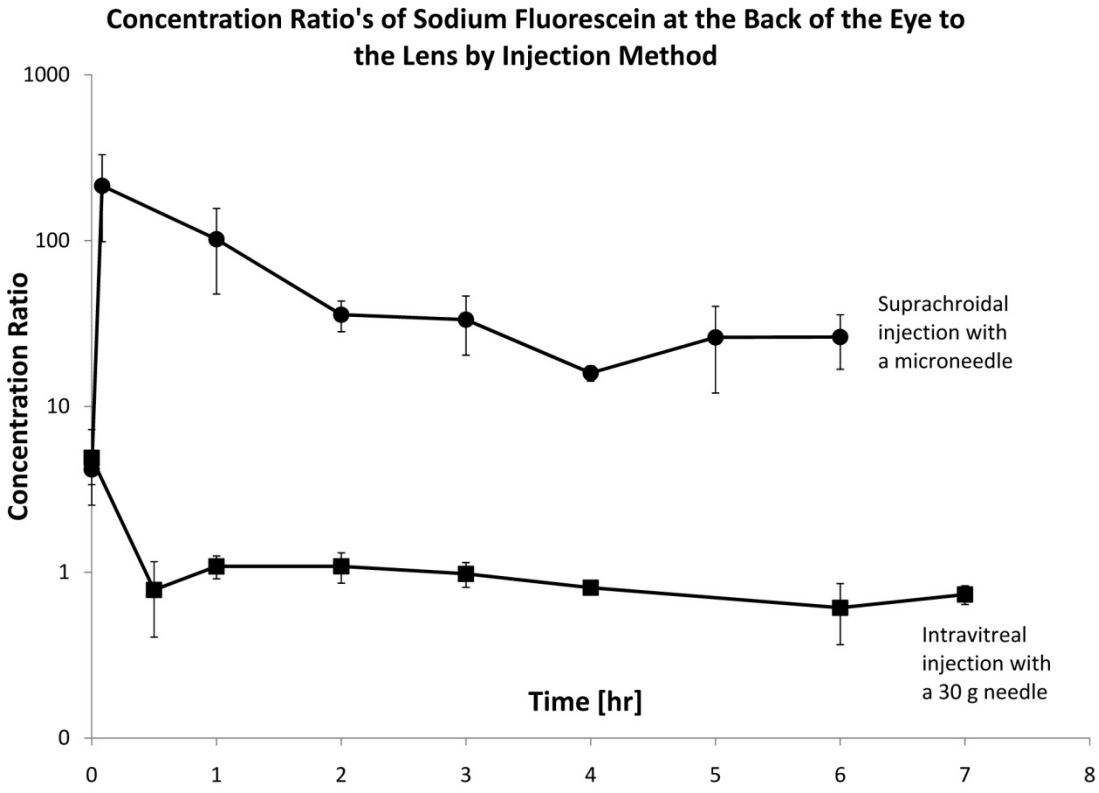

Figure 4.3.6 Graph showing the ratio of concentrations of sodium fluorescein within two locations in the eye after intravitreal (squares) and suprachoroidal injections (triangles). The ratio represents the ability of the injection to target the chorioretinal tissues. For an intravitreal injection the ratio is the concentration in the vitreous near the retina to that near the lens. For a suprachoroidal injection the ratio is the concentration in the suprachoroidal space to the concentration in the vitreous near the lens. The graph shows that the ratio is higher for a suprachoroidal injection and is statistically different at all time points after administration than an intravitreal injection. Error bars are standard deviations. n=3 per injection.

4.3.3 Injection of Macromolecules in to the Suprachoroidal Space

In addition to a small molecule such as fluorescein, we wanted to investigate the capability of a hollow microneedle to inject proteins and other macromolecules within the suprachoroidal space. As a result we injected 40 kDa and 250 kDa dextran tagged with FITC (fluorescein isothiocyanate) within the

suprachoroidal space. We also investigated the ability to inject a therapeutic antibody, bevacizumab (Avastin®), tagged with Alexa Fluro 488 within the suprachoroidal space. This antibody is a therapeutically relevant 147 kDa macromolecule since it is an anti vascular endothelial growth factor (VEGF) that has been used to treat patients with wet macular degeneration (Chappelow and Kaiser 2008). We hypothesize that macromolecules can be successfully targeted to the suprachoroidal region and will have similar localization as sodium fluorescein injected within the suprachoroidal space. Two eyes were injected for each macromolecule and the fluorescence intensities in the eyes were monitored over time.

The distribution profiles from suprachoroidal injections showed a sharp peak in the suprachoroidal space with a quick drop off in surrounding regions. As time progressed this peak dropped in value but maintained its shape (Figures 4.3.7-9). Overall the profile shapes are similar to sodium fluorescein and showed similar localization. The ratio of suprachoroidal levels as compared to levels in the lens for each of the macromolecules were above 25 up to 6 hours from time of injection. Immediately after injection the ratio was 224±101, 89±20, and 98±68 for 40kDa dextran, 250 kDa dextran and bevacizumab respectively. This indicates the injection was well targeted to the chorioretinal tissues in the back of the eye with minimal exposure to the front of the eye. Within 24 hours the fluorescence intensity of the 40 kDa dextran had reached near baseline levels. The level of the 250 kDa and dextran and bevaciszumab were slightly above baseline levels (Figures 4.3.10-12). This indicated that the macromolecules were

cleared from the suprachoroidal space in approximately 24 hours. The calculated half lives of 40kDa dextran, 250 kDa dextran and Avastin in the suprachoroidal space were 3.6±0.5, 5.6±1, and 7.9±0.5 hours respectively.

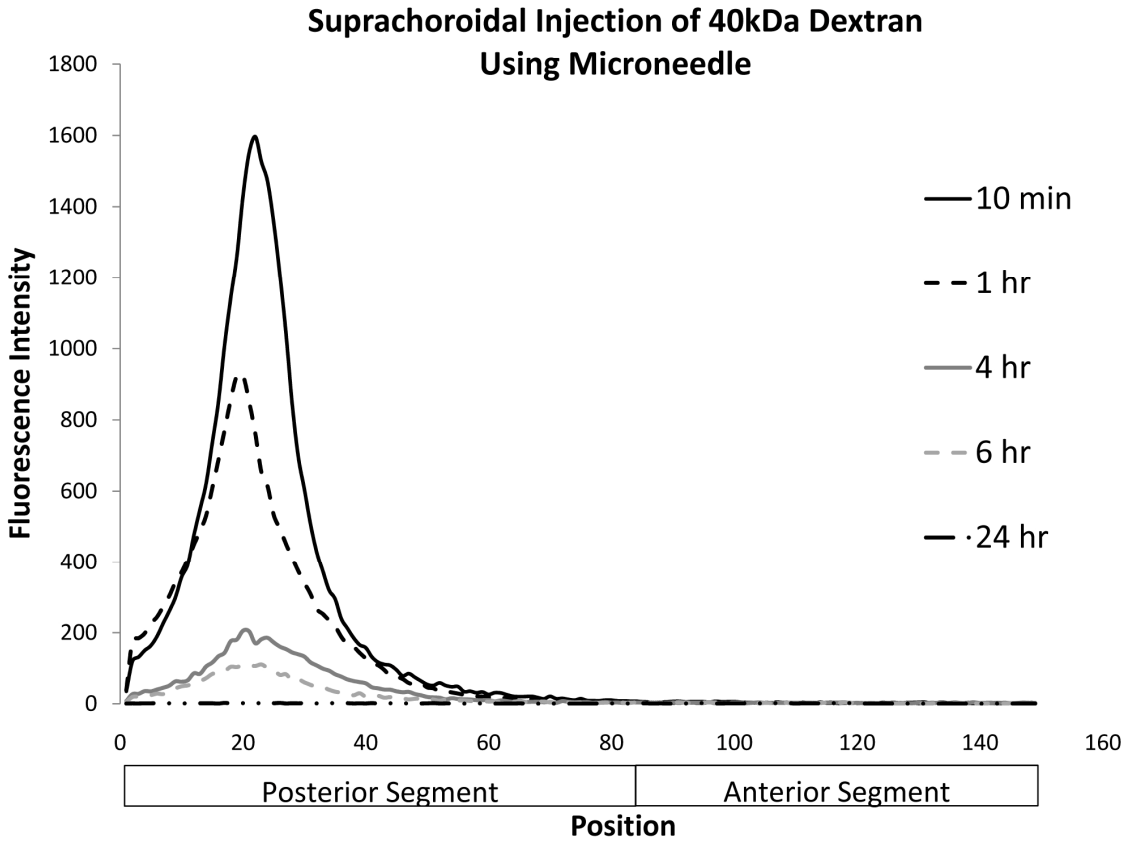

Figure 4.3.7 Representative fluorescence intensity profiles of 40kDa dextran tagged with FITC in the rabbit eye in vivo over time after a suprachoroidal injection of 50 µL using a microneedle. Each profile was created from a single scan of the eye along the visual axis. The x-axis, position, represents the visual axis of the eye with the cornea located to the right of the x-axis in the anterior segment. The approximate position of eye tissues is estimated from baseline scans of the eye. The scans show that the peak intensity remains in the suprachoroidal space.

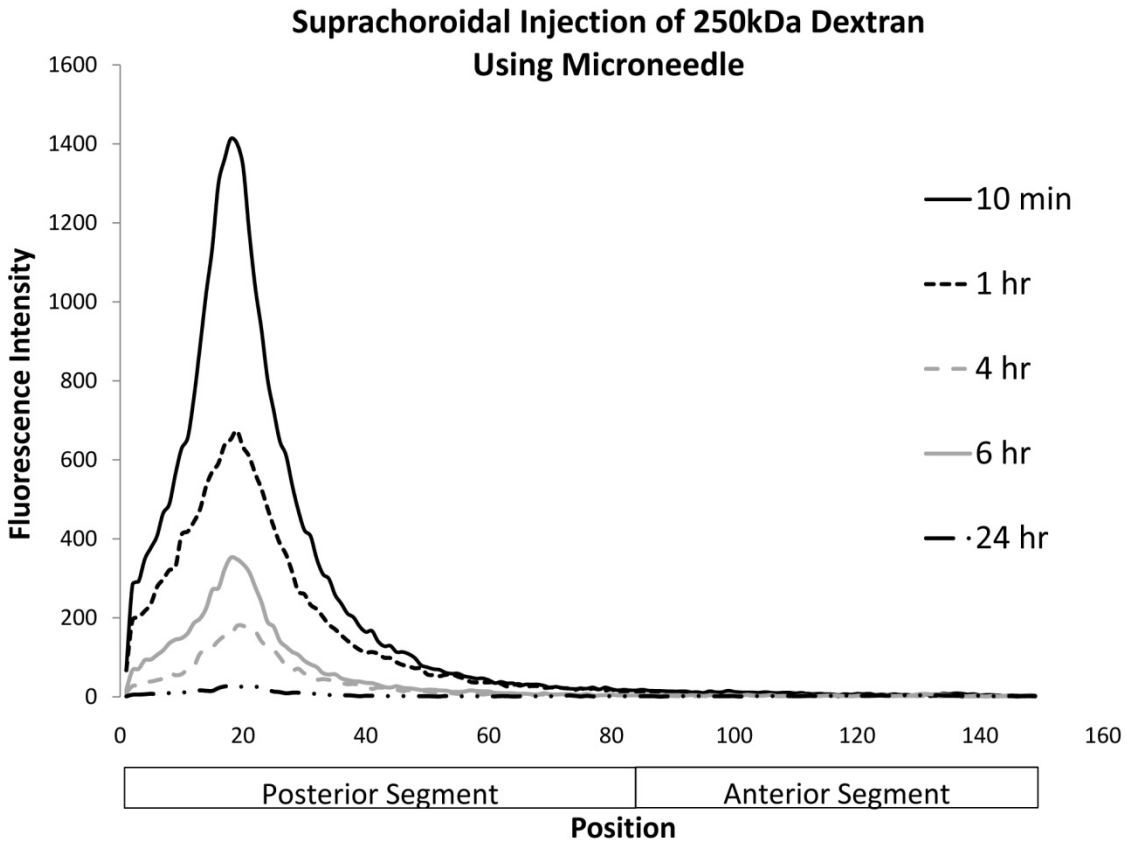

Figure 4.3.8 Representative fluorescence intensity profiles of 250kDa dextran tagged with FITC in the rabbit eye in vivo over time after a suprachoroidal injection of 50 µL using a microneedle. Each profile was created from a single scan of the eye along the visual axis. The x-axis, position, represents the visual axis of the eye with the cornea located to the right of the x-axis in the anterior segment. The approximate position of eye tissues is estimated from baseline scans of the eye. The scans show that the peak intensity remains in the suprachoroidal space.

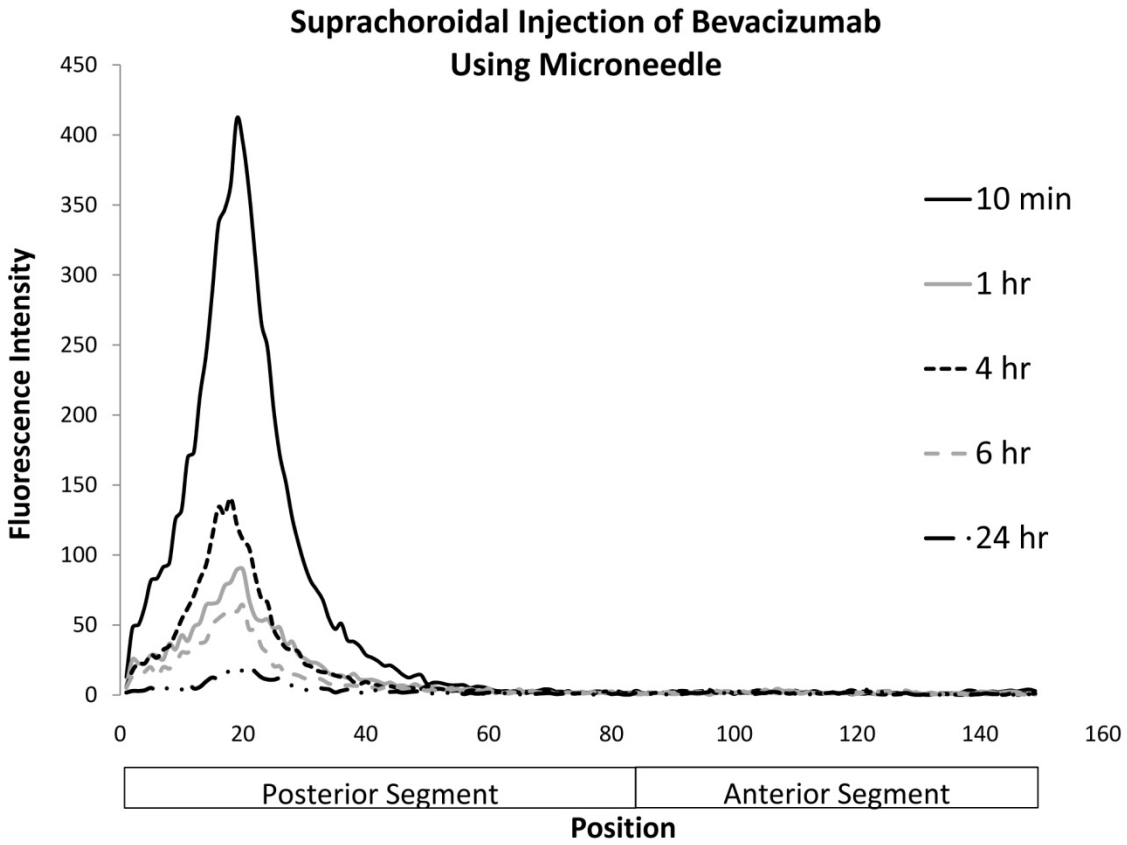

Figure 4.3.9 Representative fluorescence intensity profiles of bevaciszumab tagged with Alexa Fluor 488 in the rabbit eye in vivo over time after a suprachoroidal injection of 50 µL using a microneedle. Each profile was created from a single scan of the eye along the visual axis. The x-axis, position, represents the visual axis of the eye with the cornea located to the right of the x-axis in the anterior segment. The approximate position of eye tissues is estimated from baseline scans of the eye. The scans show that the peak intensity remains in the suprachoroidal space.

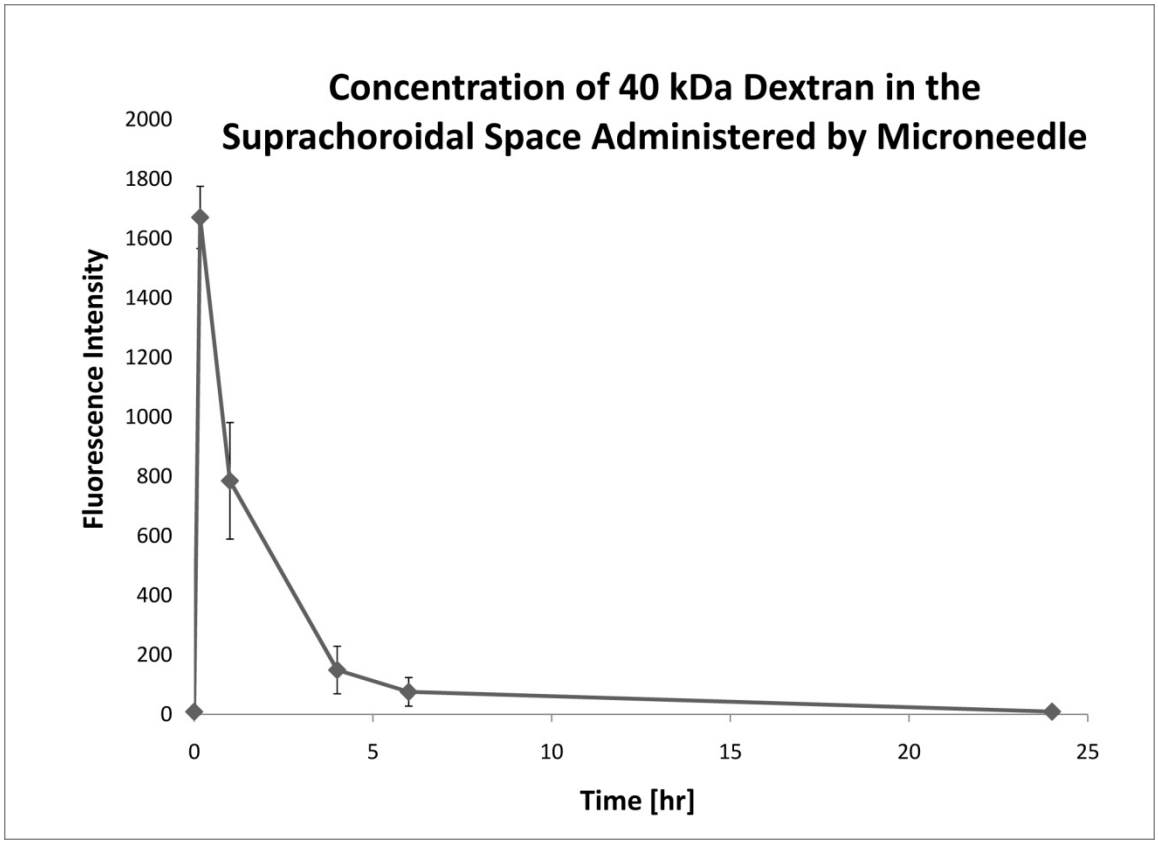

Figure 4.3.10 Average fluorescence intensity of 40 kDa dextran tagged with FITC in the suprachoroidal space over time after a suprachoroidal injection of 50 µL using a microneedle. The fluorescence intensity drops over time and the dextran is cleared from the vitreous within 24 hours after injection. (n=2 and error bars are standard deviations).

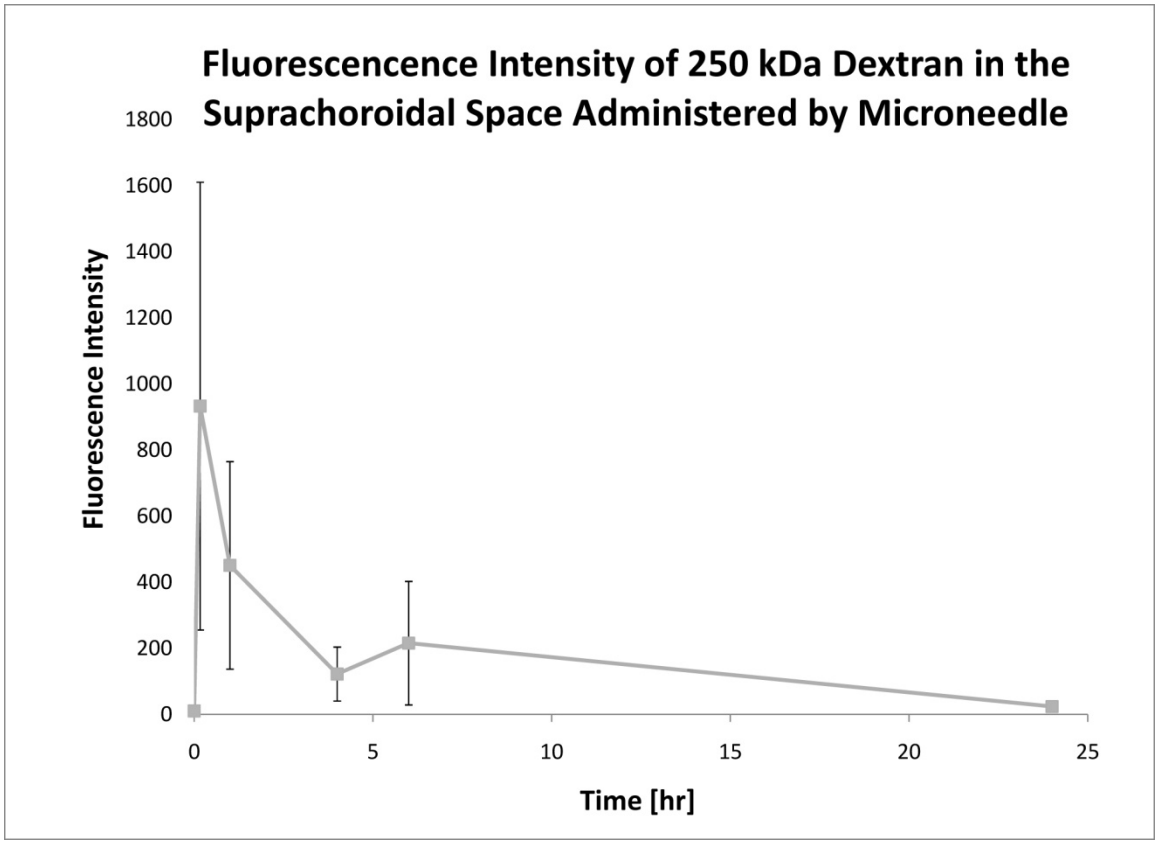

Figure 4.3.11 Average fluorescence intensity of 250 kDa dextran tagged with FITC in the suprachoroidal space over time after a suprachoroidal injection of 50 µL using a microneedle. The fluorescence intensity drops over time and the dextran is cleared from the vitreous in approximately 24 hours after injection. (n=2 and error bars are standard deviations).

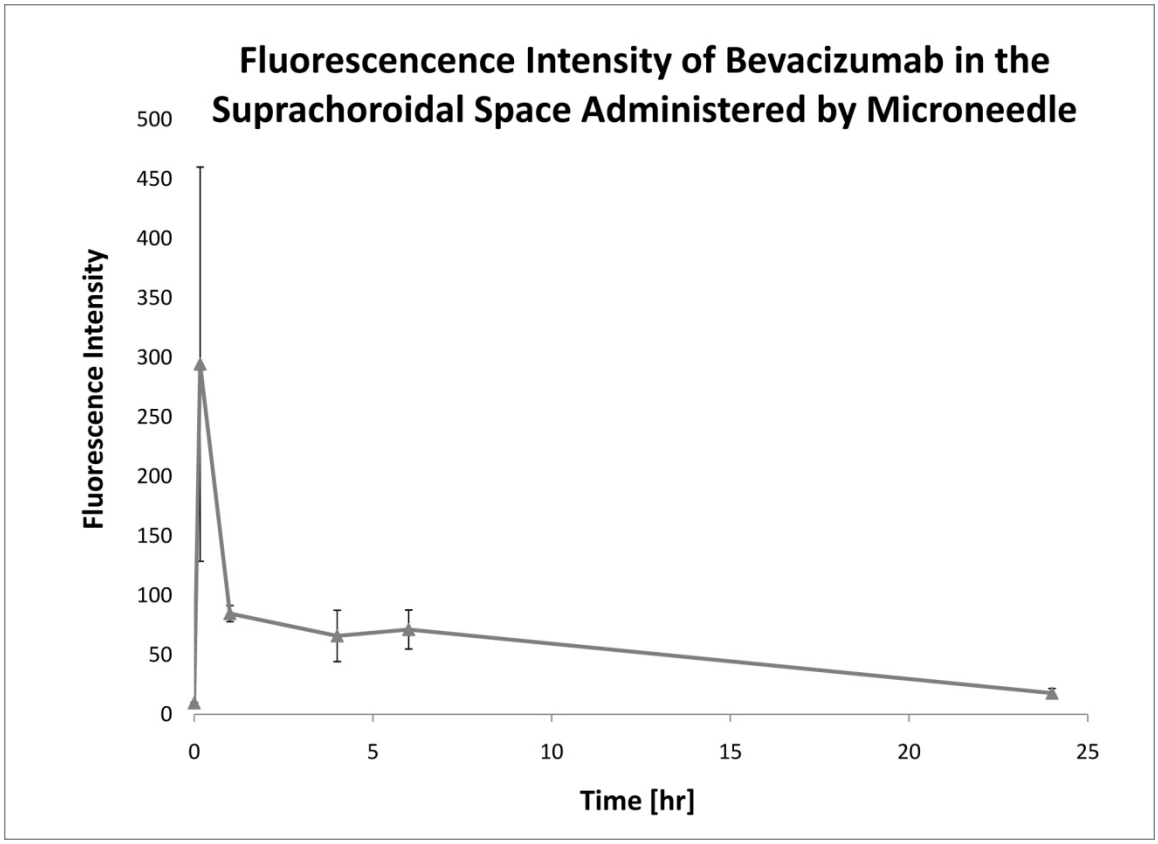

Figure 4.3.12 Average fluorescence intensity of bevacizumab tagged with Alexa Fluro 488 in the suprachoroidal space over time after a suprachoroidal injection of 50 µL using a microneedle. The fluorescence intensity drops over time and bevacizumab is cleared from the vitreous in approximately 24 hours after injection. (n=2 and error bars are standard deviations).

4.3.4 Injection of Particles in to the Suprachoroidal Space

We hypothesize that particles could be injected into the suprachoroidal space of rabbit eyes in vivo with similar targeting to the chorioretinal tissues as molecules. We further believe that particles will have a longer residence time than molecules injected into the space and thus can be used for sustained delivery. In order to test this hypothesis we injected non degradable fluorescent particles, FluoSpheres®, into the suprachoroidal space using a hollow

microneedle. These particles are designed not to leach the fluorescent dye from within the particle. As a result fluorescence scans in the eye after injection will reveal the presence of the particles and not the release of the fluorescent dye within the particle. Four particle sizes were injected into the suprachoroidal space: 20 nm, 500 nm, 1 μm and 10 μm in diameter.

Fluorescence intensity scans in the eye show that particles can be selectively injected into the suprachoroidal space of rabbit eyes (Figure 4.3.13 and 4.3.14). All eyes injected with particles showed an increase in fluorescence intensity within the suprachoroidal space within minutes after injection. The peak fluorescent intensity within each profile was located in the suprachoroidal space at all time points. The fluorescence intensity dropped off quickly in the surrounding tissues indicating that the particles had not significantly migrated into surrounding tissues. All particle injections within the suprachoroidal space exhibited the same profile shape. The particles were also well targeted to the back of the eye. Performing a similar analysis to the fluorescein injections, the ratio of fluorescence intensity in the suprachoroidal space to that near the lens was determined and it showed that for all scans the ratio was above 10 for the time periods tested. This indicates that the particles were present in the suprachoroidal space throughout this time period and were well targeted to the chorioretinal tissues.

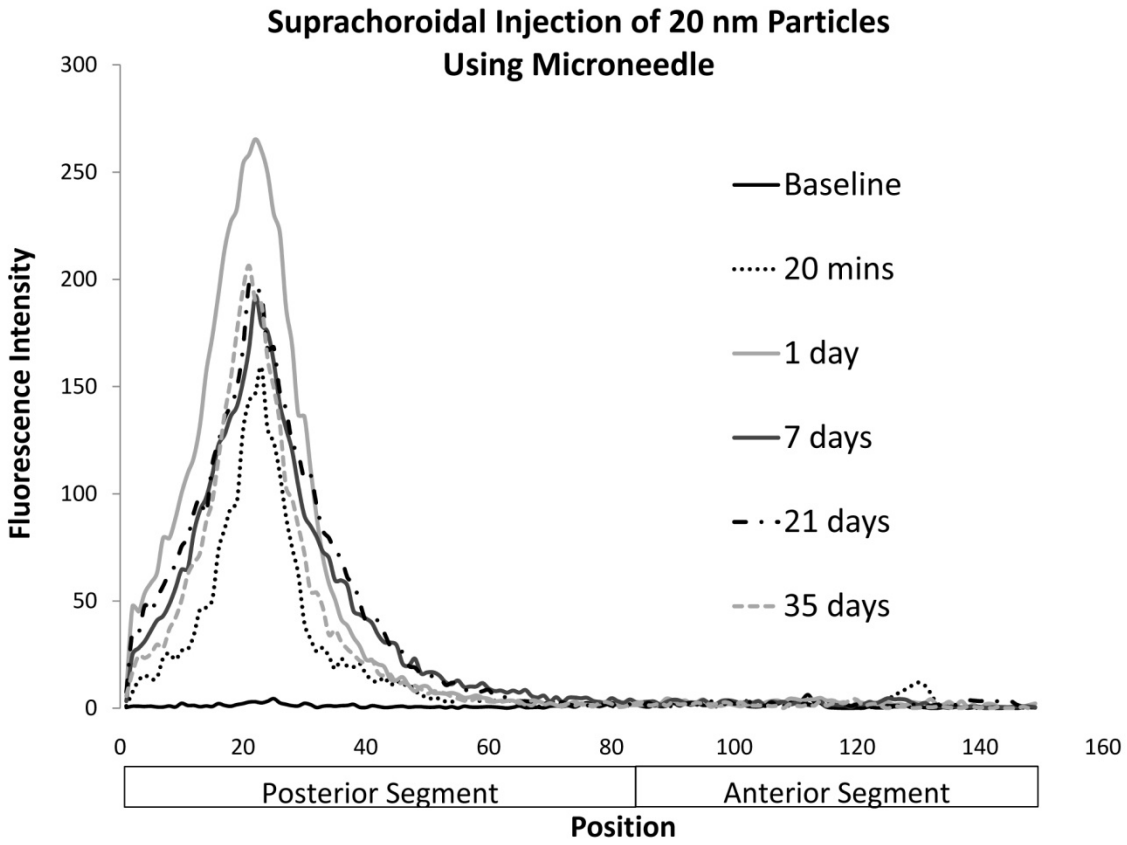

Figure 4.3.13 Representative fluorescence intensity profiles of 20 nm particles in the rabbit eye in vivo over time after a suprachoroidal injection of 50 µL using a microneedle. Each profile was created from a single scan of the eye along the visual axis. The x-axis, position, represents the visual axis of the eye with the cornea located to the right of the x-axis in the anterior segment. The approximate position of eye tissues is estimated from baseline scans of the eye. The scans show that the peak intensity remains in the suprachoroidal space and does not return to baseline in the time tested.

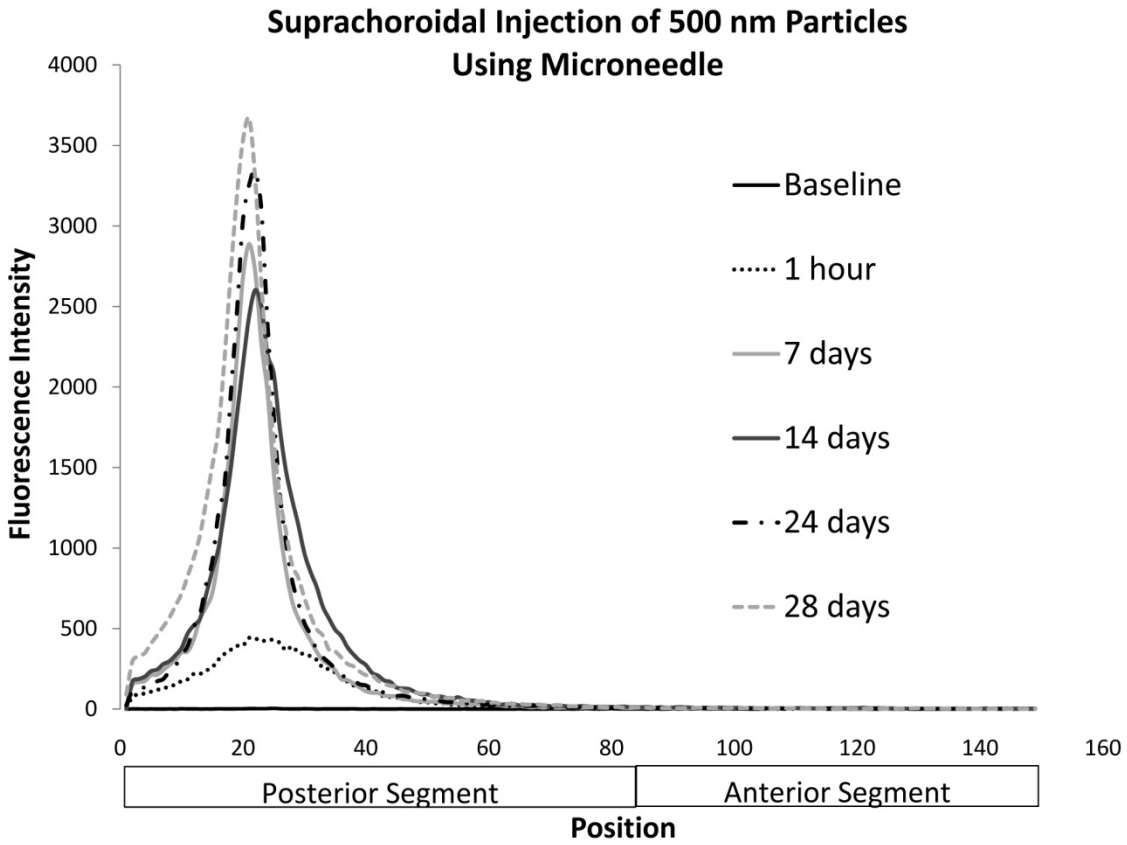

Figure 4.3.14 Representative fluorescence intensity profiles of 500 nm particles in the rabbit eye in vivo over time after a suprachoroidal injection of 50 µL using a microneedle. Each profile was created from a single scan of the eye along the visual axis. The x-axis, position, represents the visual axis of the eye with the cornea located to the right of the x-axis in the anterior segment. The approximate position of eye tissues is estimated from baseline scans of the eye. The scans show that the peak intensity remains in the suprachoroidal space and does not return to baseline in the time tested.

In order to determine if the particles were being cleared from the suprachoroidal space, the peak fluorescence intensity within the suprachoroidal space was determined over time for each particle size (Figures 4.3.15 and 4.3.16). The average fluorescence intensity within the suprachoroidal space was plotted over time for each particle size. Rabbits injected with 20 nm particles were followed for 35 days and rabbits injected with 500 nm particles were

followed for 28 days. All rabbits maintained fluorescence intensity levels within suprachoroidal similar to levels obtained immediately following the suprachoroidal injection. Statistical analysis (ANOVA $p<0.05$) revealed that all readings were similar indicating that over time the particles were not being cleared from the suprachoroidal space. Rabbits injected with 1 and 10 μm were followed for 60+ days. A plot of the fluorescence intensity over time reveals that the fluorescence intensity also does not drop over the time period tested (ANOVA $p<0.05$). This indicates that all 4 particles, once injected into the suprachoroidal space, remain in the suprachoroidal space for at least the time periods tested.

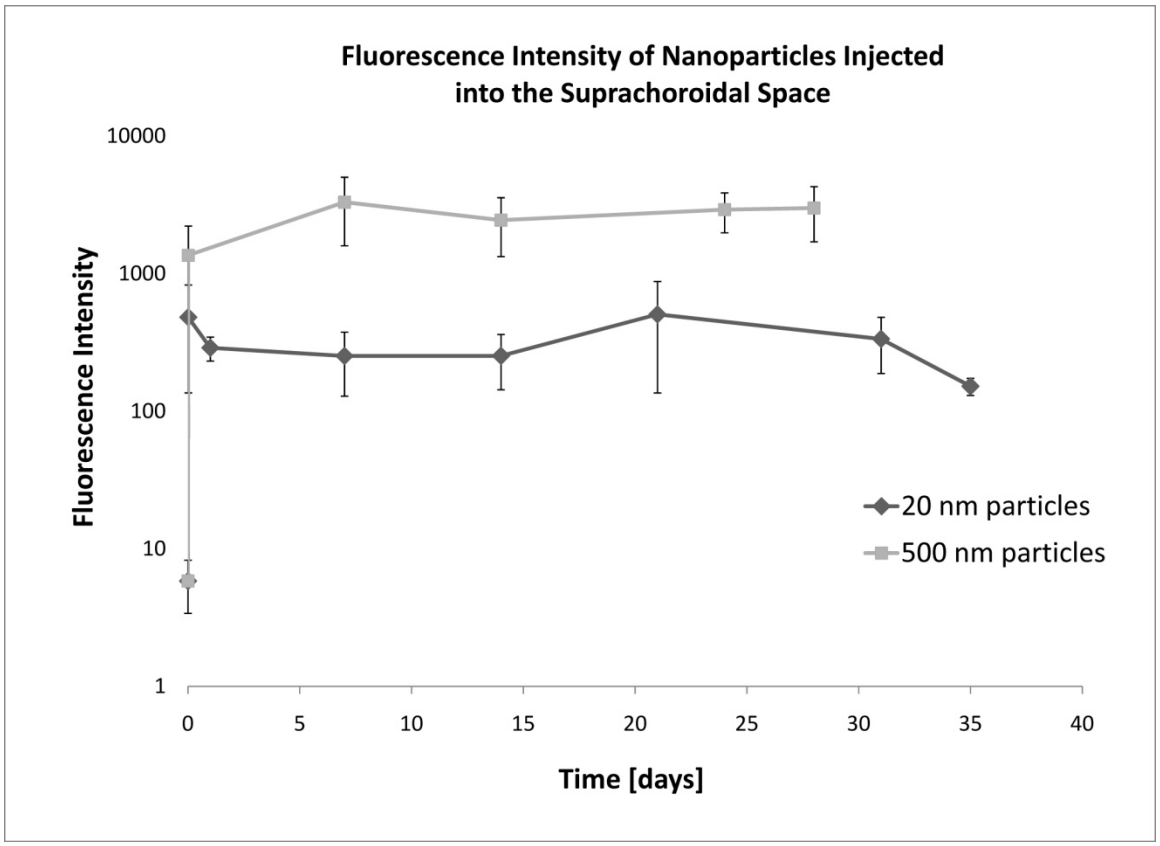

Figure 4.3.15 Average fluorescence intensity of 20 and 500 nm particles in the suprachoroidal space over time after a suprachoroidal injection of 50 µL using a microneedle. The fluorescence intensity does not drop over the time tested (ANOVA $p<0.05$) indicating the particles are still present in the suprachoroidal space in a similar concentration to the initial amount. (n=2 and error bars are standard deviations).

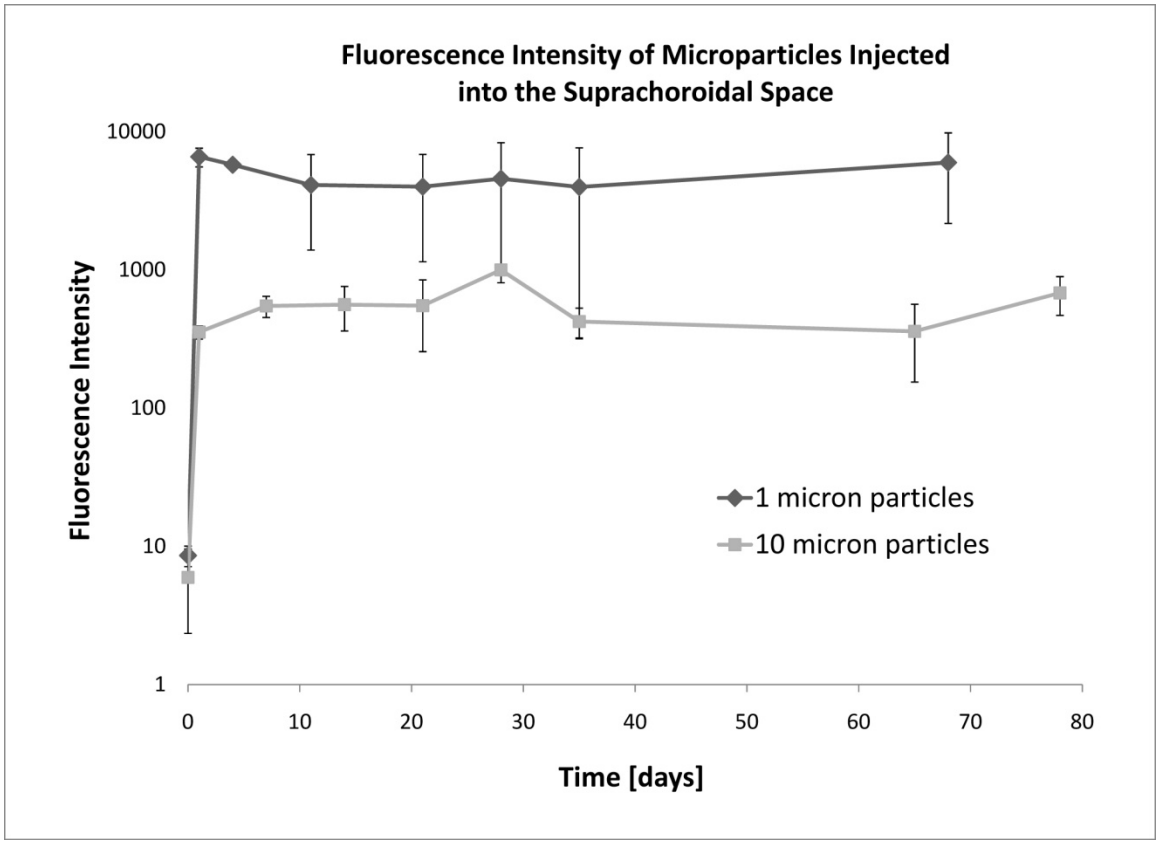

Figure 4.3.16 Average fluorescence intensity of 1 and 10 µm particles in the suprachoroidal space over time after a suprachoroidal injection of 100 µL using a microneedle. The fluorescence intensity does not drop over the time tested (ANOVA $p<0.05$) indicating the particles are still present in the suprachoroidal space in a similar concentration to the initial amount. (n=2 and error bars are standard deviations).

In order to visually confirm the presence of the particles in the eye, in vivo fundus imaging as well as histological examination was performed. Fundus photography was performed on rabbits injected with one and ten micrometer

particles (Figure 4.3.17). The fundus of the injected eyes appeared normal with no inflammation or abnormalities as compared to an uninjected eye (Figure 4.3.17 a,c,e). Fluorescence images of the fundus revealed that the particles were distributed throughout the back of the eye and had reached as far back as the optic nerve (Figure 4.3.17 b,d,f). The fluorescence images of the fundus also show that there are particles behind the chroriodal blood vessels as the blood vessels block some of the fluorescence. This confirms that even after 60 days the particles are still present. This also shows that there are still particles in the suprachoroidal space and they have not diffused into the vitreous. In order to confirm the exact location of the particles histological examination of the tissues was performed after enucleation of the eyes at the end of the study. Figure 4.3.18 shows a cross section of the rabbit tissue 28 days after injection of 500 nm particles into the suprachoroidal space. The bright fluorescence seen in the image is the 500 nm particles in the suprachoroidal space. This image confirms that the particles are still present even after 28 days and are well localized in the suprachoroidal space. Figure 4.3.19 shows a cross section of rabbit tissue 60+ days after injection of 1 and 10 μm particles. The particles are well localized to the suprachoroidal space and do not even appear in the retina. These data visually confirm the presence of particles in the suprachoroidal space and support the quantitative fluorescence data.

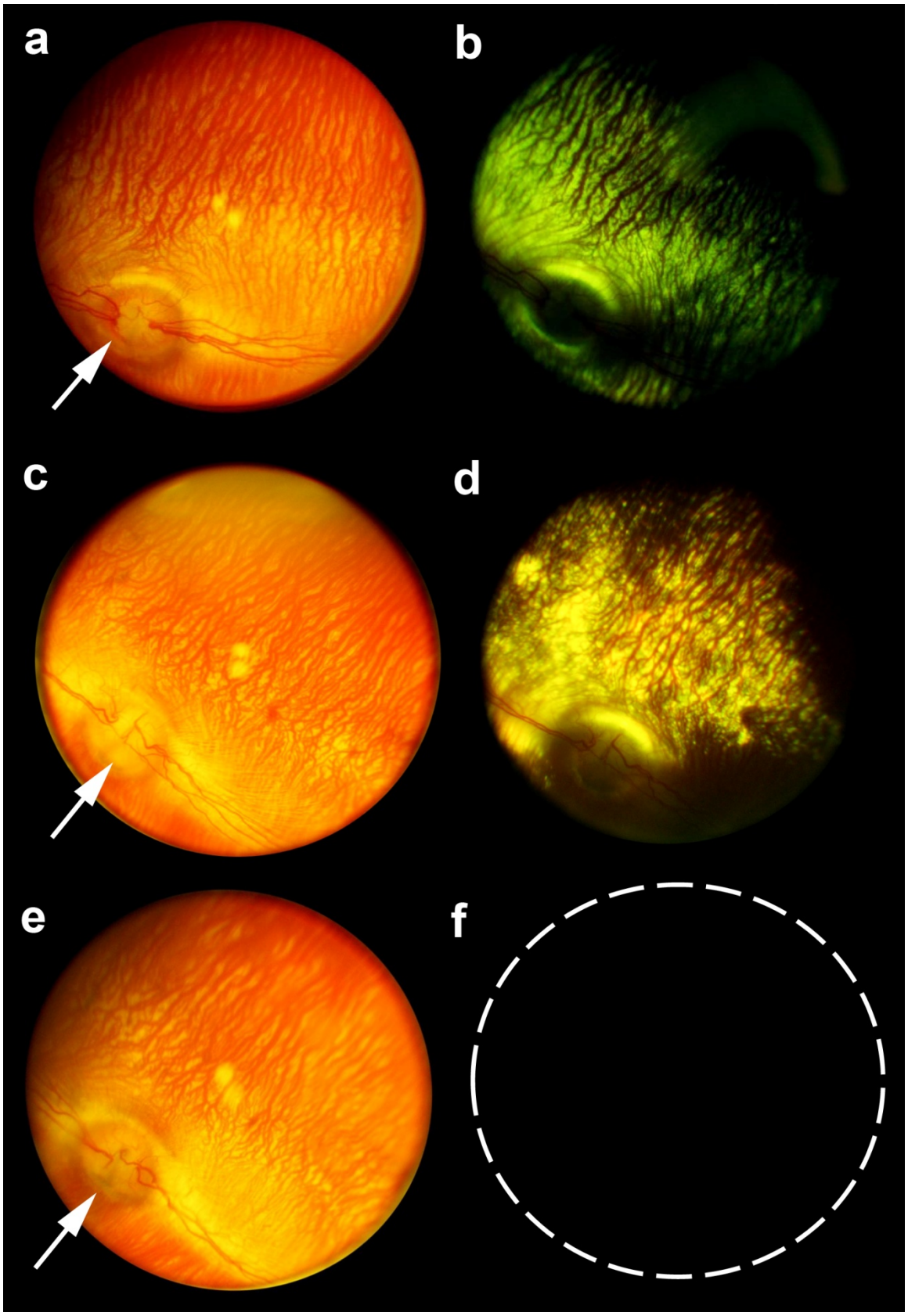
a
b
c
d
e
f

Figure 4.3.17 Fundus photography of rabbit eyes injected with (a,b) 1 μm and (c,d) 10 μm particles in the suprachoroidal space and with (e,f) no injection. Images a, c, and e are color fundus images that show the ocular anatomy while b, d, and f are fluorescence images of the fundus that show the location of fluorescent particles. Arrows indicate the location of the optic cup. The bright particles can be seen in the fluorescent images after suprachoroidal injection (b,d).

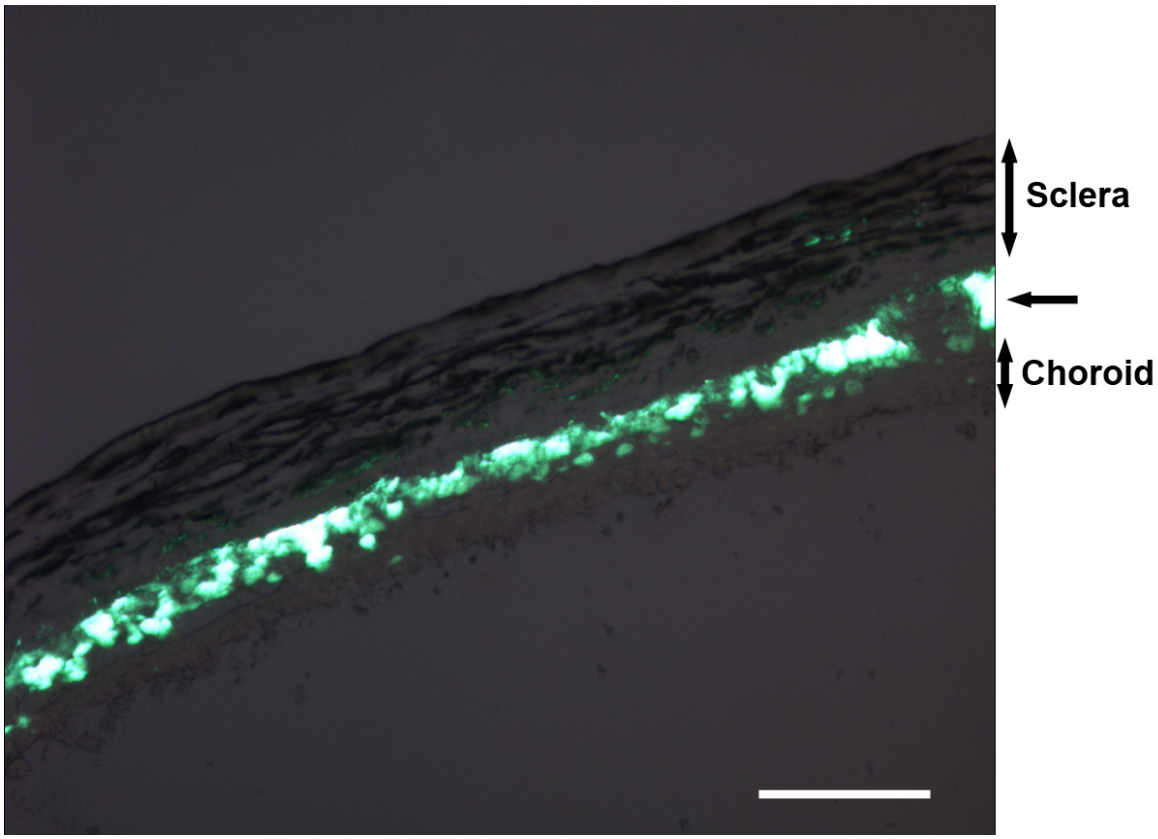

Figure 4.3.18 Cross-section of rabbit eye tissue 28 days after a suprachoroidal injection of 500 nm particles in a rabbit eye in vivo. The arrow points to fluorescent particles in the suprachoroidal space. This confirms that the particles are still present in the suprachoroidal space even after 28 days. Scale bar: 500 μm.

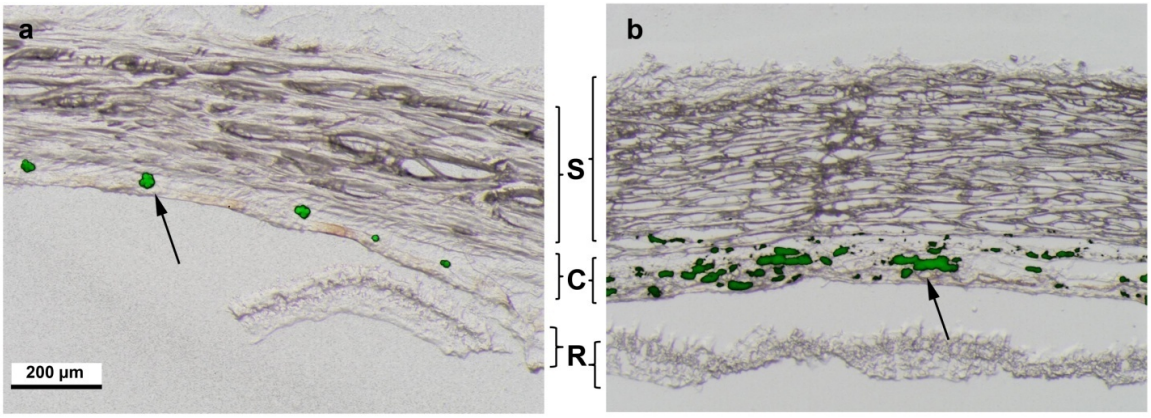

Figure 4.3.19 Cross-section of rabbit eye tissue approximately 60 days after a suprachoroidal injection of (a) 1 µm and (b) 10 µm particles in a rabbit eye in vivo. The arrows points to fluorescent particles in the suprachoroidal/choroidal space. The sclera (S) and the choroid (C) can be seen with portions of the retina (R). This confirms that the particles are still present in the suprachoroidal space even after 60 days. Scale bar: 500 µm.

4.3.5 Discussion

In this study we investigated for the first time the intraocular kinetics of materials injected into the suprachoroidal space. This work represents the first comprehensive study to examine the administration of small molecules, macromolecules, nanoparticles and microparticles into the suprachoroidal space. The work also shows for the first time that a hollow microneedle can inject a variety of materials into the suprachoroidal space of an eye in vivo. This work first characterized the intraocular concentration profile of a suprachoroidal injection and compared it to an intravitreal injection profile using sodium fluorescein as a model compound. This data showed that suprachoroidal injections were more effective at targeting the chorioretinal tissues than intravitreal injections. The study further compared the half lives of both injection methods and determined them both to be very quick, less than 3 hours for each. We further showed that

microneedles could inject macromolecules, including a therapeutic antibody, into the suprachoroidal space. An important result of this study is that it showed nano- and microparticles could be injected into the suprachoroidal space using a microneedle and were not cleared from the eye for at least 2 months.

In vivo fluorescence measurements were used in this study to determine the levels of the injected molecules in the eye. This method offers a non invasive way to measure fluorescence intensities in both the front and back of the eye in real time. As a result, the relative amounts of an injected molecule can be monitored in its normal state since no anesthesia is necessary to perform the scan. One of the biggest advantage is this approach allows longitudinal studies of fluorescent intensities in a single dimension in the eye. One of the limitations is that only a small region of the eye can be measured in any given scan and movement of molecules outside of this one dimensions will not be captured from this type of approach. A scan will not be able to capture what is occurring in the extreme periphery of the eye since the light beam will not penetrate through the pupil at angles that are not nearly perpendicular to the ocular surface. When the animal is not under the influence of anesthesia the animal is also free to move its eye and the exact spot being measured will vary from scan to scan. Additionally, this requires the molecule to be fluorescent or needs to be tagged with a fluorophore with excitation and emission wavelengths in the range that is detectable by the Fluorotron. This limits the type of molecules that can be tested and also means the doses that can be tested are dependent on the resolution of the fluorophore on the machine. Even with these limitations this approach offers

a unique way to quickly monitor the levels in the eye of an animal over time in a non invasive way and can help show the one dimensional distribution of an injected molecule.

The results from this study show that molecules injected into the suprachoroidal space are removed from this space within a 24 hour timeframe. This is true for a small molecule such as fluorescein as well as large macromolecules such as dextrans and bevascizumab. The mechanisms responsible for this clearance are uncertain and detailed studies for determining these mechanisms are still necessary. However, there may be two main mechanisms responsible for transport of these molecules from this space. One mechanism may be the transport of molecules facilitated by uveal scleral outflow pathway. Some aqueous humor is naturally removed from the anterior segment of the eye through flow into the suprachoroidal space and subsequently out of the eye through the sclera (Alm and Nilsson 2009). This bulk flow may also contribute to the transport of injected molecules directly into the suprachoroidal space. A second mechanism that may be responsible for clearance of molecules is uptake of the molecules into the choroidal blood vessels. The injection is in direct contact with the choroidal blood vessels and molecules may be absorbed into the blood circulation and carried away from the eye. The role these mechanisms play may be better addressed with actual pharmacokinetic experiments analyzing tissue concentrations within the eye and blood levels of various molecules. Fluorophotometry may not be the best way to study this

phenomena since it only provides a one dimensional view to a three dimensional problem with dynamic clearance pathways.

Particles injected into the suprachoroidal space do not appear to be easily cleared from this space. For the time period tested, the size of the particles did not influence the residence time. There may not be an active mechanism to take up the nano- and microparticles injected into the suprachoroidal space. Diffusion of particles into the surrounding region may not be possible because of barriers such as the retinal pigment epithelium and sclera that do not easily allow large particles to migrate through. Uptake of these particles in to the choroidal blood vessels may also not be occurring. As a result both nano- and microparticles remain in the suprachoroidal space. In order to determine what factors of the particles cause them to remain in the suprachoroidal space much longer than small and large molecules, further studies would need to be performed using particles made of different sizes, materials and chemistries.

What this study does show, is that there may be a way to provide sustained delivery from within the suprachoroidal space. There are materials that will be cleared from the suprachoroidal space on a time scale of hours (soluble molecules) and there are also materials that will remain in the space for months (particles). Using this understanding, it may be possible for degradable particles to provide sustained delivery from within the suprachoroidal space. If degradable particles loaded with a drug are injected within this space they can remain in this space for months. As the particles degrade their degradation products and drug will be released into the suprachoroidal space. The study of macromolecules

demonstrates that the degradation products can be cleared from the space. At the same time, the drug can be released into the suprachoroidal space to provide sustained release to the surrounding tissues. This ensures that once the particles completely broken down there is a mechanism for their degradation products to be cleared from within this space and the site can be redosed.

4.3.6 Conclusion

This study demonstrated that small and large molecules can be injected into the suprachoroidal space of live rabbits. In addition this was the first work to examine the clearance kinetics of a variety of materials from within the suprachoroidal space. The study showed that the clearance kinetics of soluble molecules is relatively fast, occurring on the order of hours. As a result drug solutions injected into the suprachoroidal space may not be ideal for sustained delivery to the suprachoroidal space. However, fluorescent nano- and microparticles injected into this space were present for up to two months within the suprachoroidal space with no appreciable drop off in fluorescent intensity. Particles may be an ideal way to provide sustained delivery from within the suprachoroidal space to the surrounding tissues.

CHAPTER 5

CONCLUSION

Delivering drugs effectively to the eye is a challenging task. One of the most challenging aspects of drug delivery to the eye is to target the delivery to the diseased tissues. In the case of posterior segment diseases, such as age related macular degeneration (AMD), drugs need to reach the choroid and retina (chorioretinal tissues) to provide a therapeutic effect. Although there are a number of drugs that have been shown to be effective at treating diseases of the choroid and retina, there are very few delivery methods that can target and localize the drug to these tissues. Most delivery methods aim to inject a drug into the vitreous or on the extraocular surface of the globe. Although these can be designed to provide sustained delivery for periods of months to years, they are still not able effectively target the drug to the chorioretinal tissues without exposing other parts of the eye to the drug. The research presented in this thesis demonstrates a novel alternative to the current approaches to drug delivery to the eye.

This first part of the work introduced our minimally invasive strategy for drug delivery to the back of the eye. It showed that a hollow microneedle can be inserted into the sclera and inject liquid solutions and suspension of particles into the suprachoroidal space of rabbit, pig and human eyes ex vivo. The suprachoroidal space is a virtual space that is located between the sclera and choroid layers of the eye. This demonstrated that the injection spreads circumferentially around the eye within the suprachoroidal space. We showed

that by optimizing parameters such as infusion pressure and microneedle length, particles are reliably delivered into the suprachoroidal space. As a result, these data could be used to design an effective device for delivering drug formulations into the eye.

Armed with this information, the second part of the study developed an in vivo device for injection into rabbit eyes. This device was shown to reliably inject India ink into the suprachoroidal space. This study represents the first study to examine the capability of a hollow microneedle to inject within the suprachoroidal space of a live animal eye. The India ink study also showed that volumes up to 100 μL could be delivered into the rabbit eye and the India ink is well localized to the suprachoroidal space. This device allowed us to study the coverage of the chorioretinal surface. We were able to show that suprachoroidal injections of India ink cover up to 36 % of the available surface a single microneedle injection of 100 μL. Further characterization of the spread showed the India ink reaches the optic nerve in the back of the eye with a volume as small as 30 μL and further injections do not cause the spread to occur further back but instead in the lateral direction around the eye. In addition, the analysis showed that volumes in excess of 50 μL can cause the suprachoroidal space to expand in thickness and these thicknesses are on the order of several hundred micrometers.

In addition we developed a hollow metal microneedle that could be easily attached to a syringe to make a simple injection device. We showed that with this metal hollow microneedle device we could inject latex within the suprachoroidal space of fresh human cadaver eyes. The work showed that it was possible to

inject up to 150 µL of latex in to the suprachoroidal space and cover up to 40 % of the chorioretinal surface. In addition, the injections were performed at a site that would be accessible on a human (8 mm posterior to the limbus) and the results show that it is possible to inject in the suprachoroidal space from such a site. In addition the volumes injected represent volumes that are currently being injected into the vitreous for treatment of diseases such as AMD. As a result, this shows that it would be theoretically possibly to inject a comparable dose into the suprachoroidal space.

The final leg of the study, examined the intraocular pharmacokinetics of materials injected into the suprachoroidal space of rabbits in vivo. This work represents the first comprehensive study to examine the administration of small molecules, macromolecules, nanoparticles and microparticles into the suprachoroidal space. We were able to characterize the intraocular concentration profile of a suprachoroidal injection and compare it to an intravitreal injection profile using sodium fluorescein as a model compound. This data showed that suprachoroidal injections were more effective at targeting the chorioretinal tissues than intravitreal injections. The study further compared the half lives of both injection methods and determined them both to be very fast, less than 3 hours for each. We further showed that microneedles could inject macromolecules, including a therapeutic antibody, into the suprachoroidal space. An important result of this study is that it showed nano- and microparticles could be injected into the suprachoroidal space using a microneedle and were not cleared from the eye for at least 2 months.

Suprachoroidal delivery represents an improvement over current periocular and intravitreal delivery methods, both of which are poorly targeted to the chorioretinal tissues affected by posterior segment diseases. Rather than injecting drug outside the eye or in the vitreous humor, microneedle technology enables precisely targeted injection within the suprachoroidal space of the ocular tunic, which bathes the chorioretinal surface with the drug formulation. Moreover, by taking advantage of the unique features of ocular anatomy, a microneedle injection does not expose the drug formulation to many tissues as do conventional injections. Instead, by targeting the suprachoroidal space, the drug formulation infuses circumferentially within the suprachoroidal space to cover the chorioretinal surface from a single injection.

This method of delivery has four important attributes of an effective drug delivery system for the posterior segment. First, the use of a hollow microneedle allows the delivery method to be minimally invasive, because the microneedle only penetrates hundreds of micrometers into the eye, which should protect the retina from mechanical damage and reduce the risk of infection. We showed with our in vivo rabbit studies that the injections could be performed without any significant surgery and can be done quickly. This is a significant improvement over past studies that have accessed the suprachoroidal space using much more invasive procedures (Einmahl et al 2002, Gilger et al 2006, Olsen et al 2006, Kim et al 2007). As a result, this may offer a safety and convenience advantage.

Second, the suprachoroidal space offers the ability to target the choroid and retina by localizing the injection immediately adjacent to these tissues. Our

kinetic study showed that the intraocular concentration profiles of all materials injected into the suprachoroidal space were better targeted to chorioretinal tissues as compared to the conventional intraviteral injection. Suprachoroidal injections maintained this targeting through the time the material was in the eye. Third, we showed the potential for sustained delivery by demonstrating injection of particles up to 10 μm diameter into the suprachoroidal space of rabbits in vivo. The ability of the suprachoroidal space to accommodate particles has not been previously reported. Our findings suggest that particles can remain in the suprachoroidal space for a period of months. This opens up the possibility of injecting drug-loaded biodegradable particles into the suprachoroidal space for sustained drug release over a period of weeks to months, which could reduce the frequency of drug administration. Finally, with the inherent simplicity of the microneedle injection and with a properly designed microneedle device, suprachoroidal delivery could be carried out as a straightforward office procedure rather than a surgical one.

Overall this work shows that suprachoroidal drug delivery is a viable new route of administration for the treatment of chorioretinal diseases. Furthermore, administration using a microneedle based device could make the device simple and minimally invasive.

CHAPTER 6

DISCUSSION AND RECOMMENDATIONS

The research presented here represents some of the first studies to examine the suprachoroidal space as a local drug delivery route for the eye. This work also represents the first attempt to use microneedles as a way to administer fluids and particles into this space. The results from this work show that this is a promising route of delivery for treating diseases of the eye. However, there are still many unanswered questions and theories that need exploring before the full potential of this strategy can be understood.

We have shown with the prototype devices that we can reliably deliver materials into the suprachoroidal space of rabbits in vivo and within human cadaver eyes. However, in order to test this type of delivery on humans, improvement of the device and method need to be addressed. In order to decrease the risk of improper delivery, the insertion of the microneedles should be properly done to access the suprachoroidal space. The device or method should allow the microneedle to reach as close as possible to the suprachoroidal space without penetrating into the choroid. This would allow the best chance of targeting the space. This could be accomplished by measuring the thickness of the patient's sclera and conjunctiva and then choosing a proper sized microneedle. An alternative would be to incorporate a feedback system within the insertion device to allow for proper positioning. Our work also showed that the infusion pressure was important. As a result, the device should allow for proper

control of infusion pressure. The device should prioritize safety and minimize trauma to the eye from both the insertion and the infusion.

Future work also needs to focus on understanding the intraocular pharmacokinetics of suprachoroidal injections. Experiments should be designed to understand how formulation changes and properties of molecules influence the pharmacokinetics within the eye. Lipophilic drugs, such as steroids, may have prolonged residence times because of their low solubility in aqueous environments. In addition, formulation changes may allow for tuning of clearance rates as well as spread within the suprachoroidal space. Gel formulations may provide slower release of drugs as well as unique spread profiles within the suprachoroidal space. As an example, if a formulation can be designed so as to limit spread of the injection just around the limbus, this formulation may have applications in glaucoma therapy. In addition, biodegradable particles with encapsulated drugs need to be evaluated within the suprachoroidal space to demonstrate sustained release. Understanding this and determining the concentration of drugs in the intraocular tissues will help determine the potential of these injections have to treat diseases.

In addition to pharmacokinetics, pharmacotherapy from within this space also needs to be evaluated. The potential to actually treat diseases from within this space still needs to be proven. One of the first things is to determine what diseases can actually be treated. Diseases of the choroid and retina appear to be the most relevant. Animal models of these diseases could be used to evaluate the potential to treat these diseases from suprachoroidal delivery. Furthermore,

the targeting to chorioretinal tissues enabled by this delivery might enable a preventative approach to treating diseases. As an example, choroidal neovascularization, is a major component of advanced AMD and anti-VEGF therapies do exist to treat neovascularization. Based on the proposed mechanisms for the disease, if antibodies against neovascularization can be delivered to the choroid it may prevent the blood vessels from growing and damaging the retina. Since suprachoroidal injections can deliver drugs directly to the choroid, injecting these antibodies during the early progression of the disease may prevent damage to the retina.

An evaluation of the safety from these types of injections will also be an important area to study if suprachoroidal injections are to be used on humans. This applies to not just the safety of the injection, but also the safety of drugs and fluids occupying the space for an extended period of time. Some of the critical things to examine are if there is any serious complication, edema, inflammation, abnormal vessel growth, or deterioration of visual function as a result of the injection. Formulations within the space may affect some of the natural processes in the eye, such as uveal scleral outflow. The effect of repeated injections in to the space also needs to be characterized. This is especially important since the patients being treated already have compromised ocular integrity.

In the context of ocular drug delivery, this work offers an exciting opportunity to explore a new strategy enabled by microneedle technology. It demonstrates that it may be possible to provided targeted, minimally invasive

and sustained drug delivery from a single device. From a research perspective there is a lot that can be learned by exploring this route and comparing it to the options that are currently available. It may serve as a research tool that can lead to the discovery of new drugs. It may also lead to optimized formulations for applications in the suprachoroidal space in the eye. We hope this work will lead to new research to explore the benefits of targeting in ocular drug delivery. We are optimistic that this work will play an important role in developing better therapy modalities and have a positive impact on the treatment of ocular diseases.

REFERENCES

The Merck Manual of Medical Information —Second Home Edition. In. Merck Research Laboratories. http://www.merck.com/mmhe/index.html. Accessed 06/14/2007.

Alm A and Nilsson SFE (2009) Uveoscleral Outflow - a Review. Experimental Eye Research 88(4):760-8

Alward WLM (1998) Medical Management of Glaucoma. N Engl J Med 339(18):1298-307

Arora A, Prausnitz MR and Mitragotri S (2008) Micro-Scale Devices for Transdermal Drug Delivery. Int J Pharm 364(2):227-36

Avery RL, Pearlman J, Pieramici DJ, et al (2006) Intravitreal Bevacizumab (Avastin) in the Treatment of Proliferative Diabetic Retinopathy. Ophthalmology 113(10):1695-705

Brazzle J, Papautsky I and Frazier AB (1999) Micromachined Needle Arrays for Drug Delivery or Fluid Extraction. IEEE Eng Med Biol Mag 18(6):53-8

Brubaker RF (1982) The Flow of Aqueous Humor in the Human Eye. Trans Am Ophthalmol Soc 80:391-474.

Chang-Lin JE, Attar M, Acheampong AA, et al (2010) Pharmacokinetics and Pharmacodynamics of the Sustained-Release Dexamethasone Intravitreal Implant. Invest Ophthalmol Vis Sci doi: 10.1167/iovs.10-5285

Chappelow AV and Kaiser PK (2008) Neovascular Age-Related Macular Degeneration: Potential Therapies. Drugs 68(8):1029-36.

Chun DW, Heier JS, Topping TM, et al (2006) A Pilot Study of Multiple Intravitreal Injections of Ranibizumab in Patients with Center-Involving Clinically Significant Diabetic Macular Edema. Ophthalmology 113(10):1706-12

Clement CI and Goldberg I (2011) The Management of Complicated Glaucoma. Indian J Ophthalmol 59(Suppl):S141-7.

Congdon N, O'Colmain B, Klaver CCW, et al (2004) Causes and Prevalence of Visual Impairment among Adults in the United States. Arch Ophthalmol 122(4):477-85

Cormier M, Johnson B, Ameri M, et al (2004) Transdermal Delivery of Desmopressin Using a Coated Microneedle Array Patch System. J Control Release 97(3):503-11.

Davis SP, Martanto W, Allen MG, et al (2005) Hollow Metal Microneedles for Insulin Delivery to Diabetic Rats. IEEE Trans Biomed Eng 52(5):909-15

del Amo EM and Urtti A (2008) Current and Future Ophthalmic Drug Delivery Systems: A Shift to the Posterior Segment. Drug Disc Today 13(3-4):135-43

Ding Z, Verbaan FJ, Bivas-Benita M, et al (2009) Microneedle Arrays for the Transcutaneous Immunization of Diphtheria and Influenza in Balb/C Mice. J Control Release 136(1):71-8.

Edelhauser HF, Rowe-Rendleman CL, Robinson MR, et al (2010) Ophthalmic Drug Delivery Systems for the Treatment of Retinal Diseases: Basic Research to Clinical Applications. Invest Ophthalmol Vis Sci 51(11):5403-20.

Edwards A and Prausnitz MR (1998) Fiber Matrix Model of Sclera and Corneal Stroma for Drug Delivery to the Eye. AIChE J 44(1):214-25

Einmahl S, Savoldelli M, D'Hermies F, et al (2002) Evaluation of a Novel Biomaterial in the Suprachoroidal Space of the Rabbit Eye. Invest Ophthalmol Vis Sci 43(5):1533-9

Einmahl S, Savoldelli M, D'Hermies F, et al (2002) Evaluation of a Novel Biomaterial in the Suprachoroidal Space of the Rabbit Eye. Invest Ophthalmol Vis Sci 43(5):1533-9

Eljarrat-Binstock E, Pe'er J and Domb AJ (2010) New Techniques for Drug Delivery to the Posterior Eye Segment. Pharm Res 27(4):530-43

Emi K, Pederson JE and Toris CB (1989) Hydrostatic-Pressure of the Suprachoroidal Space. Invest Ophthalmol Vis Sci 30(2):233-8

Fattal E and Bochot A (2006) Ocular Delivery of Nucleic Acids: Antisense Oligonucleotides, Aptamers and Sirna. Adv Drug Deliv Rev 58(11):1203-23

Feldkamp LA, Davis LC and Kress JW (1984) Practical Cone-Beam Algorithm. J Opt Soc Am A-Opt Image Sci Vis 1(6):612-9

Felt-Baeyens O, Eperon S, Mora P, et al (2006) Biodegradable Scleral Implants as New Triamcinolone Acetonide Delivery Systems. Int J Pharm 322(1-2):6-12

Gardeniers H, Luttge R, Berenschot EJW, et al (2003) Silicon Micromachined Hollow Microneedles for Transdermal Liquid Transport. J of Microelectro Sys 12(6):855-62

Gaudana R, Ananthula H, Parenky A, et al (2010) Ocular Drug Delivery. AAPS J 12(3):348-60

Ghate D, Brooks W, McCarey BE, et al (2007) Pharmacokinetics of Intraocular Drug Delivery by Periocular Injections Using Ocular Fluorophotometry. Invest Ophthalmol Vis Sci 48(5):2230-7

Gilger BC, Salmon JH, Wilkie DA, et al (2006) A Novel Bioerodible Deep Scleral Lamellar Cyclosporine Implant for Uveitis. Invest Ophthalmol Vis Sci 47(6):2596-605

Gilger BC, Salmon JH, Wilkie DA, et al (2006) A Novel Bioerodible Deep Scleral Lamellar Cyclosporine Implant for Uveitis. Invest Ophthalmol Vis Sci 47(6):2596-605 47(6):2596-605

Gill HS and Prausnitz MR (2007a) Coating Formulations for Microneedles. Pharm Res 24(7):1369-80

Gill HS and Prausnitz MR (2007b) Coated Microneedles for Transdermal Delivery. J Control Release 117(2):227-37

Gupta J, Felner EI and Prausnitz MR (2009) Minimally Invasive Insulin Delivery in Subjects with Type 1 Diabetes Using Hollow Microneedles. Diab Tech & Therap 11(6):329-37

Healey PR, Herndon L and Smiddy W (2007) Management of Suprachoroidal Hemorrhage. J Glaucoma 16(6):577-9

Henry S, McAllister DV, Allen MG, et al (1999) Microfabricated Microneedles: A Novel Approach to Transdermal Drug Delivery. J Pharm Sci 88(9):948

Hughes PM, Olejnik O, Chang-Lin J-E, et al (2005) Topical and Systemic Drug Delivery to the Posterior Segments. Adv Drug Deliv Rev 57(14):2010-32

Jager RD, Aiello LP, Patel SC, et al (2004) Risks of Intravitreous Injection: A Comprehensive Review. Retina 24(5):676-98

Jarvinen K, Jarvinen T and Urtti A (1995) Ocular Absorption Following Topical Delivery. Adv Drug Deliv Rev 16(1):3-19

Jiang J, Gill HS, Ghate D, et al (2007) Coated Microneedles for Drug Delivery to the Eye. Invest Ophthalmol Vis Sci 48(9):4038-43

Jiang J, Moore JS, Edelhauser HF, et al (2009) Intrascleral Drug Delivery to the Eye Using Hollow Microneedles. Pharm Res 26(2):395-403

Kane FE, Burdan J, Cutino A, et al (2008) Iluvien: A New Sustained Delivery Technology for Posterior Eye Disease. Expert Opin Drug Deliv 5(9):1039-46.

Kaufman P and Alm A (2002) Adler's Physiology of the Eye. 10th ed: Mosby

Kaur IP and Kanwar M (2002) Ocular Preparations: The Formulation Approach. Drug Dev Ind Pharm 28(5):473-93

Kim SH, Csaky KG, Wang NS, et al (2008) Drug Elimination Kinetics Following Subconjunctival Injection Using Dynamic Contrast-Enhanced Magnetic Resonance Imaging. Pharm Res 25(3):512–520

Kim SH, Galban CJ, Lutz RJ, et al (2007) Assessment of Subconjunctival and Intrascleral Drug Delivery to the Posterior Segment Using Dynamic Contrast-Enhanced Magnetic Resonance Imaging. Invest Ophthalmol Vis Sci 48(2):808-14

Kim SH, Lutz RJ, Wang NS, et al (2007) Transport Barriers in Transscleral Drug Delivery for Retinal Diseases. Ophthalmic Res 39(5):244-54

Kimura H, Yasukawa T, Tabata Y, et al (2001) Drug Targeting to Choroidal Neovascularization. Adv Drug Deliv Rev 52(1):79-91

Klein BEK, Klein R and Linton KLP (1992) Intraocular Pressure in an American Community - the Beaver Damn Eye Study. Invest Ophthalmol Vis Sci 33(7):2224-8

Koevary SB (2003) Pharmacokinetics of Topical Ocular Drug Delivery: Potential Uses for the Treatment of Diseases of the Posterior Segment and Beyond. Current Drug Metabolism 4(3):213-22

Krohn J (2004) Morphology and Clinical Aspects of the Aqueous Humour Drainage Routes with Special Emphasis on Uveoscleral Outflow. Acta Ophthal Scand 82(4):483-4

Krohn J and Bertelsen T (1997) Corrosion Casts of the Suprachoroidal Space and Uveoscleral Drainage Routes in the Human Eye. Acta Ophthal Scand 75(1):32-5

Krohn J and Bertelsen T (1998) Light Microscopy of Uveoscleral Drainage Routes after Gelatine Injections into the Suprachoroidal Space. Acta Ophth Scand 76(5):521-7

Kuno N and Fujii S (2010) Biodegradable Intraocular Therapies for Retinal Disorders: Progress to Date. Drugs Aging 27(2):117-34

Kuppermann B (2007) Implants Can Deliver Corticosteroids, Pharmacological Agents. Retina Today (March/April):27-31

Lai MM, Lai JC, Lee WH, et al (2005) Comparison of Retrobulbar and Sub-Tenon's Capsule Injection of Local Anesthetic in Vitreoretinal Surgery. Ophthalmology 112(4):574-9

Lee DA and Higginbotham EJ (2005) Glaucoma and Its Treatment: A Review. Am J Health Syst Pharm 62(7):691-9

Lee JW, Park J-H and Prausnitz MR (2008) Dissolving Microneedles for Transdermal Drug Delivery. Biomaterials 29(13):2113-24

Lee S, Hughes P, Ross A, et al (2010) Biodegradable Implants for Sustained Drug Release in the Eye. Pharm Res 27(10):2043-53

Lens A, Langley T, Nemeth S, et al (1999) Ocular Anatomy and Physiology. 1st ed. Thorofare, NJ: SLACK Inc.

Loftssona T and Jarvinen T (1999) Cyclodextrins in Ophthalmic Drug Delivery. Adv Drug Deliv Rev 36(1):59-79

Ludwig A (2005) The Use of Mucoadhesive Polymers in Ocular Drug Delivery. Adv Drug Deliv Rev 57(11):1595-639

Martanto W, Davis SP, Holiday NR, et al (2004) Transdermal Delivery of Insulin Using Microneedles in Vivo. Pharm Res 21(6):947-52

Martanto W, Moore JS, Kashlan O, et al (2006) Microinfusion Using Hollow Microneedles. Pharm Res 23(1):104-13

Maurice D (2001) Review: Practical Issues in Intravitreal Drug Delivery. J Ocul Pharmacol Ther 17(4):393-401

McAllister DV, Wang PM, Davis SP, et al (2003) Microfabricated Needles for Transdermal Delivery of Macromolecules and Nanoparticles: Fabrication Methods and Transport Studies. Proc Natl Acad Sci U S A 100(24):13755-60

Meek KM and Fullwood NJ (2001) Corneal and Scleral Collagens - a Microscopist's Perspective. Micron 32(3):261-72

Mittl RN and Tiwari R (1987) Suprachoroidal Injection of Sodium Hyaluronate as an 'Internal' Buckling Procedure. Ophthalm Res 19(5):255-60

Mohamed Q, Gillies MC and Wong TY (2007) Management of Diabetic Retinopathy: A Systematic Review. JAMA 298(8):902-16

Myles ME, Neumann DM and Hill JM (2005) Recent Progress in Ocular Drug Delivery for Posterior Segment Disease: Emphasis on Transscleral Iontophoresis. Adv Drug Deliv Rev 57(14):2063-79

Ockrim Z and Yorston D (2010) Managing Diabetic Retinopathy. BMJ doi: 10.1136/bmj.c5400

Olsen TW, Feng X, Wabner K, et al (2006) Cannulation of the Suprachoroidal Space: A Novel Drug Delivery Methodology to the Posterior Segment. Am J Ophthalmol 142(5):777-87

Ozkiris A and Erkilic K (2005) Complications of Intravitreal Injection of Triamcinolone Acetonide. Can J Ophthalmol 40(1):63-8

Park JH, Allen MG and Prausnitz MR (2005) Biodegradable Polymer Microneedles: Fabrication, Mechanics and Transdermal Drug Delivery. J Control Release 104(1):51-66

Park JH, Allen MG and Prausnitz MR (2006) Polymer Microneedles for Controlled-Release Drug Delivery. Pharm Res 23(5):1008-19

Patel S, Lin A, Edelhauser H, et al (2011) Suprachoroidal Drug Delivery to the Back of the Eye Using Hollow Microneedles. Pharm Res 28(1):166-76

Peyman GA and Ganiban GJ (1995) Delivery Systems for Intraocular Routes. Adv Drug Deliv Rev 16(1):107-23

Peyman GA, Lad EM and Moshfeghi DM (2009) Intravitreal Injection of Therapeutic Agents. Retina 29(7):875-912

Peyman GA, Lad EM and Moshfeghi DM (2009) Intravitreal Injection of Therapeutic Agents. Retina 29(7):875-912

Raghava S, Hammond M and Kompella UB (2004) Periocular Routes for Retinal Drug Delivery. Expert Opin Drug Deliv 1(1):99-114

Saettone MF and Salminen L (1995) Ocular Inserts for Topical Delivery. AdvDrug Deliv Rev 16(1):95-106

Stefansson E and Loftsson T (2002) Cyclodextrins in Eye Drop Formulations. Journal of Inclusion Phenomena and Macrocyclic Chemistry 44(1-4):23-7

Steinbrook R (2006) The Price of Sight - Ranibizumab, Bevacizumab, and the Treatment of Macular Degeneration. N Engl J Med 355(14):1409-12

Van Damme P, Oosterhuis-Kafeja F, Van der Wielen M, et al (2009) Safety and Efficacy of a Novel Microneedle Device for Dose Sparing Intradermal Influenza Vaccination in Healthy Adults. Vaccine 27(3):454-9

Wax MB, Camras CB, Fiscella RG, et al (2002) Emerging Perspectives in Glaucoma: Optimizing 24-Hour Control of Intraocular Pressure Am J Ophthalmol 133:s1-s10

Xie Y, Xu B and Gao Y (2005) Controlled Transdermal Delivery of Model Drug Compounds by Mems Microneedle Array. Nanomedicine 1(2):184-90

Yasukawa T and Ogura Y (2010) Medical Devices for the Treatment of Eye Diseases. Handb Exp Pharmacol (197):469-89

Zahn JD, Talbot NH, Liepmann D, et al (2000) Microfabricated Polysilicon Microneedles for Minimally Invasive Biomedical Devices. Biomed Microdev 2:295-303

Zarbin M and Szirth B (2007) Current Treatment of Age-Related Macular Degeneration. Opto and Vis Sci 84(7):559-72

Zignani M, Tabatabay C and Gurny R (1995) Topical Semisolid Drug-Delivery - Kinetics and Tolerance of Ophthalmic Hydrogels. Adv Drug Deliv Rev 16(1):51-60

VITA

Samirkumar R. Patel

Samirkumar Patel was born in Sarsa Gujarat, India. He immigrated to the United States in 1986. Mr. Patel grew up in the central valley in Stockton, California and went graduated from Tokay High School. He attended the University of California at Berkeley and received a dual Bachelors of Science degree in Chemical and Material Science Engineering in 2004. Mr. Patel worked for Alza Corporation for approximately 1.5 years before joining the Georgia Institute of Technology to pursue a doctoral degree Chemical Engineering.